University of South-Eastern Norway
Faculty of Technology, Natural Sciences and Maritime Sciences
–
Master's Thesis
Study programme: Smart Systems Integrated Solutions
Spring/Autumn 2023

Mashrur Sakib Choyon

Development of an Electrochemical Sensor for Detecting Microplastics in Aqueous Media

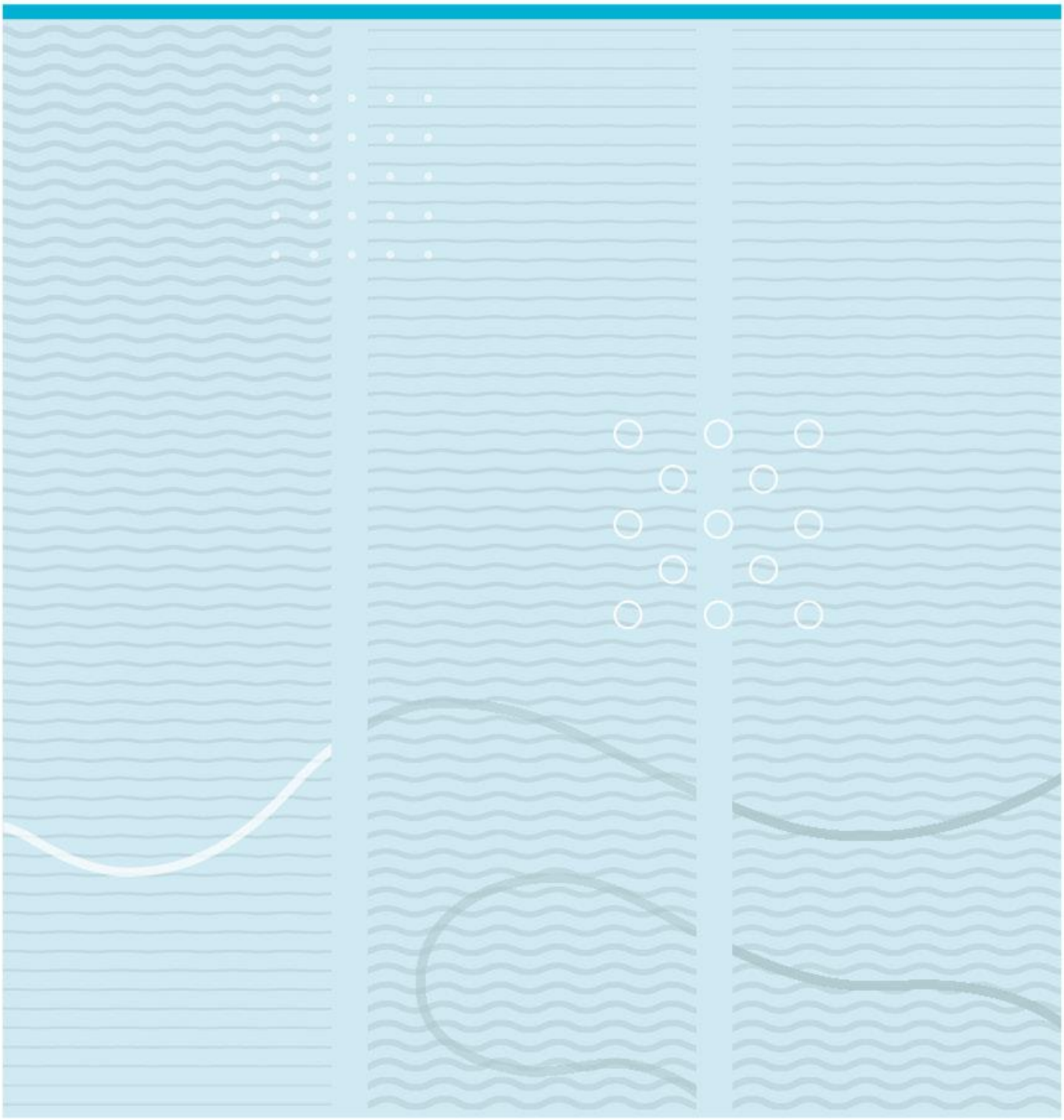

University of South-Eastern Norway
Faculty of Technology, Natural Sciences and Maritime Sciences
Department of Microsystems
PO Box 215
NO- 3184 Raveien, Norway

http://www.usn.no

This thesis is worth 30 ECTS study points

Summary

Microplastic pollution has become a significant environmental concern due to its adverse effects on ecosystems and human health. In this master's thesis, the development of an electrochemical sensor for the detection of microplastics in aqueous media is presented. The sensor was developed utilizing the “impact concept” which basically states that the microplastic particles generate a signal at the time of making impacts with the working electrode of the sensor. From the attained signals of these impacts, microplastic particles present in the aqueous sample were detected utilizing the spike counts generated from the impacts and quantified using FFT analysis. The result shows that for microplastics concentrations as volume fractions (v/v) 0.005%, 0.02%, 0.03%, and 0.04%, prominent peaks are observed around 5 Hz, 20 Hz, 21 Hz, and 24 Hz respectively, whereas the control solution of 0% displayed no such peaks. Electrochemical impedance spectroscopy (EIS) was studied as an alternative detection modality for the detection and quantification of microparticles where a calibration coefficient was determined in terms of constant phase element (CPE) for the aqueous solution with the absence of microplastics and different concentrations of microplastics in the solution.

This thesis report begins with a brief introduction to the project. A comprehensive review of literature and background studies from which the motivation for this research work emerged is also presented. The obtained results demonstrate the sensor's capability to detect microplastics utilizing a 100 nA range current and exhibit a linear response over a wide concentration range. The developed electrochemical sensor can quickly and directly detect microplastics in aqueous solutions. It is a potential instrument for environmental research and monitoring due to its relatively simple design and operation. A possible improvement of the sensor can be made on the working electrode’s diameter, as it should be reduced to below 10 µm to increase its capability to detect microplastic particles individually. The sensor is intended to be part of a system where microplastics are pre-concentrated at the sensor through an acoustic actuator focusing on an integrated microfluidic device.

Contents

Abbreviations

FFT	Fast Fourier Transform	WE	Working Electrode
LDPE	Low-density polyethylene	CE	Counter Electrode
HDPE	High-density polyethylene	RE	Reference Electrode
PP	Polypropylene	RS	Raman Spectroscopy
PS	Polystyrene	SEM	Scanning Electron Microscopy
PET	Polyethylene Terephthalate	EDX	Energy Dispersive X-Ray
PVC	Polyvinyl chloride	GC	Gas Chromatography
PP	Polypropylene	MS	Mass Spectrometry
UV	Ultraviolet	FPA	Focal Plane Array
M cells	Microfold cells	HPLC	High-Performance Liquid Chromatography
HOCs	Hydrophobic Organic Contaminants	CCD	Charge-Coupled Device
PAHs	Polycyclic Aromatic Hydrocarbons	SPR	Surface Plasmon Resonance
PCBs	Polychlorinated Biphenyls	ERs	Estrogen Receptors
CPE	Constant Phase Element	ZP-HV-SPE	Zimmer & Peacock Hyper Value Screen Printed Electrodes
WWTP	Waste Water Treatment Plant	CV	Cyclic Voltammetry
FT-IR	Fourier Transform Infrared Spectroscopy	FAM	Fast Amperometry
FT	Fourier Transform	CA	Chronoamperometry
IR	Infrared	EIS	Electrochemical Impedance Spectroscopy
ATR	Attenuated total reflection	DFT	Discrete Fourier Transform
SPR	Surface Plasmon Resonance	ER	Estrogen Receptors
R&D	Research and Development	SNR	Signal-to-Noise Ratio

Acknowledgements

The journey of this project has been quite challenging and exciting at the same time for its unique application. However, none of it would have been possible without the support, guidance, and simple encouragement from the people who were there for me.

Firstly, I would like to thank my thesis supervisor Professor Erik Andrew Johannessen for being such an influential person in my Master's study. His kind guidance and the tendency to push me towards perfection and preciseness in my studies have always been a major impact on my learning. Secondly, I want to thank Sindre Søpstad from ZP for being such a supportive Co-supervisor from ZP. His kind encouragement, guidance, teachings, and contributions to this thesis have been incomparable. I also want to thank my other Co-supervisor Hamed Salmani for his valuable thought-provoking insights into this project work. I was able to improve quite many aspects of the project from his suggestions. I am blessed to have these three persons as my supervisor and co-supervisors. I couldn't have asked for any better supervision than this.

I want to thank Zimmer & Peacock AS for providing the facilities to carry out my thesis project. Many thanks go to Martin Peacock for introducing the unique principle that worked as one of the main ideas behind this thesis. I also want to thank the brilliant and amazing people from ZP for their guidance and support, namely, Even Zimmer, Youssef Lattach, Solrun Lid, Birgette Hønsvall, Soha Sweilam, Ni Ngo, Saran, Sujith, Tatiane, Thanh, Daniel, Roger, and Kristoffer. Also thanks to Karoline Krogstad for helping me in the USN lab.

Special thanks to my elder brother Ashraf Mahbub Shawon for guiding me toward the right path in life. Thanks to Eshrat Jahan Muniya for just being there in the tough days and supporting me unconditionally. Thanks to Saltanat Askar, Georgii Pushkarev, Gayane Avetisyan for providing moral support and for just having those talks.

I acknowledge the huge opportunity that was given to me by SSIs programme committee to study in this Joint Master's programme. The project was financially supported by the Research Council of Norway NORFAB III (project number: 295864), and RFF Vestfold og Telemark (project number: 337766).

Mashrur Sakib Choyon

Horten, Norway

July 2023

1 Introduction

The production of plastic worldwide has increased dramatically in the past decades. Unsustainable disposal of used plastics has led to global pollution in all parts of the environment. Although plastics do not biodegrade easily, they break down into microplastics and nanoplastics, which are defined as small pieces of plastic debris that are less than 5 mm in length and found in different environments like water, soil, and air. Microplastics can exist in the environment for hundreds of years as they do not biodegrade and their accumulation in the food chain has made them a significant environmental concern and also a major health concern for living beings, including humans. Their presence can negatively affect animal and human health, as well as disrupt ecosystems by interfering with feeding and reproduction [1]–[5].

Most of the plastic waste gets dumped into the marine environment and after many years of degradation, these plastics become microplastics. However, there is no easy and cost-effective solution to detect microplastics in aqueous media and in order to mitigate the negative impact of microplastics, there's a need to develop mobile low-cost units for microplastics detection. Thus, facing this challenge, this research project seeks to develop such a system in which microplastics in aqueous media can be detected using electrochemical sensors.

The main inspiration was taken from the "impact concept" introduced by Shimizu et al. [6] in their research work to detect microplastics. This study examines collisions between tiny polyethylene insulating particles floating in an aqueous electrolyte solution. The publication describes the finding of current transients (spikes) that are connected to these particle collisions. Although microplastic particles of polyethylene material are insulators, the current spikes seen during impacts suggest that the current comes from the reduction of oxygen, and where the microplastic particles work as oxygen carriers. This project aims to leverage this "impact concept" as an effective method to detect microplastics in aqueous solution. Furthermore, the project utilized alternative methods such as impedance spectroscopy analysis, and signal processing techniques like FFT analysis to establish ways to interpret the signal.

This report is organized as follows. Chapter 2 explains the motivation behind this research work through literature reviews, background studies, and theoretical aspects of different technological concepts used in this project. Chapter 3 describes the methodology used for carrying out the research work. Chapter 4 displays and discusses the results obtained from the experiments carried out in this project. Chapter 5 discusses the challenges and overall outcomes of this project. Section 6 concludes and discusses the future works that this research work paved the way to.

2 Literature Review and Background

This chapter discusses the literature review and background from which the motivation for this research work emerged and different theoretical concepts that were utilized.

2.1 Microplastics

To understand the characteristics and impacts of microplastics, it is important to have a background knowledge of microplastics itself. This section gives a brief introduction to plastic pollution with different types of plastics, microplastics, and the effect of microplastics on living beings.

2.1.1 Plastic pollution and common types of plastics

Plastics, which are generated from oil or gas via polymerization, have revolutionized the industry due to their light weight, toughness, and resilience towards corrosion [5], [7]. Since the emergence of the first modern plastic called “Bakelite”, in 1907, a broad variety of plastics have been mass-produced and extensively employed in a variety of applications. Plastic manufacturing increased dramatically, reaching 390.7 million tons in 2021 [8]. Plastic is popular because of its durability, but because it is so resistant to deterioration, disposing of any sort of plastic garbage can be difficult. Municipal garbage, which accounts for 10% of the world's waste production, contains a sizable part of plastic debris, including waste from disposable things like packaging materials [9].

Marine litter occurs due to garbage dumping carried out directly or indirectly into the seas and oceans [10]. Among all marine debris, it is estimated that 80% of the plastic waste comes from terrestrial sources [11]. Numerous studies have demonstrated how freshwater systems' unidirectional flow plays a significant role in the transfer of plastic waste into marine environments or oceans [12].

Different types of plastics are used for several kinds of applications. Table 1 shows different types of plastic classes and the products that are manufactured from them which are ultimately found as marine debris.

Table 1: Different types of Plastics that are commonly found in marine debris [11], [13]

Plastic Class	Products and Typical origin
Low-density polyethylene (LDPE)	Plastic bags, six-pack rings, bottles, netting, drinking straws
High-density polyethylene (HDPE)	Milk and juice jugs
Polypropylene (PP)	Rope, bottle caps, netting
Polystyrene (PS)	Plastic utensils, food containers
Foamed Polystyrene	Floats, bait boxes, foam cups
Nylon	Netting and traps
Thermoplastic Polyester, i.e., polyethylene terephthalate (PET)	Plastic beverage bottles
Polyvinyl chloride (PVC)	Plastic film, bottles, cups
Cellulose Acetate	Cigarette filters
Polypropylene (PP)	Baby milk bottle, food grade bottle package

2.1.2 Microplastics and their sources

The freshwater sources that mostly flow down to the oceans or marine environment play a significant role in transferring plastic wastes into the marine environment. Freshwater sources are mostly rivers and lakes that are utilized by humans to collect and process the water for daily use, as well as to drink. However, these freshwater sources also get polluted with many kinds of waste, including plastic waste, at a high rate.

Small plastic pieces are produced from the degradation of bigger plastic pieces in marine and terrestrial ecosystems. Physical, biological, and chemical processes degrade the structural stability of plastics over time, leading to fragmentation. UV rays from the sun's rays cause photo-degradation, which causes the polymer matrix to disintegrate and release additives [9], [10]. Due to exposure to sunshine, plastic waste on beaches deteriorates quickly, becoming brittle and cracking. Through abrasion, wave action, and turbulence, plastics become more vulnerable to fragmentation [11]. This process keeps going until the particles are the size of microplastic. Researchers have different opinions to define the standard size of microplastics. However, the most widely acceptable size of plastic particles that can be defined as microplastics is <5mm [1], [2], [10], [11]. The smallest

microplastic fragments found in seas are around 1.6 µm in diameter [14]. Degradation of plastics that results in microplastic particles can be classified into the following categories [11]:

(a) Biodegradation is the result of living things, often micro-organisms.
(b) Photodegradation is the result of light (often sunshine when exposed outside).
(c) Thermo-oxidative degradation is a gradual oxidative breakdown that occurs at normal temperatures.
(d) Thermal deterioration, which is caused by extreme heat (not an environmental degradation process).
(e) Hydrolysis - water-based reaction.

Common polymers are usually photo-oxidatively degraded in the marine environment when exposed to UV-B rays. As long as there is oxygen available, this destruction can also proceed thermo-oxidatively without additional UV exposure. Compared to light-induced oxidation, other degradation mechanisms are substantially slower [11]. Beaches or shores are therefore the most probable location for the production of microplastics in the marine environment. Since different types of plastic waste exist in the marine environment, the microplastics generated from these wastes aren't formed of just one substance. Rather, they are a complicated mixture of hundreds of chemically distinct molecules.

Microplastics have recently been discovered in drinking water and its sources, raising serious concerns and generating debates about possible negative effects on human health. In their review, Koelmans et al. looked at fifty research that investigated microplastics in important freshwater sources such as rivers, lakes, groundwater, tap water, bottled drinking water, and wastewater [15]. Their research showed that freshwaters and drinking water frequently include microplastics. Over ten orders of magnitude (1*10-2 to 10^8 #/m3) in size, the contents of microplastics varied dramatically between various samples and water types [15]. The documented concentrations of microplastics found in both tap and bottled water vary from 0 to 104 particles per liter [15]. According to a more focused statistical analysis, greater counts are being seen for smaller-sized microplastics. Another study reports that the abundance of microplastics varies depending on the location, ranging from over 1 million pieces per cubic meter to less than 1 piece in 100 cubic meters [16]. Figure 2.1 shows the concentration of microplastics in different types of water sources which indicates a significant concern regarding the issue. The result indicates the significant amount of microplastics found in drinking water sources.

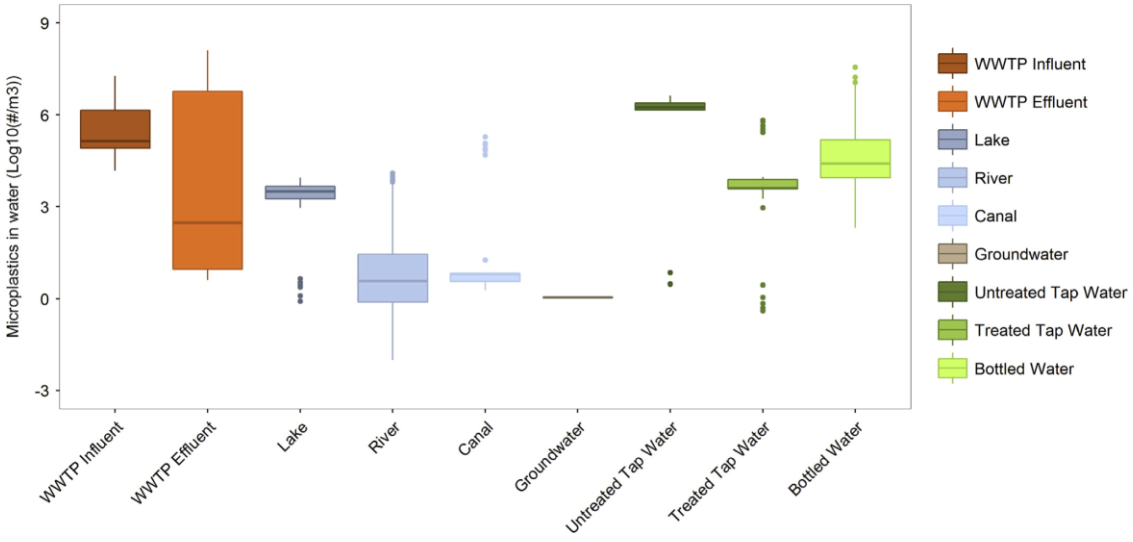

Figure 2.1 Box and whisker plot illustrating the central tendency and variability of microplastic number concentrations across different water types, based on individual sample data (WWTP = Waste Water Treatment Plant) [15]

2.1.3 Presence of microplastics in different consumer products

Due to their small dimensions and degraded conditions, microplastics have several origins and channels from where they enter the environment, making it challenging to track their origin. Microplastics' size, color, form, and polymer type, among other features, might offer hints regarding their origin. For instance, polyethylene-based spherical microbeads are typically found in personal care products. Industrial pellets are typically 3 to 5 mm long microplastics that are cylindrical or oval in form. Synthetic garments or textiles are frequently linked with colorful polyester microfibers. These distinguishing features of microplastics can also point to the sources of their introduction into the environment, such as industrial wastes, agricultural waste, stormwater runoff, the release of wastewater, recycling plants, landfills, or fishing equipment [1].

The presence of microplastics and synthetic microparticles in honey and precipitation provides evidence that they are airborne [17]. During precipitation events, fibers and pieces have been discovered in the rainfall, lending credence to the idea that microplastics are airborne. These contaminating particles may wind up on flowers and other vegetation, where they may combine with pollen and be carried to beehives by bees. Additionally, it has been shown that samples of German beer are potentially contaminated with microplastics, the most prevalent type being fragments [18]. Materials employed in the brewing process or atmospheric deposition might be to blame for the pollution. Additionally, it has been shown that store-bought sea salt contains microplastics [19]. Especially PET and PE, which most likely come from air deposition or coastal waterways, as these

seawaters are eventually used for the production of salt. Therefore, it has become quite evident that the pollution of the atmosphere by microplastics is causing their prevalence in diverse food sources. However, it is still unclear how their presence in food may affect human health.

2.1.4 Impact of Microplastics on marine life and human health

Microplastics have been detected in a wide range of marine organisms, spanning from zooplankton to whales [20]. Even though the exact impact of microplastics on human health and marine lives yet to be fully understood, some studies suggest that microplastic exposure can have adverse impacts on gene expression, survival, or reproductive output of organisms [21]. The diversity of physical and chemical characteristics of microplastics that organisms are exposed to may play a factor to determine the exact impact factors of microplastics on marine life and human health. It is suspected that even if microplastic particles are not toxic material itself, they might have the potential ability to act as a carrier of other toxic elements that are harmful to organisms and humans. Nonetheless, the impact of microplastic exposure in the long term cannot be neglected [21].

Seabirds were utilized as bioindicators in a research on marine lives affected by plastic pollution. The study reported that these creatures are at risk of getting entangled in plastic waste, which might result in skeletal damage, hunger, abrasions to the skin, and asphyxiation. Plastic consumption can also result in bowel obstruction, damage to the gut lining, illness, and death of these marine creatures [22]. Nanoplastics, which are small microplastics, can pass past digestive membranes and build up in tissues and organs. Gene expression interference, oxidative stress induction, immunological reactions, genomic instability, hormonal system problems, neurological damage, reproduction defects, embryotoxicity, and trans-generational toxicity are the suggested long-term effects indicated in the study [22]. Another research suggests that numerous elements, such as variations in the polymer type, size, form, and chemical makeup, can affect how microplastics affect organisms. Researchers have looked at various combinations of these features and corroborated these conclusions through numerous laboratory experiments. The chemical additions or component monomers utilized during the manufacturing process may be connected to the possible damage produced by various polymer types [23]. Some polymers, such as PVC and polyurethane, may have chemical components that make them possibly mutagenic or carcinogenic. This is one of the reasons why PVC is avoided in the manufacturing of consumer products [13]. In contrast, it is thought that other polymers, such as polyethylene and polypropylene, are less reactive. Additionally, tiny, elongated, or irregularly shaped microplastic particles have a larger surface area-

to-volume ratio than other types of microplastics, which increases their ability to absorb dangerous compounds that may harm organisms that consume microplastics [24]. Furthermore, the physical characteristics of microplastics, such as their size, may have an impact on their toxicity. Due to their probable capacity to move across organisms' cells and tissues, smaller microplastics, including nanoplastics, are thought to be more dangerous [25].

Another research looked at the ingestion of microplastic fibers and microplastic particles by two tiny marine creatures that are significant in the marine food chains of the North Pacific Ocean: Neocalanus cristatus (a calanoid copepod) and Euphausia pacifica (an euphausiid) [26]. Using an acid digestion technique, individual zooplankton were examined, and microplastics were discovered in both species. The encounter rate for copepods was around 1 particle per 34 individuals, whereas the encounter rate for euphausiids was 1 particle per 17 individuals. The preference for bigger food particles by euphausiids accounts for the variation in food size preferences. In addition, the study found that euphausiids ingested fewer microplastic fibers if they were farther from the shore, which is in line with earlier results from seawater samples. Because lower trophic-level creatures can confuse microplastics for food, these findings raise questions about the possible hazards to higher trophic-level species. The study also focuses on the possible effects on salmon populations, predicting that young fish in coastal British Columbia may consume 2–7 microplastic particles per day through the consumption of zooplankton, whereas adult salmon may consume more than 91 particles per day [26].

Microplastics were also discovered in ten distinct fish species during a research in the English Channel. 36.5% of the 504 fish that were tested had plastics in their gastrointestinal tracts. The 184 fish that swallowed plastic were of both pelagic and demersal species, with an average of 1.90 (± 0.10) pieces per fish [27]. Researchers found 351 fragments of plastics using FT-IR Spectroscopy, and the most frequent components were polyamide (35.6%) and rayon (57.8%) [27]. Pelagic and demersal fish did not significantly differ in the amount of plastic they ingested. The finding indicates that marine life generally consumes plastics regardless of their ingestion habit. The study also showed that most swallowed plastics were microplastic particles, defined as those smaller than 5 mm [27]. Figure 2.2 shows the frequency of plastics ingested by different fish species according to different plastic particle sizes.

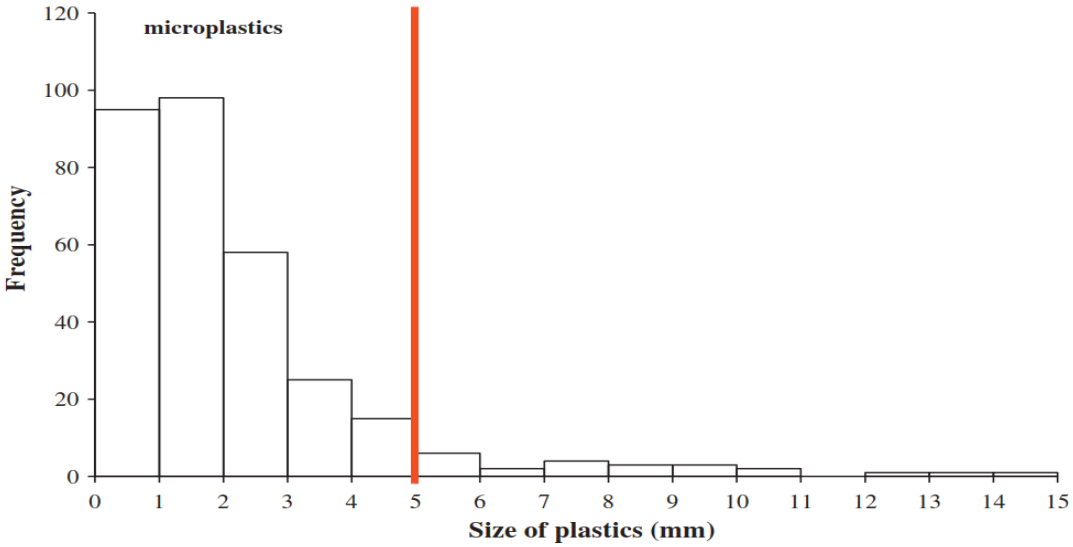

Figure 2.2 Frequency of Plastic Particles ingested by Fish Species according to Particle sizes [27]

The potential migration of microplastics from the environment to organisms, including mammals, has also raised concerns. A research by Ragusa et al. focused on six placentas taken from women who had healthy pregnancies as they looked into the existence of microplastics in human placentas [28]. The investigation found microplastic pieces in these placentas that were between 5 to 10 µm in size and had spherical or irregular forms. Microplastic fragments have been detected in the chorioamniotic membranes, maternal side, and fetal side of four of the studied placentas [28]. The study also looked at these particles' shape and chemical structure. Figure 2.3 presents hypothetical mechanisms by which microplastics can enter human tissues. Mechanism A suggests that microplastics ingested with food can be taken up by M cells in the gut and transported through the lymphatic circulation. Mechanism B proposes that microplastics may penetrate the intestinal lumen through loose junctions, aided by inflammatory states. Mechanism C explains that the upper respiratory tract's thicker mucus layer and ciliated epithelium help clear foreign particles. Mechanism D shows the lower respiratory tract, where microplastics can diffuse through the thinner mucus layer and reach circulation.

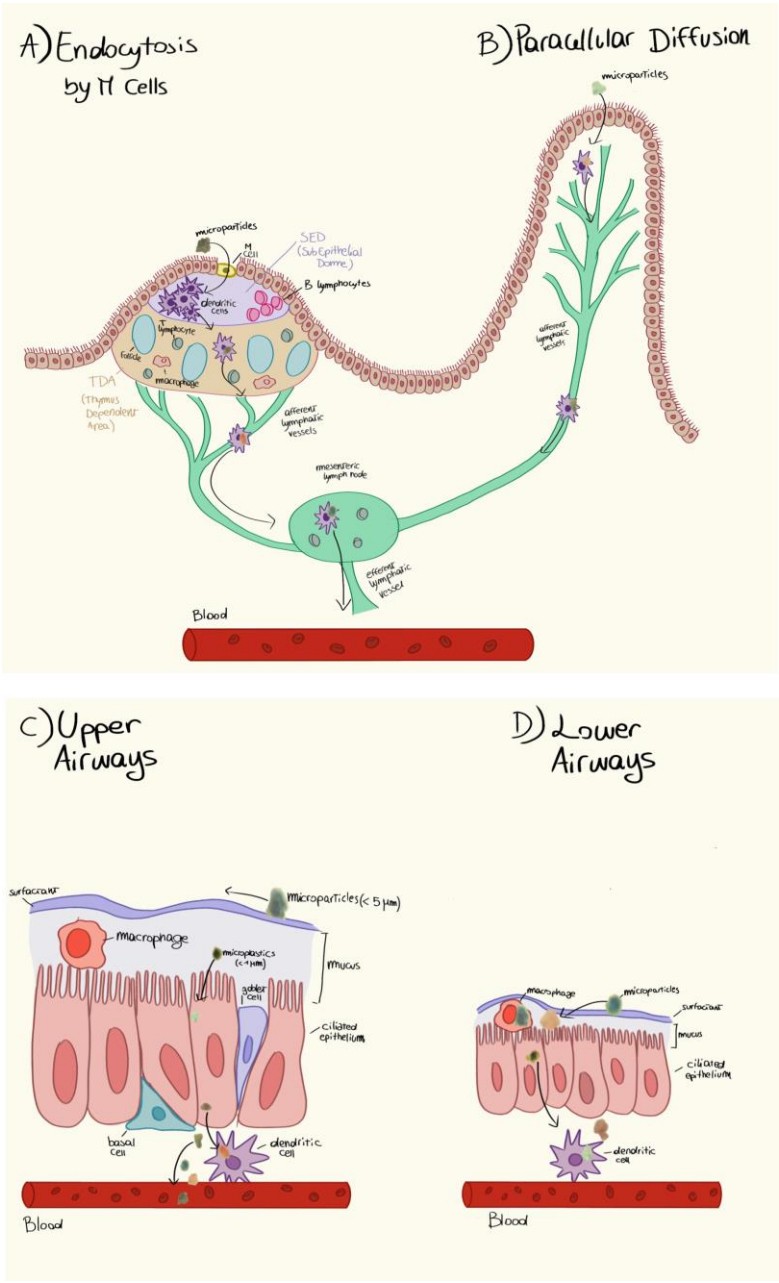

Figure 2.3 Illustration of hypothetical mechanisms for the penetration of microplastics into human tissues [28]

Another team of researchers looked at the potential for ingestion and inhalation of microplastics to have negative health effects in humans. Similarities are potentially found with particulate air pollution, where microscopic particles (<2.5 µm) can enter cell membranes and cause oxidative stress, inflammation, and an increased risk of lung cancer, cardiovascular disease, and respiratory disorders [29]. Whereas, an average eukaryotic cell size ranges from 10 to 100 µm in diameter [30]. Such ability of microplastic particles indicates the potential risk of microplastic ingestion through drinking water might also create a negative impact on the human body. Research

works on human cells in culture, rodents, and aquatic species have provided evidence that microplastics smaller than 10 µm have the ability to migrate from the gastrointestinal tract into the lymphatic and circulatory systems, resulting in widespread exposure and accumulation in various tissues such as the liver, kidney, and brain [31].

A literature review by Wright and Kelly presents an overview of the impact of microplastics on human health [32]. Microplastics can adsorb and concentrate hydrophobic organic contaminants (HOCs) such as polycyclic aromatic hydrocarbons (PAHs), organochlorine insecticides, and polychlorinated biphenyls (PCBs) to a significant degree due to their hydrophobic surface. They also gather heavy metals, including lead, cadmium, zinc, and nickel. Because endogenous chemical additives are included during the production of plastic goods, microplastics may act as carriers of these additives. These additives are prone to leaking into the surrounding media because they are not chemically bonded to the plastic polymer matrix. When microplastics are absorbed and spread to nearby tissues, these pollutants may be discharged. When inhaled or ingested, microplastics can withstand mechanical clearance, resist chemical decomposition in living organisms, and may even get stuck or entrenched. Along with the dosage, one important element that raises concern about their potential hazards is their capacity to persist in the body [32].

2.2 Microplastics Detection Techniques

There are several detection methods to identify and analyze microplastics. However, most of these available techniques require high-tech laboratory facilities. Regardless of the fact that both qualification and quantification studies on microplastics are commonly carried out by researchers using different advanced technologies, there is still no universally accepted detection or analysis technique available for detecting microplastics in aqueous media. [16].

Data collection and processing have been revolutionized by the Fourier transform (FT) approach used in infrared (IR) spectroscopy, which was made possible by reliable and powerful lasers. Modern computers have made it possible for efficient and precise analysis of IR spectrum data thanks to FTIR spectroscopy. In FTIR spectroscopy, the wavelength and intensity of absorption of IR light by a material are measured [33]. The FTIR method is based on the selective absorption of particular wavelengths by the molecular covalent bonds, which results in changes in vibrational energy. As a result of the varied frequencies that different bonds and functional groups absorb, diverse transmittance patterns are generated, which can then be plotted as an FTIR spectrum [34].

Raman spectroscopy is an analytical method that analyzes a sample's vibrational energy modes by using scattered light. The polarization of the molecular electron cloud results from the light photon's fluctuating electromagnetic field when it interacts with a molecule. The molecule is momentarily elevated to the virtual state, a higher energy level, as a result of this interaction. The photon swiftly emits as dispersed light after a brief period of time in the virtual state. Most of the time, the energy of the molecule is unaltered, and the scattered photon has the same energy and wavelength as the input photon. Elastic or Rayleigh scattering is this phenomenon, which governs Raman spectroscopy [35]. For microplastic detection, Raman spectroscopy has been one of the earliest detection methods [36].

Several methods are currently available for detecting microplastics. Each of them has their particular advantages and disadvantages. Table 2 gives an overview of different microplastic detection techniques along with their different characteristics.

Table 2. Traditional techniques for detecting and analyzing microplastics [16]

Method		Methodology	Particle Size Detection Level	Advantages	Disadvantages
Visual Method	Microscopic Counting [37]	Pre-treated samples are examined using microscopy, and the particles are directly counted. The samples are inserted through Petroff-Hausser counting chamber or hemocytometer. This causes the particles in the chamber to be separated and spread almost equally throughout the area. The chamber is placed under an optical microscope to collect visual images which is ultimately used for counting the microparticles.	The stereomicroscope can identify particles as small as a micro-meter in size.	This method allows for quick identification of samples with a high concentration of large microplastics, providing an overview of microplastic abundance.	This method alone cannot determine the nature of the samples, so it should be used in conjunction with other listed identification methods.
Spectroscopic Method	FTIR [38]	Samples are exposed to infrared radiation within a specific range, and the resulting vibrations reveal their composition and molecular structure. Plastic polymers exhibit unique IR spectra with distinct band patterns.	ATR-FTIR can analyze larger particles (>500 µm), while microscopy combined with FTIR can be used for smaller particles (down to 20 µm).	FTIR-based techniques are established, rapid, reliable, and non-destructive. Advanced FTIR imaging, like FPA, enables the quick acquisition of thousands of spectra in a single measurement and	It is crucial for samples to react to IR, and particles smaller than 20 µm may not yield interpretable spectra with sufficient absorbance. Analyzing non-transparent

				reduces the analysis time.	particles is challenging, and specialized and costly instruments require skilled operators for data processing. Factors like biofilm formation and IR-active water affect data interpretation, requiring sample pre-treatment.
	Raman Spectroscopy [39]	When laser light interacts with a sample, it causes a Raman shift in the back-scattered light, enabling the detection of substance-specific Raman spectra.	Microscopy combined with Raman Spectroscopy (RS) is suitable for particles larger than 1 µm and is the only available method for particles between 1 and 20 µm.	Microscopy-coupled RS allows high-resolution analysis of small particles (1 to 20 µm), with minimal interference from water. It is effective for non-transparent and dark particles, enabling fast chemical mapping and automated data processing.	Fluorescence from biological and impurities can hinder microplastic identification with RS. Sample purification is necessary, and selecting suitable acquisition parameters is crucial. Automated micro-RS mapping is still in development, and RS analysis can be time-consuming.
	Scanning Electron Microscopy [40]	By measuring the secondary ions resulting from the interaction of an electron beam with the sample, images of the sample are generated, offering detailed information.	The method enables the analysis of particles ranging from micro-scale and upwards.	This technique allows for the creation of high-resolution images, providing detailed views of the samples.	To conduct the analysis, samples must be coated in a high vacuum environment. However, it does not provide specific identification details.
Chromatographic Method	Thermo-analytical Method (Pyrolysis GC/MS) [41]	Samples are subjected to thermal treatment at room temperature, capturing the released gases for analysis in a GC (Gas Chromatography) column coupled with quadrupole – MS (Mass Spectrometry). The resulting pyrolysis spectra are compared to a database of commonly found plastic types.	This technique is suitable for samples larger than 500 mm, which can be manually handled using tweezers.	The method allows for the analysis of the sample and its organic plastic additives in a single run, eliminating the need for solvents and preventing background contamination. It is a reliable and sensitive approach, supported by a library of spectra data for some widely used polymers.	Each analysis run focuses on a single particle with a specific weight, and the available pyrolysis database covers only selected polymers like polyethylene and polypropylene.

	Liquid Chromatography [40]	The samples are dissolved using specific solvents, and size exclusion chromatography is utilized to measure the distribution of different molar masses. HPLC (High-Performance Liquid Chromatography) analysis is then used for quantification.	To conduct this testing method, a sufficient sample size of several milligrams is required for the chemical extraction process.	The recovery rates for the selected polymers were found to be high.	This method has limitations in determining physical characteristics such as size and is restricted to analyzing specific polymer types like PS and PET. Furthermore, its applicability to environmental samples is limited, and only a small number of samples can be analyzed in each run.
Other Methods	Tagging Method [42]	Microplastic surfaces are coated with a hydrophobic dye, resulting in fluorescence upon blue light exposure.	This visualization method allows for the counting of microplastics, including those at the microscale range.	The technique is simple and offers a quick and affordable way to screen for microplastics. It involves counting the fluorescent particles and potentially identifying them.	It's crucial to consider that the dye may stain other particles, such as organic debris, leading to an overestimate of the actual abundance of microplastics.

Apart from these traditional techniques, researchers have been working on developing more convenient methods to detect microplastics. Asamoah et al. developed a portable optical sensor prototype specifically designed for identifying translucent microplastics in freshwater environments. They employed commercial PET plastic, known for its transparency, and LDPE plastic, which has a translucent property. These plastic samples were combined and examined using a handheld optical device powered by a battery and equipped with a CCD (Charge-Coupled Device) camera. By utilizing the measurement principle of the handheld device along with the imaging capabilities of the CCD camera, they achieved successful detection and evaluation of curved plastic items. The exceptionality of this prototype lies in its capability to detect microplastics on non-flat surfaces, making it a valuable tool for nonplanar sample analysis [43]. Using a similar optical technique and combining it with Raman Spectroscopy, Iri et al. developed a prototype device utilizing an optical system to detect microplastics in water. This low-cost system is based on a Raman spectrometer and costs around $370. It consists of components such as a collimated laser (5 mW), a sample holder, a notch filter, a diffraction grating, and a CCD sensor, all integrated into a 3D printed case. Through their experiments, they demonstrated that this system is capable of detecting microplastics in water even at concentrations as low as 0.015% w/v [44].

In contrast to spectroscopic methods, the thermal analysis approach is utilized for assessing any form of changes in the chemical and physical characteristics of substances based on their thermal stability. By assessing the thermal stability or thermal degradation of polymers, thermal analysis can provide information on their composition [45]. Another study aims to investigate the movement mode of microplastics and develop a method for detecting low concentrations of microplastics using surface plasmon resonance (SPR). The researchers prepared 20-micrometer microplastics by grinding and filtering and studied their characteristics using SPR. Chromatographic analysis revealed that the elution time of microplastics depends on their surface charge, while estrogen receptors (ERs) play a supporting role. The SPR sensorgram showed distinct patterns of microplastics, this indicates their rolling movement on the ERs. The analysis demonstrated that the number of microplastics on SPR had a linear relationship with the response unit, allowing for quantification. [46].

2.3 Theories

This chapter explains some of the theories of technology and analysis that were utilized for this project. The chapter also explains some of the basic principles that were utilized for this project.

2.3.1 Electrochemical Sensor

A sensor can be defined as a device or a system that detects and responds to a specific physical phenomenon or a certain change in the surrounding environment and converts these changes into an electrical signal. This electrical signal is then received and analyzed by other parts of the system for further processing, conversion, or analysis of the signal to make it more recognizable. Sensors are most commonly used for measuring or monitoring various parameters such as temperature, humidity, pressure, chemicals, materials, etc [47].

An electrochemical sensor can be defined as a device or a system that carries out the detection, and quantification of a certain chemical or material through an electrochemical reaction. An electrochemical sensor usually consists of electrodes made of conducting materials (gold, silver, carbon, etc.) that also work as the interface which interacts with the electrochemical reaction of the electrolyte. The electrochemical sensor produces a computable signal according to the electrochemical reaction that takes place in the experimented sample. This signal is later analyzed for further verification of the targeted analyte in the sample [48].

An electrochemical sensor usually consists of three electrodes: Counter Electrode (CE), Working Electrode (WE), and Reference Electrode (RE). The counter electrode plays the role of the

source or sink of electrons depending on the reactions. The reference electrode maintains a stable voltage difference from the working electrode when an electrochemical reaction takes place. The working electrode is the primary electrode of an electrochemical sensor where the electrochemical reaction of interest occurs [49]. Figure 2.4 shows the screen-printed electrodes (ZPS HYP-000-00150, Zimmer & Peacock AS, Norway) that were used in this project. The CE and RE are made of Silver/Silver Chloride (Ag/AgCl) materials, while the working electrode is made of Carbon. The electrode materials are printed on a PET sheet that is 250 µm thick [50]. Figure 2.5 shows all dimensions of the electrodes.

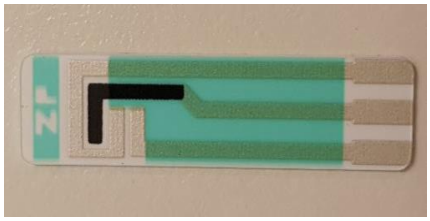

Figure 2.4 ZP Hyper Value screen printed electrodes [50]

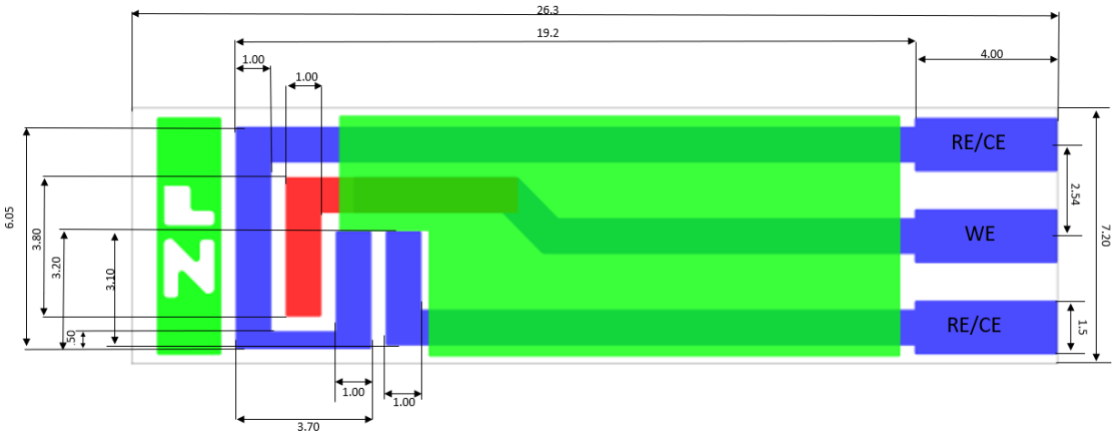

Figure 2.5 Schematic design with dimensions of the ZP hyper value screen printed electrode. All dimensions are in millimeters (mm) [50].

2.3.2 Potentiostat Device (PalmSens4)

In order to carry out electrochemical measurements with sensors, electrochemical instruments like potentiostat devices play a crucial role. The potentiostat is a device that controls the applied potential on the electrodes of the sensor for carrying out electrochemical measurements. On the other hand, a galvanostat controls the applied current on the electrochemical cells [49].

2.3.3 Fast Amperometry

While amperometry analysis can be defined as an electrochemical technique for measuring the current flow through an electrode over a defined period of time when a stable voltage is applied [49], fast amperometry (FAM) is known for its high sampling rates where the amperometry analysis is carried out in a very short time [51]. The fast amperometry analysis helps to measure very small changes in a relatively shorter time frame, which is helpful for analyzing electrochemical reactions that take place very quickly. Figure 2.6 represents how the signal is applied to PalmSens4 device for carrying out the FAM analysis. The figure also shows that in each $t_{interval}$ timespan, the electrochemical change is recorded through the signal and this makes the FAM analysis a suitable method for this project.

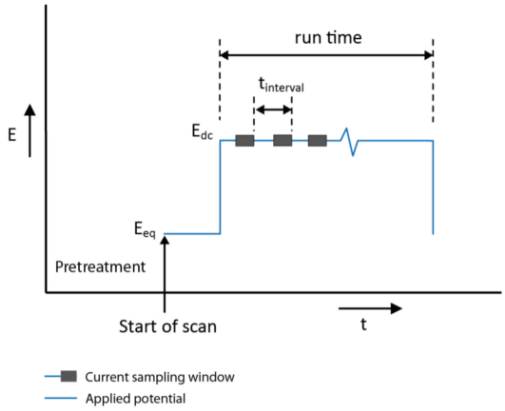

Figure 2.6 Signals in PalmSens4 device during Fast Amperometry Analysis [51]

2.3.4 Cyclic Voltammetry

Cyclic Voltammetry is another electrochemical measurement technique that mainly utilizes voltage waveform as an input to measure the current response. The voltage is usually applied linearly increasing or decreasing with time in order to record the resultant current response. The cyclic voltammetry analysis is usually used for studies that involve electron transfer kinetics, redox potentials, and also to analyze analyte concentrations [49]. If the applied voltage is 'E' during the time 't', then the scan rate 'v' in a cyclic voltammetry can be represented with the following equation.

$$v = \frac{\partial E}{\partial t} \qquad (1)$$

Figure 2.7 represents a typical cyclic voltammetry analysis in terms of voltage vs time. During an electrochemical measurement with cyclic voltammetry, the applied voltage is kept at a state where no electrochemical reaction takes place (Evertex1). Then, the voltage is applied linearly in the

direction of the formal potential of the species (E0') that is being examined. The linear voltage gets increased continuously until reaching the set voltage. When the applied voltage reaches the set voltage or vertex potential (Evertex2), it is then inverted to create a reverse voltage sweep. The applied voltage ultimately returns to the initial voltage after completing the full cycle through this forward and reverse voltage sweep. In PalmSens4, the two vertex points can be selected before running the measurement and thus, the voltage would sweep between these vertex points [52].

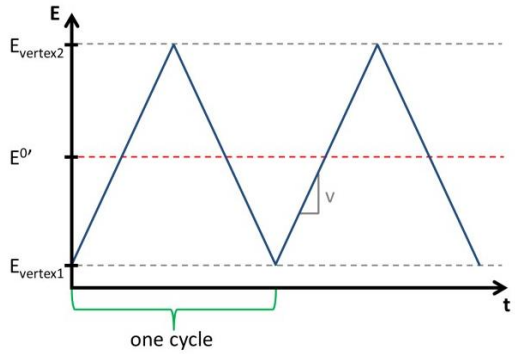

Figure 2.7 Applied voltage vs time in cyclic voltammetry analysis. Here, Evertex = vertex potentials, E0'= Formal voltage of the investigated species, and V = scan rate [52]

During cyclic voltammetry, the oxidation or reduction causes the current flow. A perfect condition results in the sigmoidal current. However, the real-life scenario reveals that diffusion limits the current flow. Increasing the voltage results in the increment of the current flow until it reaches the diffusion limit which ultimately forms a peak. Subsequently, the reverse sweep goes through the events in a reverse manner. The voltammogram (curve of I vs E) determines the parameters faster by plotting the E vs t and I vs t on top of each other where the time (t) is common in both cases, producing a compact I vs E curve as shown in Figure 2.8 [52].

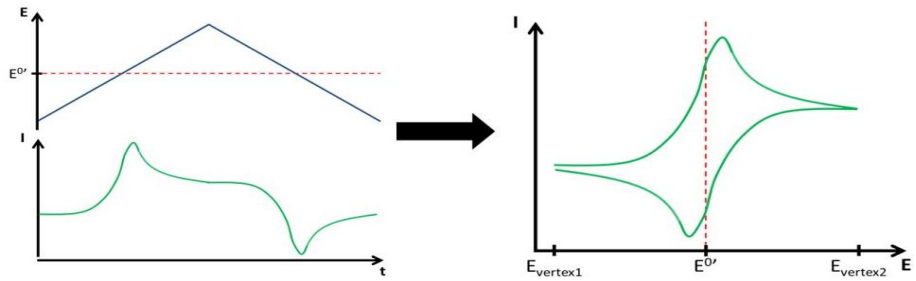

Figure 2.8 Combination of E vs t and I vs t curve to represent the I vs E curve in Cyclic Voltammetry [52]

CV analysis of a reversible redox couple on an inert electrode, such as carbon, results in a specific 'duck-shaped' plot, as a signature for this reversibility. Significant deviations from this indicate other processes are at play, such as a less inert seed layer being exposed to the test solution [53]. Figure 2.9 shows a typical 'duck-shaped' CV curve of a carbon electrode. The current turns positive signifying an oxidative electrochemical reaction at the WE. The current grows stronger as the voltage rises until it reaches a peak known as the anodic peak. Due to the presence of reactants close to the electrode at this time, the oxidation process is happening at its fastest pace. As the voltage rises further, the supply of reactants becomes diffusion-limited, resulting in a lower and occasionally constant value for the current. The oxidized species can be reduced by switching the direction of the voltage sweep, which causes a cathodic peak to be observed [49], [53], [54].

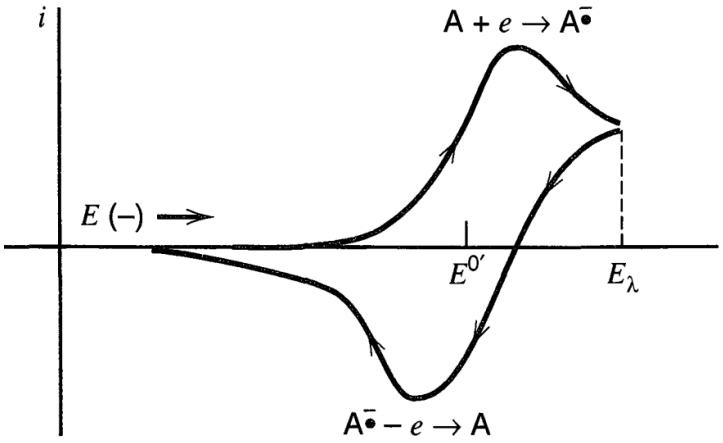

Figure 2.9 A typical 'duck-shaped' curve resulted from a CV analysis on carbon electrode [49]

From such comparison between the obtained CV curves, it is usually a practice to identify a carbon electrode or whether an electrode has proper carbon coating or not, as the carbon electrode tends to provide the signature 'duck-shaped' curve from the CV analysis.

2.3.5 Impedance Spectroscopy

Electrochemical Impedance Spectroscopy (EIS) carries out the measurement of impedance depending on the AC voltage frequencies. Considering two periodic waves of voltage and current, when they have the same frequency, there is a time shift between these waves as one wave is generated from the other. This phase shift is annotated with Φ and considered as a vector of the sine function in a polar coordinate system. The ratio of the voltage and current amplitude represents the impedance. However, the impedance is a complex number. The impedance is expressed with Z as

the vector's length and Φ as the angle. The PalmSens4 measures the impedance by applying a potential wave to the WE (Working Electrode) while recording the current wave. The potentiostat calculates and plots the Z, Φ, Z', and Z" from these waves as shown in Figure 2.10 [55].

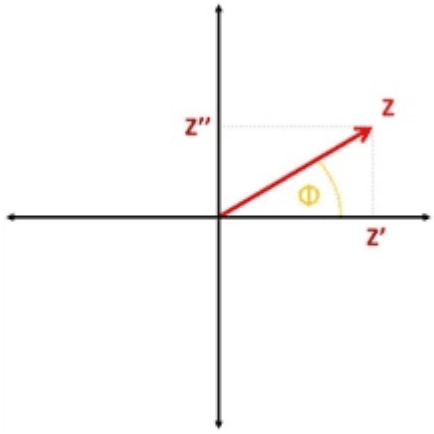

Figure 2.10 Impedance plot of Z (resistance), Z' (real), Z" (Imaginary), Φ (angle) [55]

2.3.6 Oxidation reaction on carbon electrode

Carbon electrodes have become very popular in electrochemical analysis for their greater advantage in multiple aspects. The carbon electrodes have the potential to replace other metals for performing as the working electrode in the electrochemical cell due to their appropriate electronic properties, hydrophobic attributes, high conductivity, thermal stability, and chemical stability [56]. Researchers have revealed certain advantages of using carbon electrodes to detect the oxygen reduction reaction in electrochemical analysis. The oxygen species are adsorbed on the carbon surface which results in the oxygen reduction reaction. Therefore, oxidation reactions taking place on the surface of the carbon electrode may also form surface oxides as well as other functional groups [57], [58]. Equation 3 takes place on the surface of the carbon electrode usually when oxygen comes into contact with it. Here, the oxygen molecules attain electrons in the water solution, which ultimately produces hydroxide ions.

$$O_2 + 2H_2O + 4e^- \rightarrow 4OH^- \qquad (3)$$

In addition to the electrochemical aspects of carbon electrodes, it also costs very little compared to other conductive materials like gold, silver, copper, etc. This is also another reason for carbon being used so widely in electrochemical sensor development.

2.3.7 Fast Fourier Transform (FFT) Analysis

The Fast Fourier Transform (FFT) analysis interprets frequency-related characteristics from a signal by computing the Discrete Fourier Transform (DFT) of the signal. Through this analysis, the breakdown of the time domain signal is carried out to represent its frequency domain signal. This calculation is conducted by converting the time domain signal into multiple sinusoidal signals where each of them represents a certain frequency level. This phenomenon enables the detection of the dominant frequency levels and also their amplitude in the signal. By analyzing a signal's characteristics, the FFT enables the identification of significant attributes like periodicity, harmonic patterns, and prominent frequency spikes. In summary, the FFT analysis calculates the average frequency components of a signal throughout the entire time duration from which the signal was attained [59], [60]. A visual representation of FFT analysis is shown in Figure 2.11. Here, the time domain signals are converted to frequency domain signals where each time domain signal's specific characteristics on a certain frequency zone and amplitude are interpreted through the FFT analysis. It is to be pointed out that a certain time-domain signal has a frequency level with a variation in amplitude compared to other time-domain signals.

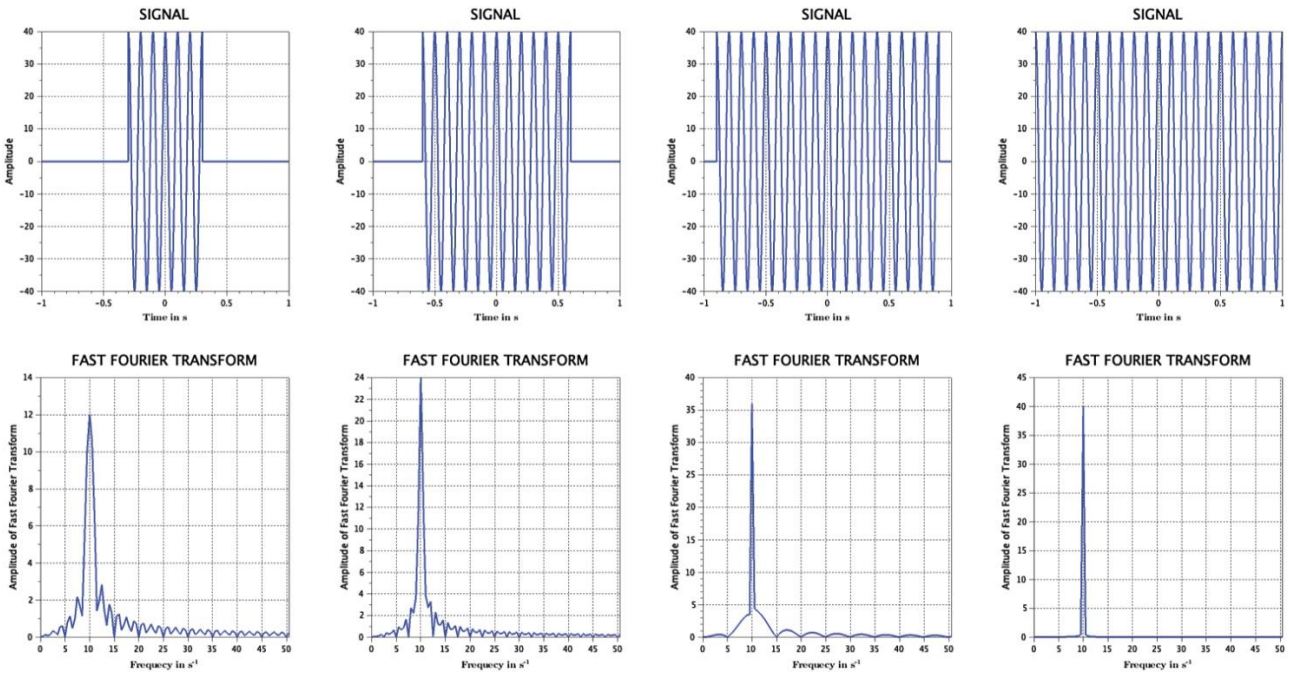

Figure 2.11 Conversion of time-domain signal to frequency-domain signal through FFT analysis (top row plots are the time-domain signal and their corresponding frequency-domain plots are shown below them in the bottom row) [59]

3 Methodology

The route to developing the electrochemical microplastic sensor for this project has been quite dynamic and unveiled new findings along the way. Even though the inspiration for the initial starting points in different stages of this project has mostly been taken from the work carried out by Shimizu et al. [6], alternative methods have also been examined and established for proceeding with this research work due to different kinds of challenges and limitations. This chapter describes the methodology of this research work chronologically.

3.1 Equipment and Materials

Table 3 represents a complete list of equipment and materials that were used for this research work. Most of the equipment and materials were provided by Z&P in their laboratory facilities. A few tools and equipment were also facilitated by USN.

Table 3. List of equipment and materials used for this project

Categorized Group	Name of the Equipment or Material
Chemicals and Microparticles	Carbon Paste (C2180626D6, SunChemical, United Kingdom)
	Microplastic Particles (72986-5ML-F, Sigma Aldrich, Germany) [61]
	KCl (Sigma Aldrich, Germany)
	Na2SO3 (Sigma Aldrich, Germany)
	MgSO4 (Sigma Aldrich, Germany)
	$Fe(CN)_6$ (Sigma Aldrich, Germany)
	Nail Polish
	NaCl Salt
	FeCN Solution (Wafer Mapping Solution)
Electrodes	ZP Hyper Value Screen Printed Electrode (ZPS HYP-000-00150, Zimmer & Peacock AS, Norway)
Cleaning tools	DI Water
	N2 Gas
Laboratory Instruments	PalmSens4 Device
	5-pin Connecting Cable compatible with PalmSens4
	Beaker (5ml, 10ml, 20ml, 50ml, 1L)
	Magnetic Stirrer
	Ultrasonic Bath Chamber

	Oven (Heraeus Instruments)
	Weighing Scale (ABT 120-4NM)
	Electrode Holder Stand
	Pipette
	Hemocytometer
Personal Safety Equipment	Surgical Hand Gloves
	Lab Coat
	Surgical Face Mask
High-tech Lab Instrument	Optical Microscope (Olympus IX51/TH4-200)
	Scanning Electron Microscopy (Hitachi SU 3500)
Software and Programming Language	PSTrace 5.9
	OriginPro 2023
	Djuli 1.6.6
	Julia Programming Language 1.8

3.2 Aqueous Test Solution

The preparation of the aqueous solution was considered from various aspects of this project. A trade-off between real-life scenarios and a controlled laboratory test setup mainly drove the outcome of preparing the aqueous test solution for the experiments. Deionized (DI) water itself couldn't be used as all of the minerals and ions are absent in it and it also provides very generic signals in fast amperometry analysis due to its high resistivity [62]. On the other hand, typical tap water contained minerals and ions like cations (sodium, calcium, iron, copper) or anions (chloride, sulfate); but the amount of any of these ions are unknown. In addition, in the attempt to create a similarity with ocean water, adding typical NaCl salt to DI water also wasn't efficient as the amount of salt was not measured properly. Therefore, none of these three approaches could be considered a controlled test setup. Finally, in order to create a more controlled test setup with known measurements of ions that is suitable for the experiments, the aqueous test solution was prepared as Shimizu et al. [6] did for their experiments as it had enough ions for completing the circuit between the electrodes in the aqueous solution while maintaining the electrical neutrality and pH neutrality.

The measured 1.491 grams of KCl was added to 1L DI water to create the 20 mM aqueous solution and stored at room temperature for further experiments. For each experiment, microplastic particles were added to the aqueous solution that was collected in a beaker to create the solution with microplastics. Another beaker containing KCl solution without microplastic particles was used as

a control. The microplastic sample was bought from Sigma Aldrich for the experiments of this project [61]. The sample was polystyrene-based microplastics that were produced for R&D purposes. The aqueous suspension was a total of 5 ml that had 10% solids. The particle size was 10 µm in diameter with a standard deviation of <0.2 µm and a coefficient variation of <2%. Around 1.05 g/cm^3 particles were produced for the suspension. The sample needed to be stored at 2-8° C temperature. In this project, the concentration of microplastics was added to a 10mL beaker containing the aqueous solution. Commonly the microplastic suspension is collected in 10 µL, 20 µL, 30 µL, and 40 µL. Therefore, the concentration of microplastics can be represented in volume fraction (v/v) as a percentage of solid per 10 mL aqueous solution as per the following calculation:

For 10 µL suspension, ((0.1*0.01)/10) * 100 = 0.01%

Similarly, for 20 µL = 0.02%, for 30 µL = 0.03%, and for 40 µL = 0.04%.

For each aqueous solution of both conditions (with microplastics and without microplastics), the measurements were carried out in either stirred condition or unstirred condition. At the later stage of the project, the stirring setup was replaced with an ultrasonic bath system to ensure a homogeneous suspension.

3.3 Electrodes: Modification, Fabrication, and Verification

One of the crucial parts that were realized and addressed in this project was the development of the working electrode. According to Shimizu et al. [6], a carbon fiber microwire electrode was used that was 7 µm in diameter and 1mm in length. The primary plan was to use the ZP-HV-SPE as the main sensor to detect the microplastics in the solution. However, with the progress of the project, it was realized that the size of the working electrode needed to be as small as possible to detect such tiny particles as microplastics. The rationale behind this idea takes into account that the generic background noise scales with the electrode size, whereas the signal generated from the microplastics hitting the sensor remains constant. In that respect, the noise floor will ultimately be reduced and thereby improve the signal-to-noise (SNR) ratio so that the “impact” event is seen.

3.3.1 Working Electrode of screen printed electrode

Initially, the screen printed electrode (ZP-HV-SPE) was used in the experiments without making any modification to its working electrode. This result did not produce a significantly different signal when comparing recordings taken in the presence and absence of microparticles. The working electrode of screen printed electrode had a width of 1mm and a length of 3.80 mm as shown in Figure

2.8. From the resultant signal, it was suspected that the working electrode size was too large to recognize the microplastic particles impacting its surface and it was only collecting generic signals (noise) inside the solution. Based on this assumption, the printed working electrode on the PET was stripped off to reduce the size of the working electrode. This 'modified screen printed electrode' was used for a few measurements and the resultant signal appeared to be much improved than the previous condition with the original screen printed electrode (see section 4.1). This finding established the concept to reduce the size of the electrode (and thereby the noise) as much as possible, which paved the way for further development of the working electrode. Figure 3.1 shows the modified screen printed electrode with a surface area of 1mm^2 being used in one of the measurements in the aqueous solution.

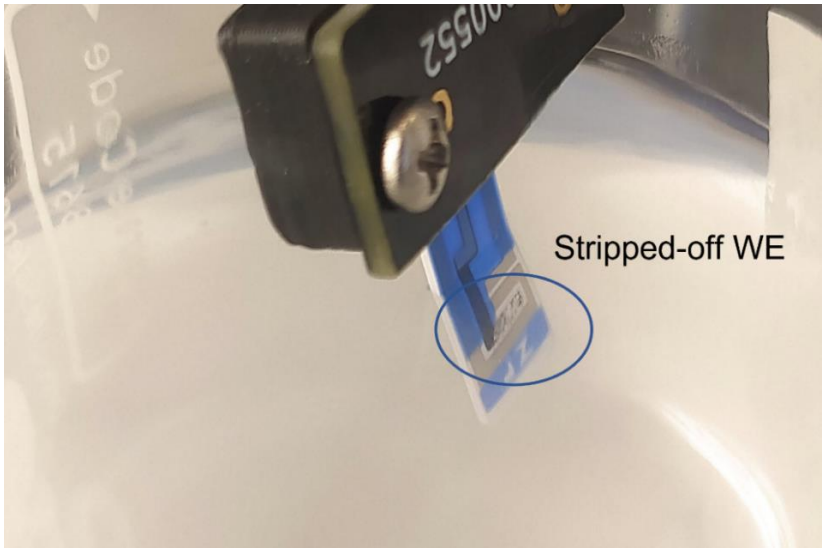

Figure 3.1 Modified ZP-HV-SPE by stripping off the WE and reducing its size

3.3.2 Wire based (working) electrodes (Type-1, Type-2, and Type-3)

After establishing the fact that the WE size plays a significant role in the detection of tiny microplastic particles, it was necessary to develop a working electrode with a very low footprint. So, the focus shifted towards developing "needle" type wire electrodes with a narrow diameter in the sub-mm regime and a length in the mm regime. Thus, a single strip of conducting wire was used as the basis for electrode manufacture. These were considered to have an effective cylindrical shape permitting impact from microparticles in all directions. The ZP-HV-SPE couldn't avail this feature as the electrodes are printed on a PET sheet, permitting impacts of particles from one side only. Therefore, considering the fact that the aqueous solution would carry particles from all directions, the cylindrical-shaped electrode was taken as a reference shape of the WE.

In order to make the desired working electrode, a typical silver wire or copper wire was taken, and the outer rubber insulator was stripped off. Some wires have multiple threads of conductor strings spiraled together, so only one string was taken from such wires. These wires were taken from the in-house collection of the ZP laboratory. As the WE needed to be a carbon electrode, the silver or copper wire string had to be coated with carbon. Carbon electrode was chosen particularly for its better oxidation reaction as stated in Section 2.3.6 and also because of the fact that the use of carbon electrode provided fruitful results in the experiments conducted by Shimizu et al. [6] for detecting microplastics using the 'impact concept'.

To develop a carbon electrode, the same kind of carbon paste that was used for printing the WE of screen printed electrode (ZP-HV-SPE) was obtained. The single string of wire (silver or copper) was first polished thoroughly with laboratory tissue. Then it was cleaned carefully with DI water and dried using nitrogen gas without touching the targeted area. Then the string was dipped inside the carbon paste for 5 seconds from a 90-degree angle at a length of approximately 1 cm and then pulled back off from the paste. This short process was counted as 1 dip. After each dip, the string was kept at room temperature for at least 10 seconds to let the carbon paste that was stuck with the targeted area be dried at an initial level. Making any sort of contact with the carbon-coated area was completely avoided. It was noticed that multiple dips after a certain interval time (i.e. 10 seconds) would increase the coating depth. Mostly the strings would go through only 1 dip. However, if the angle of dipping somehow gets inaccurate or the structure of the string causes any complications in making a proper coating, multiple dippings were carried out to ensure that the entire targeted area of the string was properly coated with carbon paste and no spot was left uncovered, especially on the tip of the string. After making the coating around the targeted area of the string, the strings were inserted into the oven for baking at a higher temperature to make the carbon coating permanently dried. At the initial stage of the project, the coated strings were kept inside the oven for 15 minutes at a temperature of 40° C. This condition sometimes causes the carbon coatings to get peeled off if any physical contact with solid objects was made accidentally and this causes the verification analysis to produce errors. Therefore, the baking conditions were later changed to 40 minutes at 95-100° C temperature. As the temperature of the oven increases gradually from room temperature to the targeted temperature, the initial time phase that required the temperature to rise was considered to be left out to be marked as baking time, and only the baking time at the targeted temperature was counted.

Based on the diameter of the metal wire found and used in this project, they were named “Type-1”, “Type-2”, and “Type-3” electrodes after the carbon coating procedure. Here, Type-1 has the largest diameter, Type-2 has a lower diameter than Type-1, and Type-3 has the lowest diameter among these 3 types of electrodes. The resultant diameters of the electrodes before and after carbon coating is presented in Table 4 of Section 4.2.1. After dipping, coating, and baking, each new electrode went through a verification process to ensure that the carbon coating was properly covering the entire surface area of the conductor string and that no spot was left uncovered on the targeted surface area of the electrode. This procedure was done by running a cyclic voltammetry (CV) analysis with FeCN solution, also known as the wafer mapping solution. Only the electrodes that resulted in the signature duck-shaped plot in the CV analysis as explained in Section 2.3.4, were then used for the next step of the project for measurements.

3.3.3 Type-4 Electrode

After acquiring better results with Type-3, it became apparent that if the electrode diameter was further reduced, the results would have the potential to become more accurate. At such a stage, conducting fibres with even lower diameter was obtained from electrodes used to facilitate electrophysiological measurements in the eye (Figure 3.2). The conductor strings were used for making the Type-4 electrode following the same procedure as before by cleaning, dip coating, baking, and verification through CV analysis.

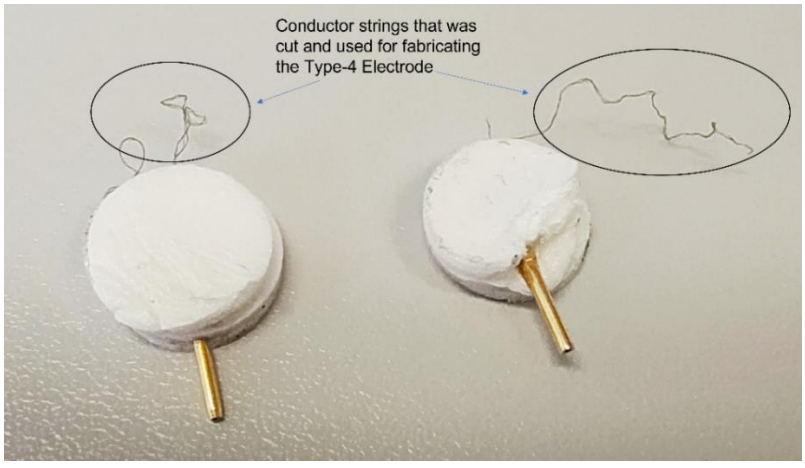

Figure 3.2 Conductor strings that were used for making the Type-4 Electrode

As the fibre strings were very short and limited, only a small length (approximately 5 mm) of the fibre was cut from the main body to make the electrode. However, the challenge was that the fibres were too short in length to connect to an alligator clip from the PalmSens4 device’s cable and

insert the rest of the electrode within the aqueous solution. To solve this issue, about 1-2 mm length of the fibre was attached with a thin copper tape that worked as the extended conductor of the fibres. Then the alligator clip from the PalmSens4 device's cable could hold on to the copper tape body and the free part of the fibre could work as the electrode in the aqueous solution. Due to its lower diameter and good conductivity, Type-4 resulted in much better accuracy to detect the impact signals (see Section 4.3.3). Thus, the Type-4 electrode continued to be used for the rest of the measurements in the project.

3.4 PSTrace Analysis Setup

The main software used in this project to carry out the measurements and to detect signals, was the PSTrace (version 5.9). The software is used for controlling the PalmSens4 device. For this project, there were mainly two types of analysis done most frequently: Fast Amperometry, and Cyclic Voltammetry. These two analysis were carried out to establish the "impact concept". However, Electrochemical Impedance Spectroscopy (EIS) was also carried out as an additional method for detecting the presence of microplastics. The reason is that microplastics are dielectric particles that will replace an equivalent volume of conducting electrolyte when present, and thereby increase the overall solution resistance. Also, the electrode will change its capacitive behavior if microplastics attach or are getting adsorbed onto its surface. Such changes will be visible in the EIS. In addition to the Fast Amperometry analysis, the chronoamperometry analysis was also carried out in some measurements to understand if chronoamperometry analysis had any significant advantage here or not. Also, Multi-Step Amperometry was carried out for verifying the electrochemical reaction taking place on the electrode. The main settings of these analyses in PSTrace were fixed as following:

- Chronoamperometry:

  Current Range = 1nA to 10 µA
  Equilibration time = 10 s
  DC potential = -0.4 V
  Time interval = 0.0005 s
  Run time = 10 s

- Multistep Amperometry:

  Current Range = 100nA to 10 µA
  Equilibration time = 0 s
  Interval time = 0.1 s
  Cycles = 12
  Level = 2
  Potential level 1 = -0.5 V for 10 s
  Potential level 2 = 0.65 for 10

(c) Impedance Spectroscopy:

Current Range = 100 pA to 1 µA
Equilibration time = 10 s
DC potential = 0.0 V
AC potential = 0.01 V
n frequencies = 31=10/dec
Maximum frequency = 5000 Hz
Minimum frequency = 5 Hz
Minimum sampling Time = 0.5 s
Minimum sampling Time = 5.0 s

3.4.1 Fast Amperometry Analysis setting in PSTrace

For the Fast Amperometry Analysis, the aim was to keep the operating current range for the electrodes as low as possible. However, depending on the electrodes, aqueous solution, the particles contained in the solution, and the length of the electrode submerged inside the solution, the current range sometimes pushes to overload or underload conditions. At the initial stage, the current range was chosen to be in the range of 10 nA to 1 µA depending on the condition of the experiment setup. It is to be noted that the fast amperometry analysis allows only one current range to be fixed. At the later stage of the project, the current range was aimed to be kept constant in every measurement as 100 nA. The DC voltage was kept at -0.4 V in most cases as the oxidation and reduction reaction occurs within the -0.2 V to -0.7 V range as per Shimizu et al. [6]. The sampling frequency or the time interval for every scan was kept at 0.0005 s or 0.05 ms. This sampling frequency was fixed according to Shimizu et al. [6] as well. At the initial stage of the project, this scan rate was kept at 0.05 s mistakenly, but it was corrected later on. The analysis setting in PSTrace for Fast Amperometry analysis is as follows:

- Fast Amperometry:

  Current range = 100 nA

  Equilibration time = 0 s

  Potential equilibration = 1 V

  DC potential = -0.4 V

  Time interval = 0.0005 s

  Run time = 10 s

3.4.2 Cyclic Voltammetry Analysis setting in PSTrace

The cyclic voltammetry analysis was mainly run as a verification process to ensure that the electrodes had proper carbon coating as explained in Section 2.3.4. The current range for the cyclic voltammetry analysis was kept in the ranges of 1 nA to 1 µA. The peak voltages were 0.5V and -0.5, with a step voltage of 0.01 V, and a scan rate of 0.05 V/s. The scan starts from 0 V and it finishes at 0 V as well after a complete scan. The analysis setting in PSTrace for Fast Amperometry analysis is as follows:

- Cyclic Voltammetry:

  Current range = 1 nA to 1µA

  Equilibration time = 0 s

Potential begin = 0 V

Potential vertex1 = 0.5 V

Potential vertex2 = -0.5 V

Potential step = 0.01 V

Scan rate = 0.05 V/s

Number of Scan = 1

3.5 Electrode insulation (Nail Polish)

One of the techniques used for reducing the electrode exposure to the aqueous solution was by insulating the electrode with nail polish. As nail polish works as a good insulator [63], it was used in one of the experiments in this project to reduce the surface area of the Type-2 electrode in order to test the method whether the insulation could be a feasible option in the experiments or not. Furthermore, the Type-2 electrode was inserted through a pipette tip to reduce the exposure to aqueous solution. The nail polish was helpful in this case to reduce the exposure size of the electrode that comes out of the pipette tip. However, it's difficult to make an accurate coating with nail polish to leave a precise and measured area exposed. As this coating with nail polish was carried out in hand, sometimes the electrodes get overcoated. To remove some part of the nail polish covering the electrode, acetone was used as a remover. Even though acetone removes the nail polish from a certain area that it gets in contact with, it also affects the carbon coating beneath it and damages the carbon coating too. As a result, the metal beneath the coating gets exposed, which ultimately makes the electrode lose its validity to be used in the experiments. For these reasons, the electrode insulation concept was not further pursued, and the insulation was applied to no other types of electrodes.

3.6 Experimental Protocol

Every measurement carried out in this project emerged through iterative trial and error. Such practice finally developed an experimental protocol that was followed to fabricate the electrodes and carrying out the experiments. Figure 3.3 shows a complete block diagram explaining the different steps of the experiments. When there is no need to fabricate a new electrode as a previously fabricated electrode can be used in an experiment, the old electrode is simply cleaned with DI water in an ultrasonic bath and then dried with nitrogen gas. The aqueous solution containing microplastics was re-used for a few days to avoid producing waste and to reduce consumption, as the suspension

amount was limited. However, after each week interval, the microplastic solution was treated as a non-toxic chemical waste, and the microplastic waste was disposed of by separating them in a waste container and labeling it as per the guidelines following the laboratory health and safety protocol. As the microplastic particles wouldn't lose their characteristics over time in the KCl solution it was stored in a fridge at a temperature of 2-8° C. Therefore, the reusability of the microplastic solution was a valid aspect of this project. To carry out the measurements, the RE and CE of ZP-HV-SPE were connected with the PalmSens4 potentiostat, and the fabricated carbon-coated electrode was connected as the WE with the device. The aqueous solution was taken in a beaker in a volume of 10 mL usually and the electrodes were held with a lab stand in such a way that the RE and CE got completely submerged in the solution and the WE are submerged at a minimum level (approx. 0.5 mm to 1 mm). Figure 3.4 shows a typical setup for an experiment in this project.

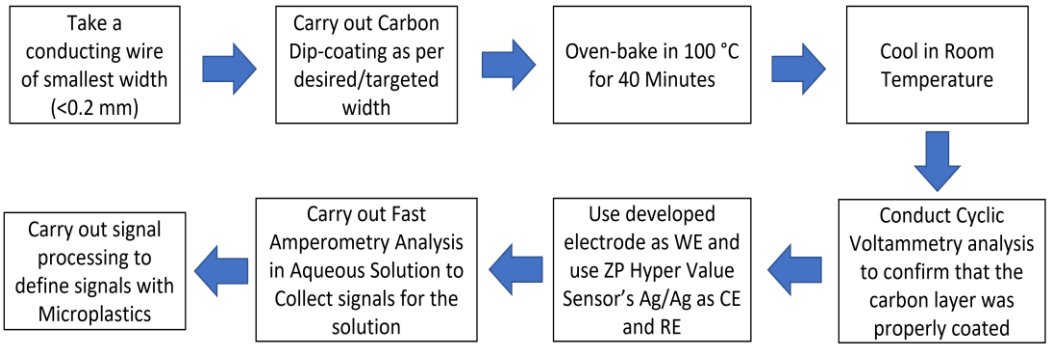

Figure 3.3 Block diagram showing the sensor fabrication and experimental protocol

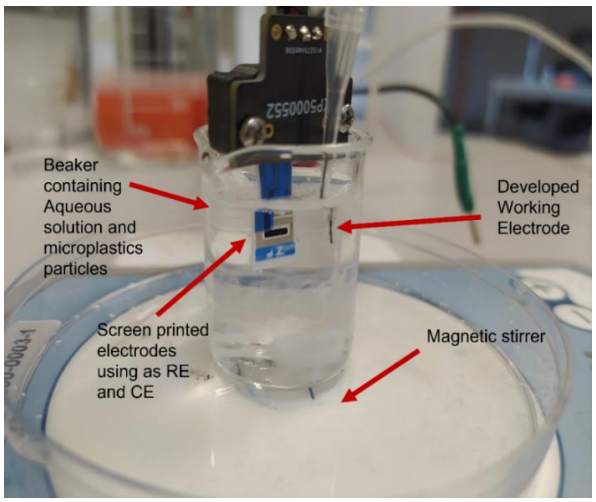

Figure 3.4 Conducting a measurement in the aqueous solution with a Type-2 electrode immersed in a 10 mL beaker on top of a magnetic stirrer

3.7 Verification of the impact experiment

In order to verify whether the electrodes can detect the impacts, an experiment with larger plastic particles was carried out. A substantial amount of “dummy” particles were made from a PET sheet by cutting a portion of it into very little pieces of around 20-30 mm diameter. The size of the particles was approximately equal to or a bit larger than the Type-1 electrode’s diameter size. These particles were visible to the naked eye, and they were released into the aqueous solution and subjected to stirring. The experiment was carried out using a Type-2 electrode. The particles were seen to be making impacts with the Type-2 electrode when it was being stirred, and the resulting signals were recorded. After verifying that the electrodes can actually detect the impacts of particles as shown in Section 4.3.1, further experiments were conducted with real microplastic particles.

3.8 Noise Identification and Mitigation

One of the novelties of this project was that the microplastic impact would be seen as noise among the acquired signals from the measurements. Therefore, there is periodic noise, instrumental noise, external environmental noise, and noise generated from the impact of the microplastic particles with the working electrode. Therefore, it was vital to understand where these undesired noises were coming from and how to minimize them as much as possible.

3.8.1 Magnetic mixer

The aqueous solution was stirred in half of the total number of measurements carried out in this project. The stirring condition was used to make the microplastic particles in the aqueous solution have rapid impacts on the electrodes. However, this method creates noise that is also not repeatable at the same RPM in every case as the magnetic stirrer creates an undefined stirring rate. A metal stir bar immersed in the liquid spins inside the beaker due to a rotating magnet below the beaker as shown in Figure 3.4. Although the magnetic stirrer has the option to increase the speed or decrease the speed of stirring, it does not remain constant always. Also, the height and position of the beaker on the magnetic stirrer cause variations in the stirring quality.

To mitigate these flaws, the beaker is always placed at the centre of the magnetic stirrer and the stirring speed is always kept constant in every measurement. The magnetic stirrer device is either powered on or off to cause the solution to mix. The results with stirring and without stirring were compared to subtract the changes in the signal caused by the stirrer alone.

3.8.2 Ultrasonic Bath

In the attempt to distribute the microparticles in the aqueous solution equally, the motion inside the liquid was initiated with the ultrasonic bath. The ultrasonic bath causes high-frequency pressure waves to vibrate the liquid, which as a result mixes the particles inside the aqueous solution. Due to the ultrasonic bath, the microplastics that settle to the bottom level of the beaker if left unshaken for a long period of time, would eventually vibrate and be distributed equally throughout the entire aqueous solution. For the experiments, the beaker containing the aqueous solution was held inside the ultrasonic bath for 3 minutes and then at least 10 measurements were carried out with the solution.

3.8.3 Deoxygenating the Aqueous Media

One of the hypotheses made by Shimizu et al. was that the microplastic particle works as an oxygen carrier when it makes an impact on the carbon electrode. According to the hypothesis, the microplastic particles work as oxygen carriers, and the following reaction takes place when the particles make an impact with the WE.

$$O_2 + 2H^+ + 2e^- = H_2O_{2(aq)}$$

In order to verify this, all the background oxygen inside the aqueous media was attempted to be deoxygenated and verify whether the microplastic particles would still generate the noises due to impact. To deoxygenate the aqueous media, Na_2SO_3 and $MgSO_4$ were used in separate experiments. Therefore, signals were acquired and analyzed for the aqueous solution containing microplastics and the deoxygenating agent. The resultant signal was also compared with the results obtained from the solution without microplastics, and deoxygenating agent as well as the solution containing only deoxygenating agent. In this way, specific contributions from each entity could be identified and understood. If a deoxygenating agent was added to the aqueous solution, it was measured and the same amount was added to the other solution to nullify the effect of any unequal amount. Thus, the effect of the deoxygenating agent could be identified accurately.

The deoxygenation procedure with Na_2SO_3 was carried out for the statistical spike count analysis (see Section 4.5.2) and $MgSO_4$ was utilized to carry out FFT analysis (see Section 4.5.3). The reason for using a different deoxygenating agent was to observe whether the deoxygenation process can be properly carried out with more than one process or not and whether the microplastic particles show different characteristics or not. Also, the deoxygenation process with $MgSO_4$ was carried out as it also serves the purpose of deoxygenation and does not remain as electrochemically active as the

Na_2SO_3 does in the aqueous solution. Here, different types of solutions were prepared for experimenting with each case (statistical spike count analysis and FFT analysis). For the statistical spike count analysis, the aqueous solution was prepared in three types: without any microplastics or deoxygenating agent Na_2SO_3, with only microplastics, and with both microplastics and deoxygenating agent Na_2SO_3. For the FFT analysis, one aqueous solution would contain deoxygenating agent $MgSO_4$ as well as the microplastic particles. Whereas the other aqueous solution would only contain the $MgSO_4$. Through this procedure, the effect of microplastics can be clearly understood. Here, both solutions contained 20 M KCl and 0.52 g $MgSO_4$. The difference was that only one of the solutions contained microplastics.

3.9 Signal Processing and Data Analysis

After carrying out all the procedures for collecting the signals from experiments, the last crucial part was signal processing and data analysis. As it was stated previously, the experimental setup catches a lot of noise from multiple sources including the noise generated by microplastic particles' impact on the electrode. Therefore, these noises were identified and analyzed in the signal-processing step of the experiments to filter out the noise caused by microplastic particles only. The signals and data obtained through PSTrace software were analyzed with OriginPro and Julia Programming Language. The signals were processed through two different methods mainly: statistical analysis to count the highest number of impacts that resulted through a signal for a specific condition, and the Fast Fourier Transform (FFT) analysis to filter out the noise that's being caused by the microplastic impact. Some pre-processing steps as explained in Section 3.9.1, were carried out as well to utilize these data in the statistical analysis mainly.

For the FFT analysis, the experimental setup was made with a 20 mM KCl solution with microplastic particles and another solution without these microplastic particles. Both solutions were processed with an ultrasound bath so that the particles in the solution would be distributed equally throughout the entire aqueous solution. Then, FAM analysis was run with a fixed current range of 100nA for both solutions. The resultant signals were collected and then processed further in the FFT analysis.

Furthermore, to observe the specific change in the resultant FFT signal for different microplastic concentrations, microplastics sample was added to the aqueous media at different concentrations for different measurements. Here, the microplastics were added at the v/v concentration of solid per mL for 0.02%, 0.03%, and 0.04%. The concentrations of the microplastics

suspension were determined as per the data obtained from the datasheet of the microplastics that were discussed in Section 3.2. Also, the probable particle count was obtained through optical microscopy and calculations shown in Section 4.5.1. After adding each new concentration of microplastics to the aqueous solution, the microplastics were distributed equally throughout the entire solution using an ultrasonic bath. Then for each of these concentrations, multiple measurements were carried out with FAM analysis. The obtained signals were later processed with FFT analysis to produce the final result with a unique frequency level indication for each specific concentration of microplastics.

3.9.1 Differentiation (d/dx) of the Signals

The signals obtained from the experiments through PalmSens4 device using the FAM analysis were viewed on the PSTrace software. These signals had their unique characteristics individually and also were in different current amplitude levels. In addition, the spike amplitudes of a particular signal had different amplitudes as well. Which made the process to analyze the signals and compare between different signals quite difficult. To mitigate this issue, the signals were differentiated in terms of time and all signals were brought to the zero level of the current amplitude. This made the comparison process simpler as it allows to find the dominant peaks in amplitudes and also make a statistical count to find out how many spikes a signal may have above a certain threshold level. Figure 3.5 shows how the signals are processed by differentiation. The raw signals obtained through FAM analysis are shown in Figure 3.5 (a), which was measured for three different aqueous solutions: with microplastics, without microplastics, and microplastics in deoxygenated solution. When all three signals are differentiated together in the same plot, they all come down to the base level of zero as shown in Figure 3.5 (b). If a certain area is zoomed in, the difference between the amplitude of the spikes from different signals can be seen in Figure 3.5 (c).

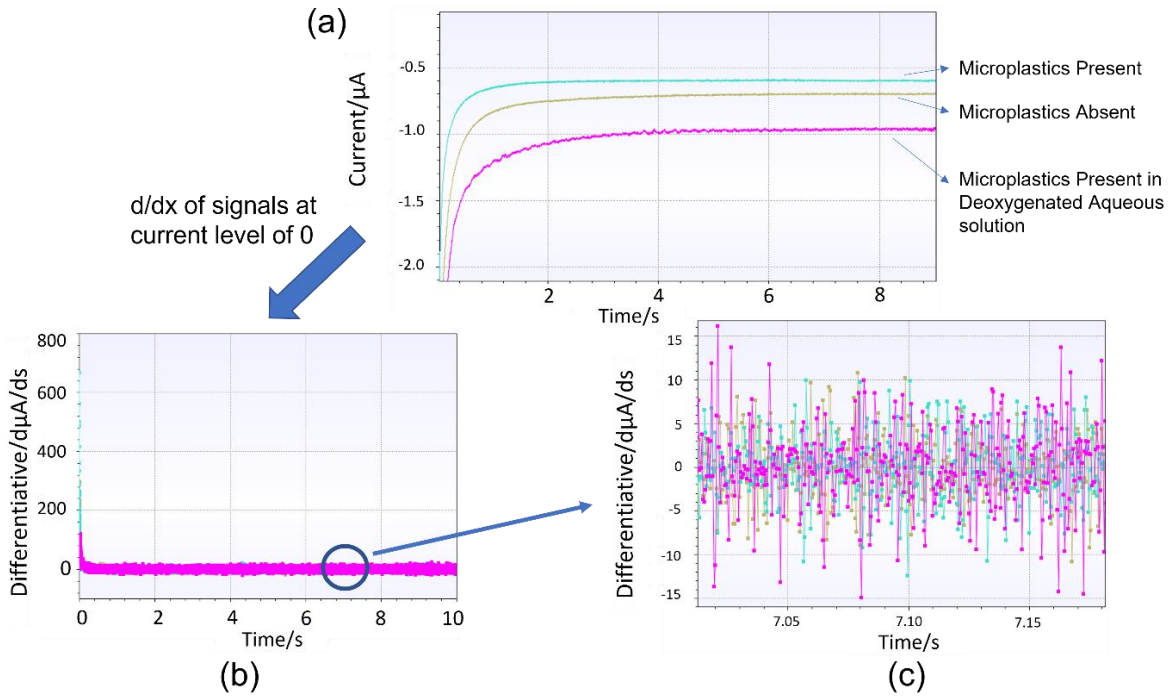

Figure 3.5 Differentiation of FAM signals; (a) raw signals, (b) differentiated signals brought to base level, and (c) zoomed-in differentiated signals zoomed in the range 7.00s-7.20s timeframe

3.10 Electrochemical Impedance Spectroscopy (EIS) Analysis

Besides aiming to establish the "impact concept", other approaches like impedance spectroscopy analysis was also considered in this project for detecting the microplastic concentration in an aqueous solution. With the addition of microplastics in the aqueous solution, it was also suspected that the impedance of the aqueous solution would also change. Thus, the EIS analysis was also carried out to investigate whether it could be a feasible method for detecting microplastics in aqueous media. The EIS analysis was carried out for different microplastics concentrations at 0.01%, 0.02%, and 0.03%. Here, each unit volume of the microplastics suspension contains a certain amount of microplastics particles as explained in section 4.5.1. The microplastics concentration was added from the 0.01% and then increased afterward in the same solution by an additional 0.01% microplastic concentration. The results were obtained in the Nyquist plot and then the circuit fitting was carried out on the obtained results in the PSTrace software. The final results as shown in Section 4.4 proves to be a promising indication that due to the change in microplastics concentration, the impedance also changes.

In order to validate the EIS results and prove its repeatability, a calibration test was also performed for EIS analysis where a new set of measurements were carried out. This test was carried

out in three steps. In the first step, 7 measurements were carried out with 5 minutes interval time in between each measurement. In the second step, the aqueous solution was kept the same and 0.005% microplastics concentration was added to the aqueous solution. Then the 3 EIS measurements were carried out. In the last step, the entire solution was changed, and a new fresh solution was added that contained no microplastics in it. Finally, 8 more measurements were carried out with 5 minutes time intervals in between each measurement.

In order to carry out a calibration test analysis, different parameters of the components were analyzed from the obtained raw signals. The values of these parameters are shown in Table 8. Here, the R^2 usually is a number between 0 and 1 indicating how well the body of the data fits with the model. X and Intercept are coefficients that describe the model equation. They can also be seen as an annotation on the fit graph. The standard error associated with each coefficient is represented as a percentage of the coefficient value. The limit of blank represents the highest quantity value, of blank material, that may be observed and is expressed as a probability. The limit of detection represents the lowest quantity that can be detected from a signal. The limit of quantitation represents the smallest concentration of a substance that is detectable from a signal. C1 and C2 are reciprocal coefficients because it can be more convenient to rewrite the model equation from (Y = X+ intercept) to (X =C1 x Y + C0).

3.11 Scanning Electron Microscopy (SEM) and Optical Microscopy

As the electrodes were developed from conducting wires or fiber strings found in the laboratory, the material that these conductors were specifically made from was not absolutely confirmed, especially in the case of Type-4 electrode fibers. In order to remove any contradiction on what kind of material was used in the development of the WE, the conductors were analyzed with Scanning Electron Microscopy (SEM). The conductors and electrodes were attached to a Cu tape and then placed in the vacuum chamber of SEM. The resultant data from SEM analysis shown in Section 4.2.2 confirms the materials of the conductor.

In addition, the microplastic particles count in a unit amount was also unknown. Therefore, to make a close approximation, the microplastic particles were counted for making an estimation and to understand how many microplastic particles were available in a unit solution. Here, the microplastics were collected from the source container of the 5ml sample through a pipette and diluted with DI water to make a proportion of 1:10 before releasing the microplastics in the hemocytometer. Through this dilution process, the concentration of cells or particles in the sample

is reduced. Thus, it avails easier counting and ensures that the cell distribution on the hemocytometer grids is suitable for accurate analysis. Figure 3.6 (a) shows the hemocytometer used in this project for counting microplastic particles under the optical microscope. Figure 3.6 (b) shows a chamber design model of the hemocytometer. Each chamber has four large squares and each large square contains 16 blocks in total. Here, an estimated count was carried out by carefully counting the particles contained in the first 4 blocks, and then multiplying it by 4 to get an estimated value for the entire 16 blocks that represent the total value of microplastic particles contained in one large square.

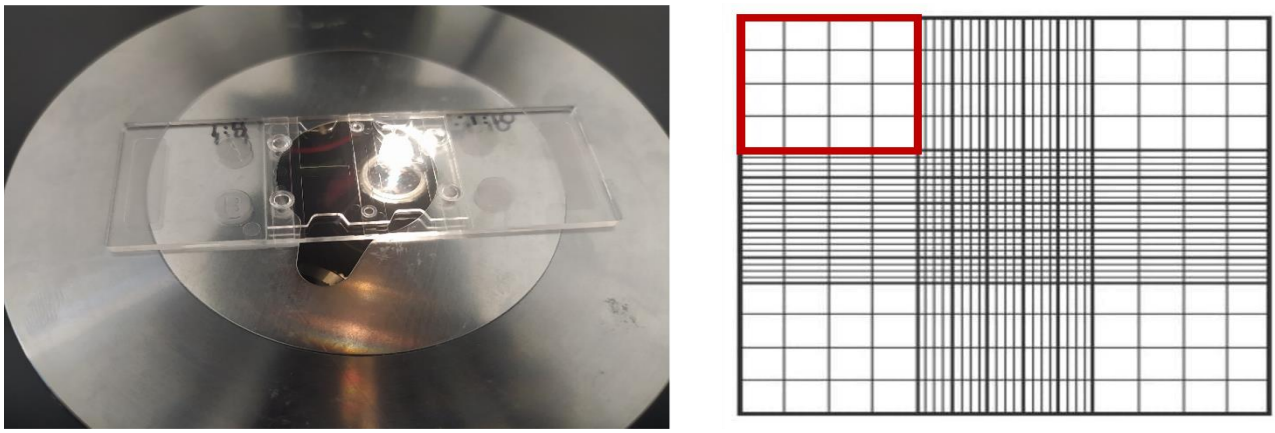

(a) (b)

Figure 3.6 (a) Hemocytometer containing microplastic particles with a dilution factor of 1:10 under the optical microscope for accurate particle counting (b) Hemocytometer chamber design model

4 Results

In this chapter, all the results obtained in different approaches for this project are presented.

4.1 Difference between original ZP-HV-SPE and Modified ZP-HV-SPE

The investigation into reducing the WE size was first observed through the modification of the ZP-HV-SPE sensor by stripping off a majority of its WE to reduce its area. Considering the current density to be the same, the signal would scale down with electrode area in order to meet the lower and more sensitive range of the measurement system without reaching saturation. The original electrode couldn't reach the lower ranges normally as the area of the working electrode was much larger. Thus, causing a higher range of current transfer. The background noise level picked up by the electrode also scales with size (see argument in section 3.3) and by reducing the electrode area the SNR was improved to a level where the signals from the microplastics impact events could be seen. Figure 4.1 shows the difference between the two types of signals from the original and modified types of the ZP-HV-SPE WE. As this test was carried out only to establish the theory that the reduced area size of WE can reach a more sensitive range of the measurement system, the test was carried out in PBS solution without any microplastic particles. Thus, only the effect of the reduced area of WE can be identified. Both signals were collected at the same condition by applying a WE potential of -0.03V and the current range of the measurement system was kept at 10 nA for the fast amperometry analysis. The modified electrode had a lower range noise level. Which was the targeted scenario, to be able to record more noise signals in less time. At this point, it was expected that with microplastics added to the solution, it would cause an increase in the spike count. If a two-second spectrum between 4 s and 6 s is looked at, it can be seen that the modified electrode had the average peak-to-peak value of approximately 12 nA, whereas the modified electrode had approximately 7.5 nA.

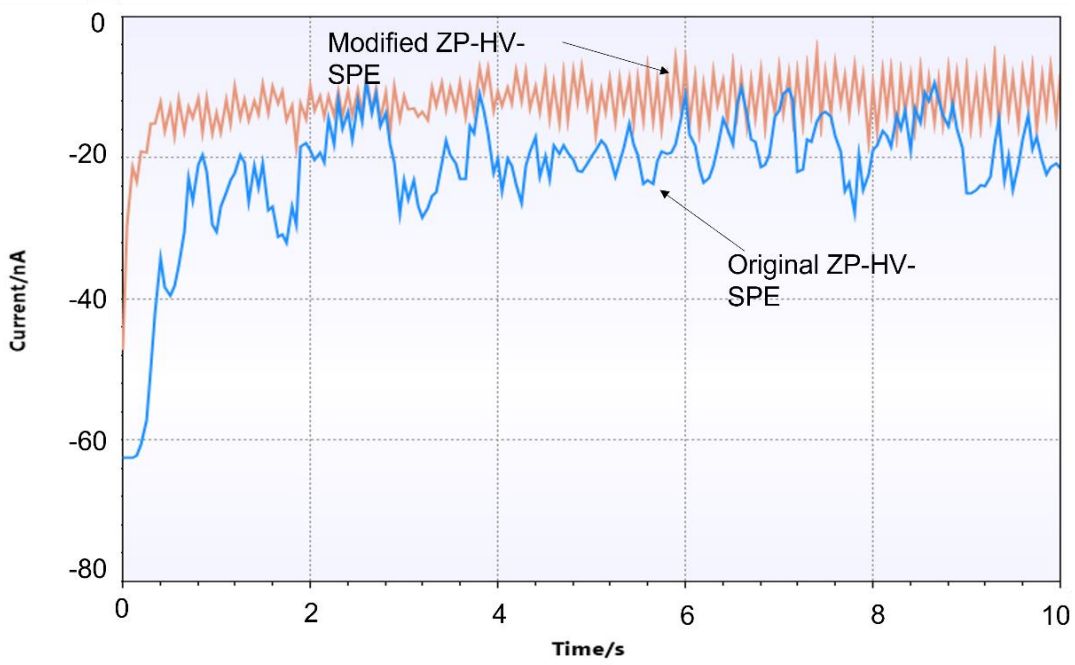

Figure 4.1 Comparison between the signals obtained through modified screen printed electrode and original electrode at the same experiment condition

Figure 4.2 shows the comparison between the two electrodes in terms of their capability of functioning at low voltage and low current range. The original electrode mostly carried out its operation in the range of -8 to -16 nA at -0.075 V in the 10 s time period of the measurement without any overload state. However, the modified electrode performed within the -1.7 to -2.5 nA range at -0.03V. Here, the negative sign in both cases of the current range is present due to there being a net reduction at the electrode surface. It was also noticed that the original electrode required 0.045V more than the modified electrode to avoid the overload state. This phenomenon might have been caused due to larger electrodes being more difficult to polarize. These findings report that the size of the electrode plays a crucial role by using a smaller current range to produce higher signal amplification of the potentiostat. Therefore, the WE needed to be developed to a much smaller surface area and diameter to attain the ability to detect signals in the nA range.

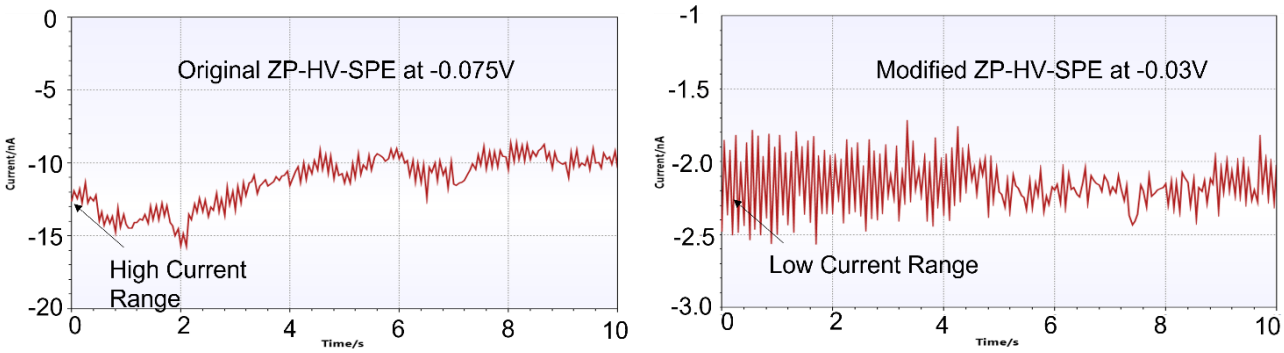

Figure 4.2 Comparison between Original ZP-HV-SPE and modified ZP-HV-SPE in terms suitable operating current range and voltage range

4.2 Comparative analysis of the Working Electrodes

4.2.1 EDX results of the Developed Electrodes and their conductors

Figure 4.3 shows all four types of electrodes that were fabricated. Although having a different conducting wire or fibre underneath, all four types of electrodes were coated with carbon.

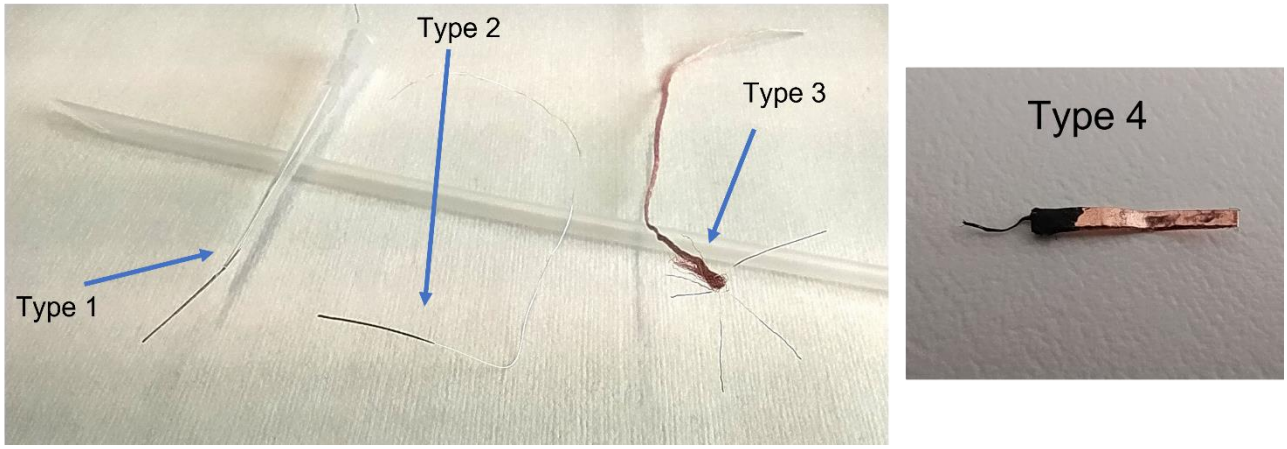

Figure 4.3 Developed four types of electrodes

The metal wire conductor that was used for developing the electrodes was put under EDX analysis with SEM for confirming the material of the conductor. Some of the analysis was carried out with point scan while others were done with an area scan. With point scan, the materials in the particular point of the conductor are analyzed and possible materials identified from molecular series are shown as the result. On the other hand, the area scan focuses on a larger area than point scan and identifies the materials available within the focused area. The area scan is commonly carried out

when multiple materials are suspected to be present in the analyzed sample. Otherwise, point scan is commonly carried out if it is confirmed that the sample is made of only one material.

Figure 4.4 shows the EDX analysis results of the conductor that was used to develop the Type-2 WE. From the result, it is confirmed that the conductor was made of silver. The presence of copper in this case was due to the fact that the conductor was placed on copper tape, which may have influenced the SEM to detect copper in the scan as well. Other insignificant materials detected in the scan are considered to be negligible as SEM works on the principle of electron scattering in the material's electron shells and sometimes the SEM detects atoms incorrectly or at an insignificant rate. Such insignificant amounts are mostly neglected and only the materials that resulted in a high percentage of atomic values are considered to be correct.

Figure 4.5 shows the EDX analysis results of the Type-3 WE which was coated with carbon. Here, the point scan was carried out in the EDX analysis and the results confirm that the coating was of carbon. The conducting wire beneath the carbon layer was known and confirmed beforehand to be copper. Figure 4.6 shows the EDX analysis results of Type-4 WE conductive fibre which was mainly unknown at the earlier stage of the project. Through a point scan, the result shows that the conductive fibre was mainly silver material. To further validate this result, an area scan on the fibre was also carried out. The result of the area scan also confirms that the conductive fibre was made of silver as shown in Figure 4.7.

(a)

Spectrum: s1

Element	Series	unn. C [wt.%]	norm. C [wt.%]	Atom. C [at.%]	Error (2 Sigma) [wt.%]
Copper	K-series	11.39	12.62	19.24	0.61
Silver	L-series	78.54	86.97	78.14	5.02
Aluminium	K-series	0.06	0.06	0.22	0.06
Nitrogen	K-series	0.31	0.35	2.40	0.24
	Total:	90.31	100.00	100.00	

(b)

Figure 4.4 SEM analysis results of Type-2 WE conductor through a point scan (a) SEM image of the conductor, (b) identified materials data

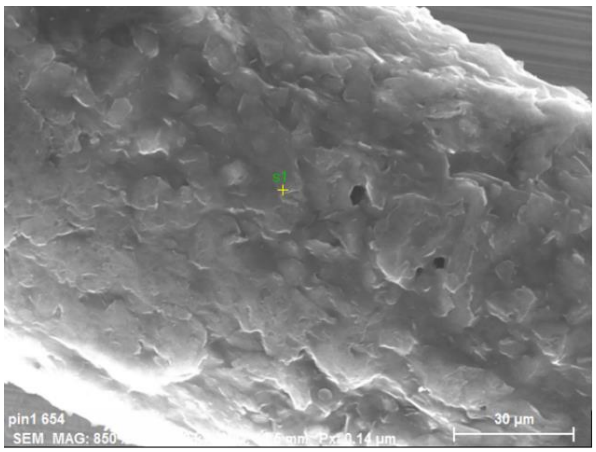

(a)

Spectrum: s1

Element	Series	unn. C [wt.%]	norm. C [wt.%]	Atom. C [at.%]	Error (2 Sigma) [wt.%]
Oxygen	K-series	4.21	12.82	12.39	1.81
Copper	K-series	1.99	6.05	1.47	0.16
Carbon	K-series	24.94	75.93	83.84	6.37
Sulfur	K-series	0.22	0.67	0.32	0.07
Chlorine	K-series	1.49	4.54	1.98	0.16
Total:		32.84	100.00	100.00	

(b)

Figure 4.5 SEM analysis results of Type-3 WE with carbon coating through a point scan (a) SEM image of the WE, (b) identified materials data

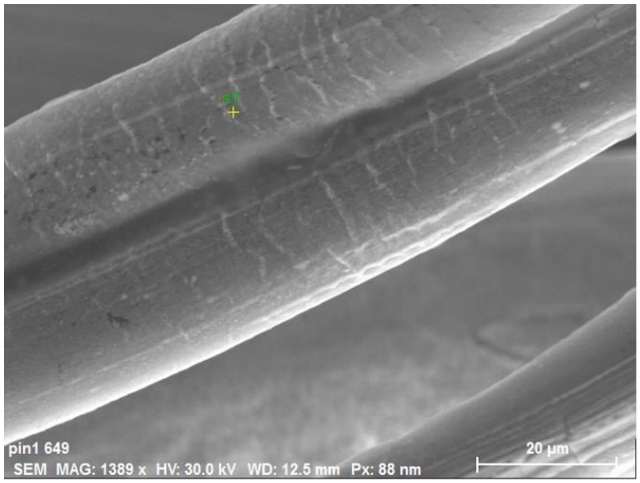

(a)

Spectrum: s1

Element	Series	unn. C [wt.%]	norm. C [wt.%]	Atom. C [at.%]	Error (2 Sigma) [wt.%]
Silver	L-series	39.77	98.87	97.49	2.58
Titanium	K-series	0.45	1.13	2.51	0.09
Total:		40.22	100.00	100.00	

(b)

Figure 4.6 SEM analysis results of Type-4 WE conductive fibre through point scan (a) SEM image of the WE, (b) identified materials data

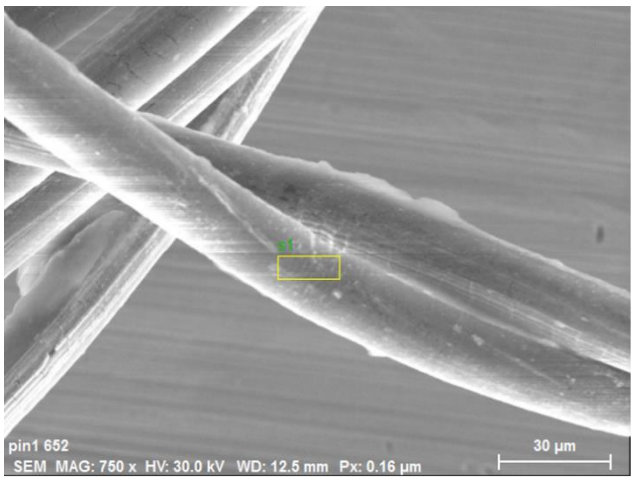

(a)

Spectrum: s1

Element	Series	unn. C [wt.%]	norm. C [wt.%]	Atom. C [at.%]	Error (2 Sigma) [wt.%]
Silver	L-series	42.85	69.53	57.10	2.77
Copper	K-series	18.64	30.25	42.16	0.98
Aluminium	K-series	0.14	0.23	0.74	0.07
	Total:	61.63	100.00	100.00	

(b)

Figure 4.7 SEM analysis results of Type-4 WE conductive fibre through area scan (a) SEM image of the WE, (b) identified materials data

Table 4 shows the difference in the diameter of the electrodes before and after carbon coating. The diameters were measured with a digital slide calliper at the area that gets submerged in the aqueous solution, which is at a maximum of 1mm from the tip of the electrode. The resultant diameter of the developed electrodes shows a significant reduction of size compared to the original ZP-HV-SPE which had a surface area of 3.80 mm^2 and the modified ZP-HV-SPE which had a surface area of 1 mm^2.

Table 4. Diameters of the fabricated electrodes

Electrode Type	Materials of the Conducting fibre/wire used	Diameter without Carbon Coating	Diameter with Carbon Coating
		(µm)	*(µm)*
Type-1	Silver	190	210
Type-2	Silver	130	150
Type-3	Copper	50	70
Type-4	Silver	25	40

4.2.2 Verification of Electrodes

Whenever any of the electrodes were fabricated, they went through the verification process by carrying out a cyclic voltammetry analysis with the electrode. The cyclic voltammetry analysis verifies whether the electrode had a proper carbon coating or not. If the electrode had a proper

carbon coating, it would show a certain duck-shaped graph plot in the analysis result. However, in the case of improper carbon coating, or the metal conductor beneath the coating leaks through at any area of the electrode, there would be some crossover between the plotted lines. In addition, crossing lines also occur due to the growth of some other material over the carbon layer due to the electrochemistry occurring for the particular solution, making the surface area bigger. Hence, this indicates that the carbon coating was not properly settled around the electrode or the electrode needs proper cleaning to remove the grown residues over the electrode. This verification step is always carried out with $Fe(CN)_6$ solution, as the carbon electrodes tend to display their signature duck-shaped plot with CV analysis in the $Fe(CN)_6$ solution [64]. Figure 4.8 shows the difference in resultant CV analysis between (a) proper carbon-coated electrode and (b) flawed carbon-coated electrode.

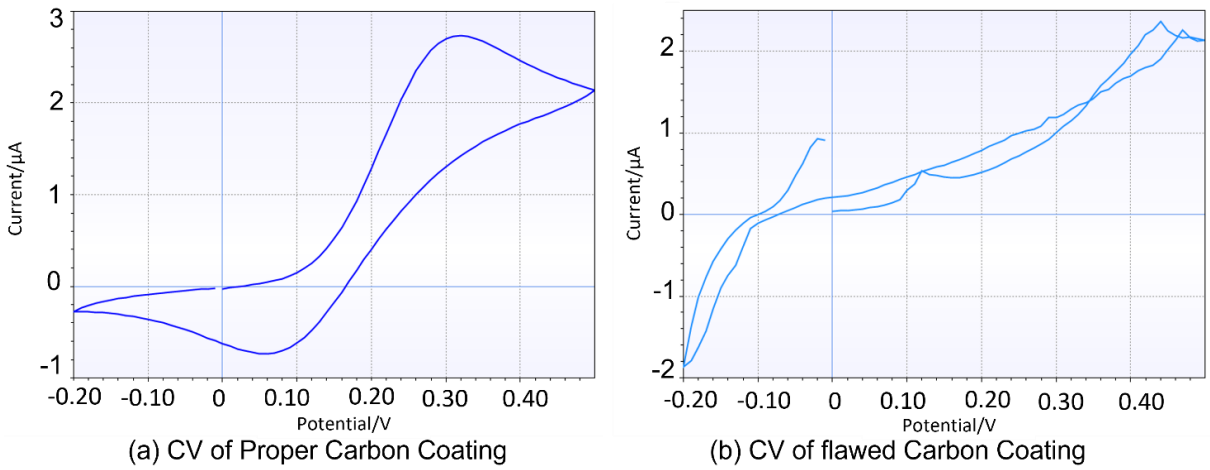

Figure 4.8 CV analysis of Type-2 electrode with (a) proper duck-shape, and (b) distorted duck-shape, at the verification process of the electrodes

If any electrode doesn't pass the verification step with a good duck-shaped plot in the CV analysis, that electrode was never used in the further step of the measurements. Figure 4.9 shows the resultant CV analysis of four types of electrodes developed for the project. At the earlier stage of the project, when the first three types of electrodes were developed, the verification was carried out at the range of -0.2V to 0.5V. However, it was later noticed that the targeted oxidation and reduction reaction takes place at the range between 0V to -0.7V, and the FAM analysis was mainly run at -0.4V, this oversight was corrected at the verifications of the Type-4 electrode. Thus, the CV of the Type-4 electrode was run between the range of -0.5V to 0.5V. Although the CV curve of Type-4 showed a different shape than the other three types of electrodes, it was considered to pass the verification as

there was no crossover between the lines in the plot. Also, another reason for this different plot could be that the conductor that was used for fabricating Type-4 was basically conductive fiber made of silver whereas the other three types of electrodes had more rigid wire strings either made of silver or copper. The data that was used for signal analysis at a later stage, were collected with Type-4 as it had the lowest diameter and was considered to be more responsive to microparticles than other types of electrodes. Although Type-1 and Type-2 had produced a better duck-shaped curve in the CV analysis, these two types of electrodes were not used at the later stages of the project after developing the Type-4 electrode. The reason behind this action was that the Type-4 electrodes had the ability to utilize a lower current range in the nA scale to detect the signals, whereas the Type-1 and Type-2 had a larger diameter size and couldn't utilize a lower current range in the nA scale.

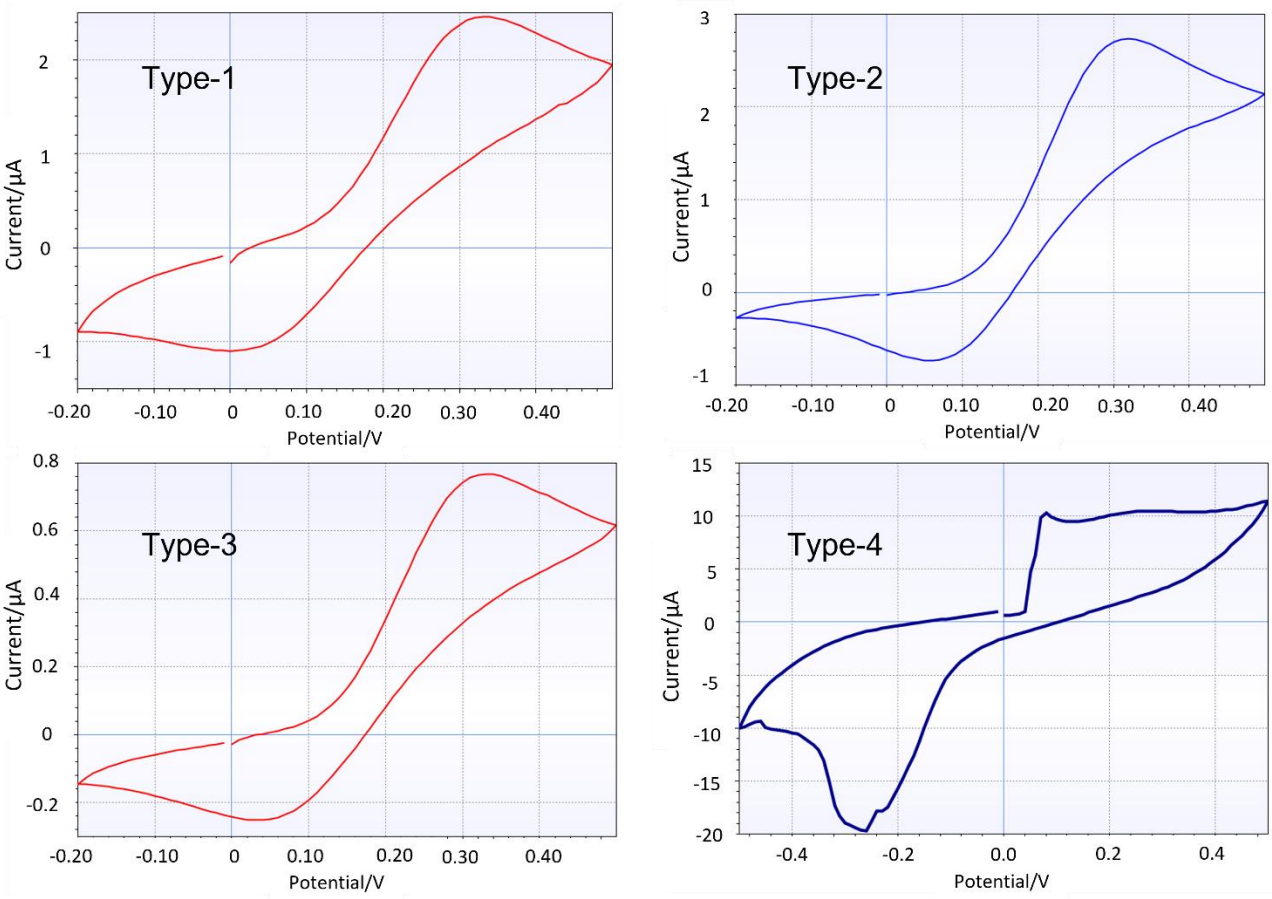

Figure 4.9 CV analysis of fabricated four types of electrodes showing no cross over in the plot and hence passing the verification process

4.3 Detecting the Presence of Microplastics

4.3.1 Verifying the impact detection method

The resultant signals from larger PET particles with the solution stirred suggested that the electrodes can detect impacts. In this particular experiment performed at an earlier stage of the project, only Type-2 electrode was used. Also, this experiment was carried out to validate the hypothesis of signal variation could cause due to particle impact, just on a larger scale. Figure 4.10 shows the comparison between two signals with and without the PET particles. There were multiple measurements taken for this experiment, but only two results are shown in this Figure 4.6 for simple comparison. Unlike microplastic particles, these larger PET particles were visible to the naked eye and seen to be making impacts with the electrode when being stirred. The figure proves the fact that the fabricated electrodes are able to recognize physical impacts by the particles on them and represent these impacts in the resultant signal. The signal representing no particle impacts is quite flat and unchanged throughout the time as it showed almost no spikes in the signal. Whereas the signal representing PET particle impacts has a lot of spikes in the signal. The expected number of impacts per second is approximately between 3 to 5. However, this number is not proven to be precise in all measurements due to the uncertainty of the stirring rate of the magnetic stirrer. Also, the PET particles tend to attach together in the aqueous media while being stirred. Furthermore, the PET particles used in this case are heavier and larger than the microplastic particles as mentioned in Section 3.7. Thus, requiring a high stirring rate to lift the particles to the upper level in the aqueous media. As a result, there were often more than 5 impacts or sometimes less than 3 impacts occurring in the measurements. The test was performed with chronoamperometry analysis to identify PET particles' impact over a longer time period. The obtained signals were compared with real-time visual inspection to confirm that impacts were certainly being recorded. The applied potential for this test with chronoamperometry analysis was kept at -0.5 V as mentioned in Section 3.4.

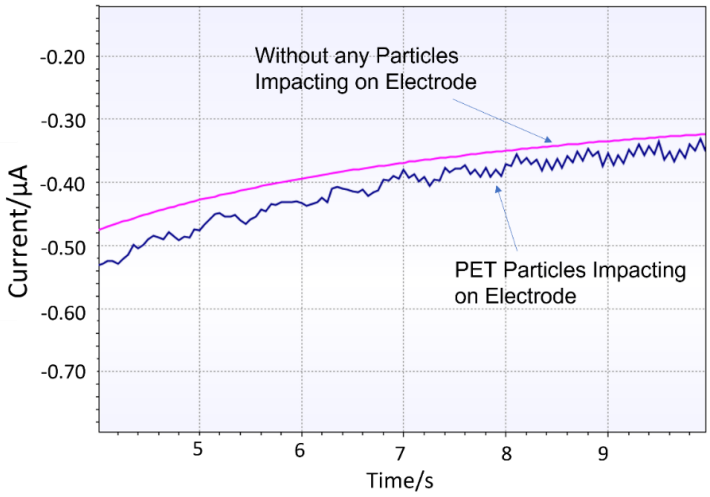

Figure 4.10 Verifying impacts being recognized by the fabricated electrodes

4.3.2 Detecting the Presence of Microplastics with Type-3

The presence of microplastics in an aqueous solution was observed from the resultant signals as they had more spikes than the signals obtained from the solution without microplastics. Figure 4.11 shows a clear indication of how microplastics can cause a difference in the obtained signals by producing spikes in the signal through impacts with the WE. These signals were obtained in both stirring and unstirring conditions. Regardless of the stirring conditions, the presence of microplastics can be clearly distinguished from the spike amplitudes of the signals. All the measurements were taken in the same current and voltage range with the fast amperometry analysis settings as mentioned in section 3.4.1. The electrode used for collecting these signals was the Type-3 electrode.

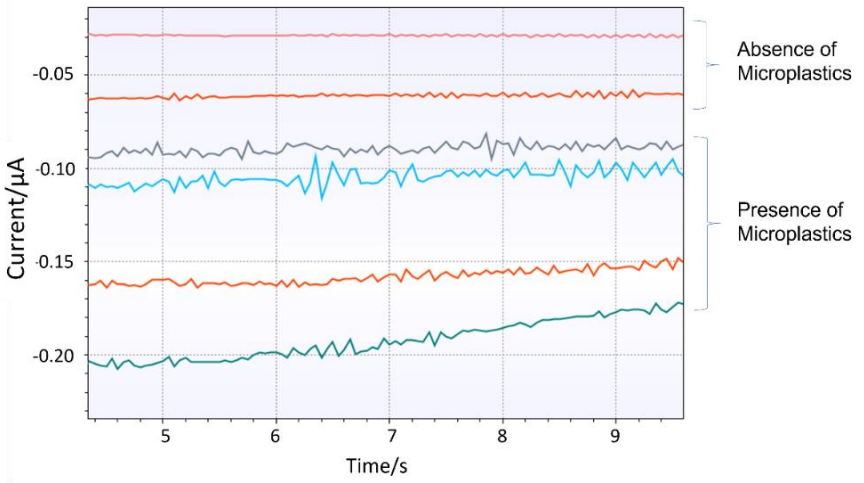

Figure 4.11 Detecting the presence of Microplastics in Aqueous solution with Type-3 electrode

4.3.3 Detecting the presence of Microplastics with Type-4 electrode and higher sampling frequency

The Type-4 electrode having the lowest diameter was considered to be the most reliable electrode among all four types of electrodes. On a different note, the scan rate of the measurements was kept at 0.05 s mistakenly in measurements that were carried out up to this stage. However, after developing the Type-3 electrode, the scan rate was modified to 0.0005 s or 0.05 ms. This implies that the electrodes would scan and obtain signals at every 0.05 ms interval. This made a significant difference in obtaining the signals for detecting microplastic impacts as it would be able to record particle impacts happening at faster intervals than 0.05 s. Figure 4.12 shows the difference between obtained signals for aqueous media containing microplastics in comparison to the absence of microplastics at a 0.05 ms scan rate. The microplastics are producing current oscillations of approx. 6 per second. In addition, with a higher sampling frequency, current spikes obtained at a shorter time interval can be analyzed using FFT, and the results are explained in section 4.5.1.

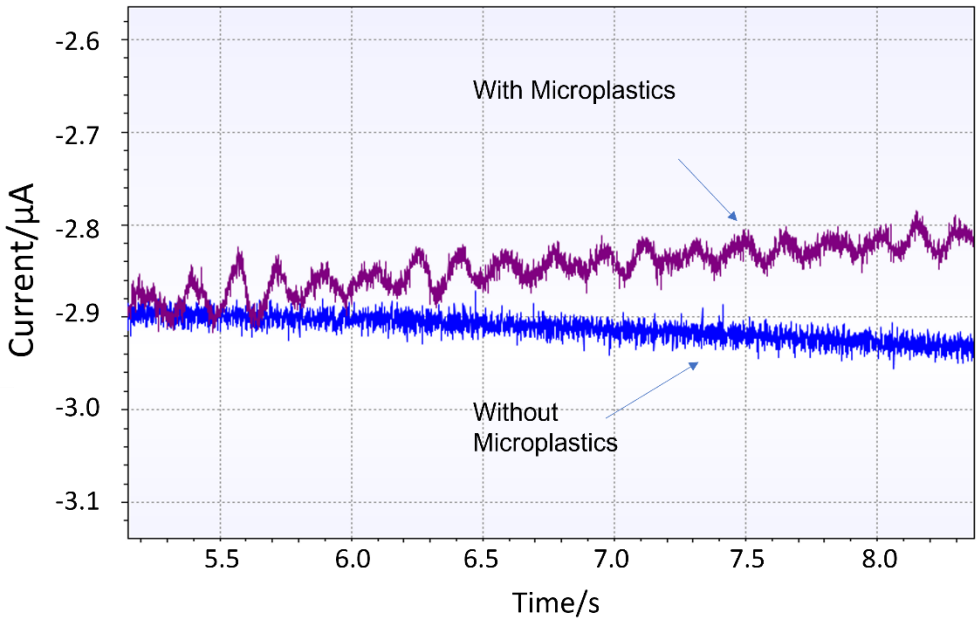

Figure 4.12 Detecting the presence of microplastics with Type-4 electrode with a lower scan rate

4.3.4 Deoxygenation of Aqueous Media

Figure 4.13 shows the CV analysis plot for a 10 mL 20mM KCl aqueous solution without any Na_2SO_3 (red plot), with 5 mg Na_2SO_3 (green plot), and with 50 mg Na_2SO_3 (pink plot). Here, the region of interest is the -0.4 V region where the oxygen reduction takes place and its respective magnitude

level. From the figure, it can be seen that the endpoint of the CV curve of a normal aqueous solution in the negative region shifts from approx. 38 µA to a lower current magnitude level of approx. 32 µA after adding 5 mg Na_2SO_3 to the solution. The equivalent current range for the CV analysis at the potential of -0.4 V was kept at 10nA to 1µA. However, even after adding 10 times more (50 mg) Na_2SO_3 in the solution, the endpoint of the CV curve did not change much. Whereas the positive region showed a significant change due to this high amount of Na_2SO_3 addition. This could be because the deoxygenation taking place in the negative region was completed with 5 mg Na_2SO_3 in the first case and there was no more free oxygen left in the aqueous media to be deoxygenated. However, the change by a high concentration of Na_2SO_3 caused a change in the positive region due to SO_3 being electrochemically active in that region. Depending on the pH level, the SO_3 is likely to exist in different forms, but some fraction of it be in the form of SO_2 (aq) which can be directly reduced at around -0.7V with the carbon WE and CE, RE of Ag/AgCl. However, the positive region is not the deoxygenation region in this case. This finding concludes that the deoxygenation with Na_2SO_3 does indeed make a significant effect in the aqueous media and all the oxygen in the aqueous media is removed. On the other hand, when the microplastics are added to such deoxygenated solution, only the oxygen attached to each microplastic particle remains and they are released at the event of making impacts with the WE.

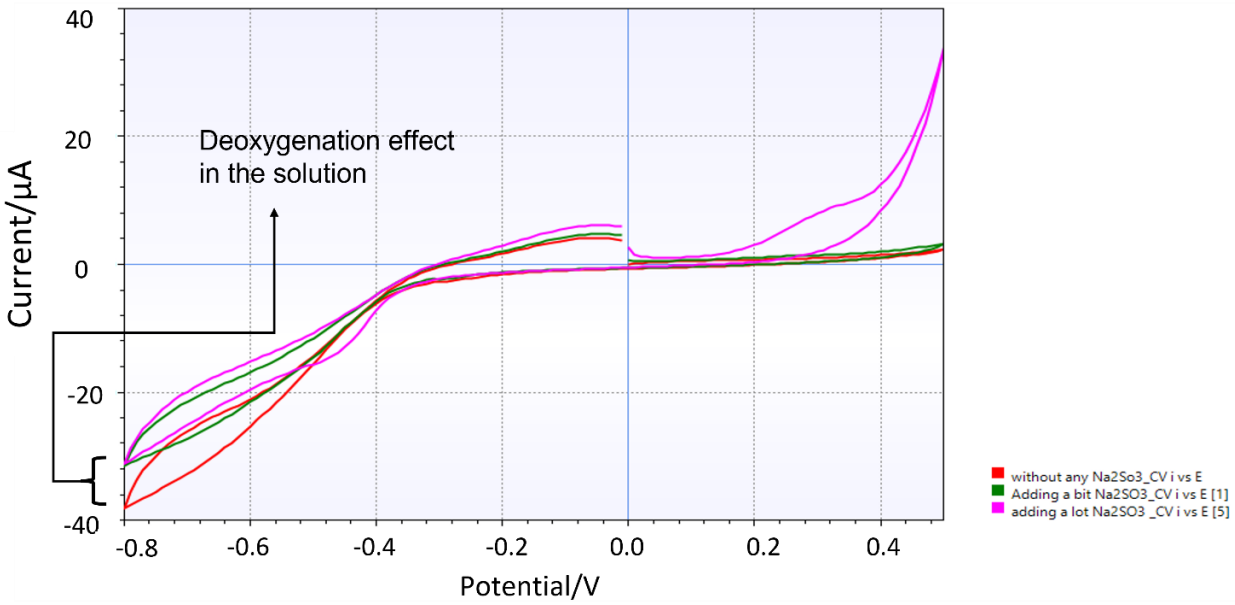

Figure 4.13 Deoxygenation effects observed in the Aqueous media through CV analysis

Another technique that was used for investigating how microplastics work as oxygen carriers was the multi-step amperometry analysis. Figure 4.14 shows the resultant signal from multi-step

amperometry analysis. Each cycle of the multi-step analysis has a negative potential in one half, and a positive potential in the other half. When the microplastics hit the WE, it releases oxygen to the WE. At the negative potential, the WE consumes the released oxygen. On the other hand, at the second step of the cycle, the electrode releases the oxygen at the positive potential of the cycle. The potential in this case changes its polarity from negative to positive in an instance, which causes the sudden rise of the current amplitude.

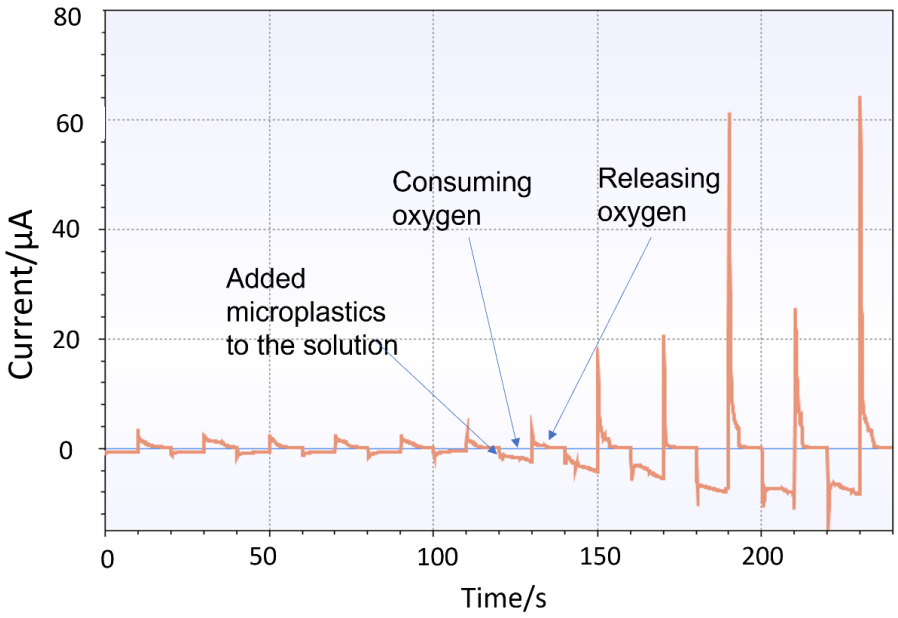

Figure 4.14 Multi-step amperometry analysis showing consumption and releasing oxygen on the electrode as microplastics make impacts

4.4 EIS Analysis

In this section, the EIS analysis results are presented. The analysis was carried out with two platforms: 'PSTrace' and 'djuli'. PSTrace was mainly used for collecting the signals from the test setup and analyzing them for circuit fitting. On the other hand, djuli was mainly used for calibration analysis with the signals obtained with PSTrace.

4.4.1 EIS signal collection and circuit fitting with PSTrace

Figure 4.15 shows the Nyquist plots for impedance spectroscopy analysis of different microplastic concentrations. Here, it can be seen that an increase in the microplastic concentrations causes a change in the impedance of the solution. The increment of microplastic concentrations significantly increases the real impedance or the resistance of the media as it shifts towards higher

values. The aqueous media was experimented with conditions of no microplastics, 0.01% microplastics concentration, 0.02% microplastics concentration, and 0.03% microplastics concentration. Here, all concentrations are represented in v/v percentage. Repeated measurements were also performed to check whether the response was the same or not, and the results showed that the responses were mostly at the same level for the specific concentration of microplastic particles.

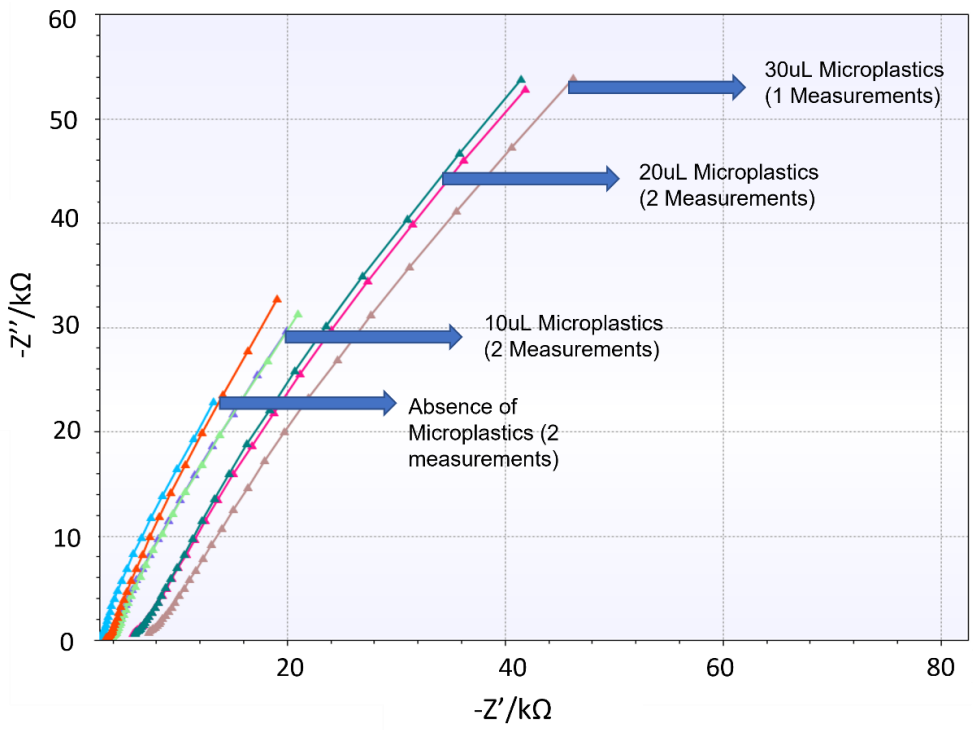

Figure 4.15 Nyquist plot by Impedance Spectroscopy analysis for different microplastics suspension of 10 µL, 20 µL, and 30 µL representing microplastics concentration of 0.01%, 0.02%, and 0.03% respectively

Figure 4.16 shows the circuit fitting for the aqueous solution without any microplastics present. Here, the usual capacitor for EIS circuit fitting was replaced with a CPE (Constant Phase Element) according to Du et al. [65] in EIS circuit fitting. Table 5 shows the detailed value of circuit fitting for the aqueous solution without any microplastics. Figure 4.17 shows the circuit fitting for the aqueous solution with 0.01% microplastics concentration while Table 6 shows the fitted values for all of its components. Figure 4.18 shows the circuit fitting for the aqueous solution with 0.02% microplastics concentration while Table 7 shows the fitted values for all of its components. Lastly, Figure 4.19 shows the circuit fitting for the aqueous solution with 0.03% microplastics concentration while Table 8 shows the fitted values for all of its components. Here, it can be observed that the

impedance value of R1 and R2 increases whereas Q1 tends to decrease with the increment of microplastics concentration.

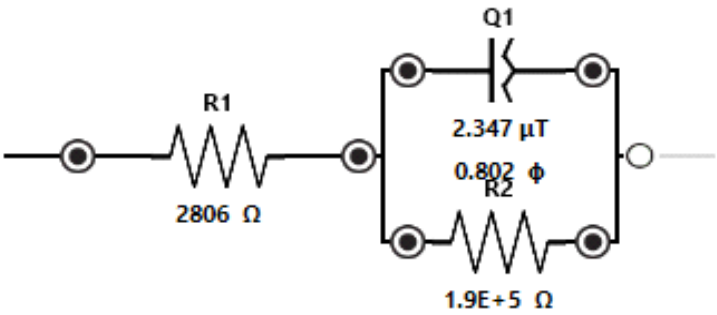

Figure 4.16 Circuit fitting for the aqueous solution without microplastics

Table 5. Resultant values of circuit fitting for the aqueous solution without microplastics

Circuit:	**R(QR)**	**Title:**	**Fresh/absence of microplastics**	**Measurement:**	**EIS**	
Fixed	***Element***	***Fitted Value***	***Min Value***	***Max Value***	***Unit***	***Error%***
False	R 1	2806	1.00E-6	1.00E+12	Ω	0.496
False	Q 1	2.347E-6	1.00E-12	1.00E-3	T	2.461
False	n 1	0.802	0	1.00	ϕ	0.577
False	R 2	1.903E+5	1.00E-6	1.00E+12	Ω	11.61
		Chi-Squared:	0.0003	Iterations:	7	

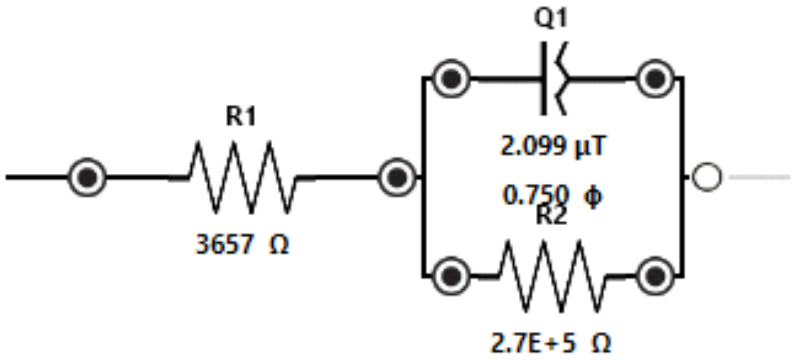

Figure 4.17 Circuit fitting for the aqueous solution with 0.01% microplastics concentration

Table 6. Resultant values of circuit fitting for the aqueous solution with 0.01% microplastics concentration

Circuit:	**R(QR)**	**Title:**	**10µL microplastics**	**Measurement:**	**EIS**	
Fixed	***Element***	***Fitted Value***	***Min Value***	***Max Value***	***Unit***	***Error%***
False	R 1	3657	1.00E-6	1.00E+12	Ω	0.707
False	Q 1	2.099E-6	1.00E-12	1.00E-3	T	3.314
False	n 1	0.750	0	1.00	ϕ	0.806
False	R 2	2.725E+5	1.00E-6	1.00E+12	Ω	16.63
	Chi-Squared:	0.0004	Iterations:	6		

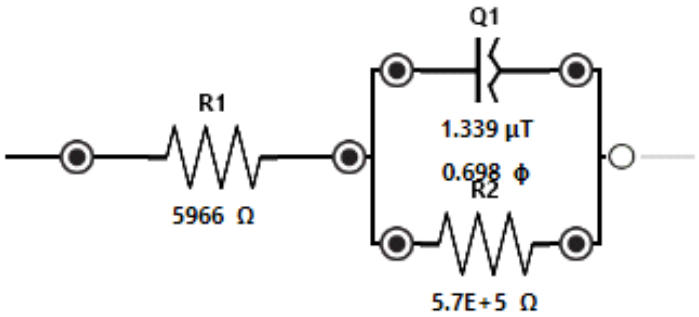

Figure 4.18 Circuit fitting for the aqueous solution with 0.02% microplastics concentration

Table 7. Resultant values of circuit fitting for the aqueous solution with 0.02% microplastics concentration

Circuit:	**R(QR)**	**Title:**	**20µL microplastics**	**Measurement:**	**EIS**	
Fixed	***Element***	***Fitted Value***	***Min Value***	***Max Value***	***Unit***	***Error%***
False	R 1	5966	1.00E-6	1.00E+12	Ω	0.963
False	Q 1	1.339E-6	1.00E-12	1.00E-3	T	3.944
False	n 1	0.698	0	1.00	ϕ	0.988
False	R 2	5.660E+5	1.00E-6	1.00E+12	Ω	22.32
	Chi-Squared:	0.0006	Iterations:	1		

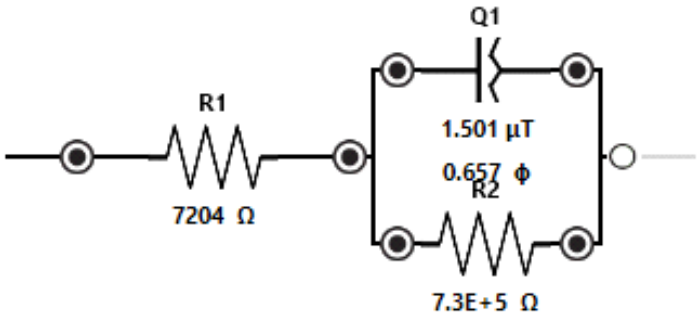

Figure 4.19 Circuit fitting for the aqueous solution with 0.03% microplastics concentration

Table 8. Resultant values of circuit fitting for the aqueous solution with 0.03% microplastics concentration

Circuit:	**R(QR)**	**Title:**	**30µL microplastics**	**Measurement:**	**EIS**	
Fixed	***Element***	***Fitted Value***	***Min Value***	***Max Value***	***Unit***	***Error%***
False	R 1	7204	1.00E-6	1.00E+12	Ω	0.952
False	Q 1	1.501E-6	1.00E-12	1.00E-3	T	3.990
False	n 1	0.657	0	1.00	ϕ	1.054
False	R 2	7.281E+5	1.00E-6	1.00E+12	Ω	27.46
	Chi-Squared:	0.0005	Iterations:	5		

4.4.2 Calibration test results using PSTrace and djuli

Figure 4.20 shows the raw signals of the calibration test result to prove the sensor's repeatability in the EIS measurements. The resultant EIS plot for the 1st step shows to be on almost the same line with not much of a difference. But there is still some insignificant small drift of the signal between the measurements which may have been caused due to temperature change, or instrumental error, or solution evaporation. On the 2nd step, a significant shift occurred toward a higher impedance range after inserting 0.005% microplastic concentration. The repeated 3 measurements show to be on the same line without altering any other parameter in the test setup indicating that the impedance has changed only due to the addition of microplastics. For the 3rd step, the signal has shifted towards a lower impedance range again. This time, the signals shifted to a lower

impedance range than the previous fresh solution with the absence of microplastics. This may have been caused due to temperature change on the WE due to the new solution. The sensor's WE in all measurements was kept at the same submerged range from the surface of the aqueous solution.

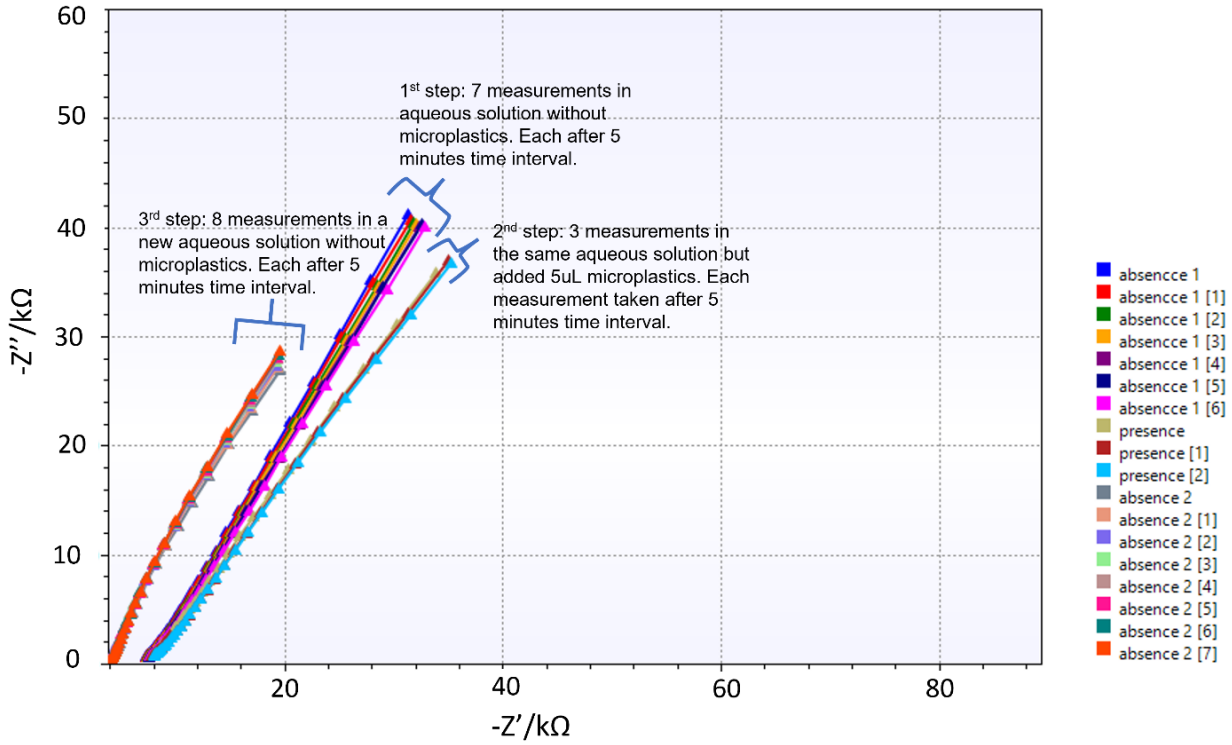

Figure 4.20 Raw signals for EIS analysis in aqueous solution for the case of microplastics being absent and present in the aqueous solution.

A calibration analysis was performed using djuli on the attained raw signals to determine a coefficient threshold of the impedance analysis, which can be used for determining whether a certain aqueous solution contains microplastics or not. The raw signals shown in Figure 4.20 are simply categorized into two groups to define a solution with microplastics and without microplastics. Figure 4.21 shows these two categorized groups for the raw signals in the real impedance vs imaginary impedance graph. From the graph, it is evident that the resultant signal representing the presence of microplastics has a higher real impedance than those that represent the absence of microplastics. Figure 4.22 shows the parameter plot of the circuit fitting components as an average of all resultant EIS signals. The two categories of "0.0" representing the absence and "1.0" representing the presence of microplastics. For EIS analysis in this project, the CPE is taken as the reference parameter for carrying out the analysis. The circuit fitting components P1n and P1w represents the P1 of the circuit fitting, which is the Constant Phase Element. Here, the CPE in djuli is represented as P1 which was

previously represented as Q1 in PSTrace. Among them, the P1w resulted in the most distinguishing feature that had the predicted concentration range at the lowest and separated from other components' range.

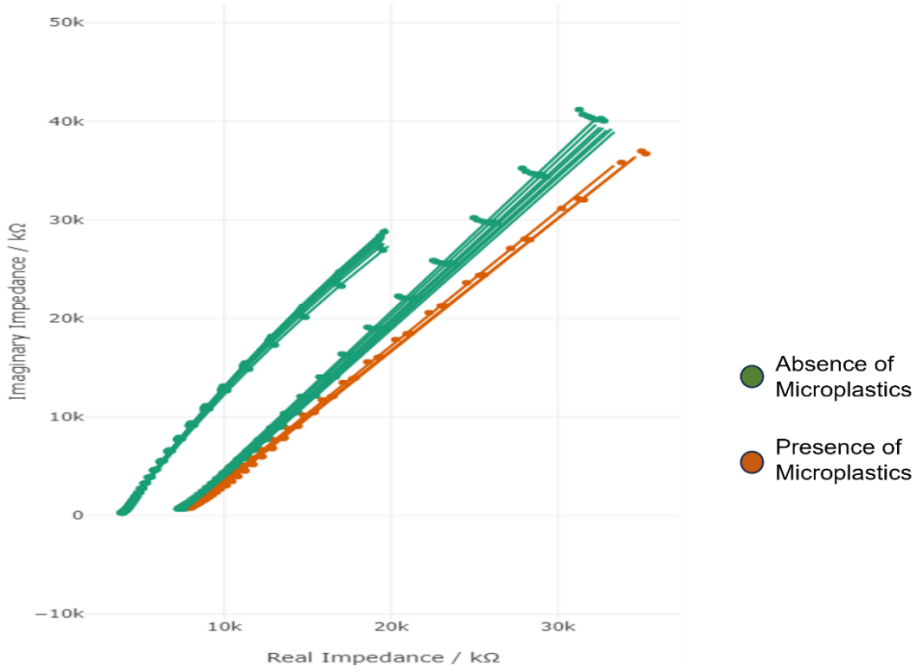

Figure 4.21 Categorized resultant raw signals for absence and presence of microplastics from EIS analysis

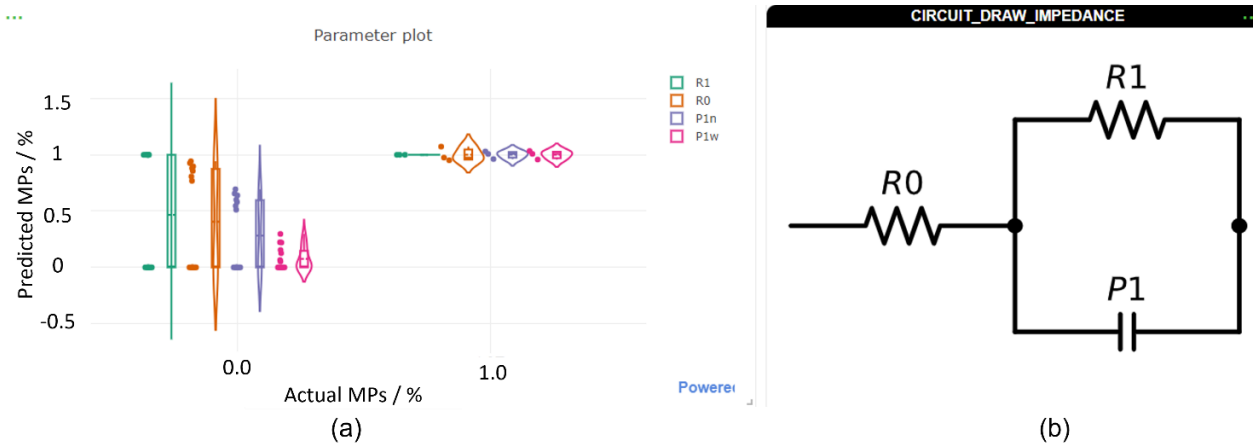

Figure 4.22 (a) Parameter plot of circuit fitting components obtained from the EIS analysis results categorized in two groups where "0.0" representing absence and "1.0" representing presence of microplastics (b) Circuit fitting for the EIS

Table 9 shows the resultant components' value in different parameters. From the table, it can also be proven that the value of R^2 is highest for P1w among the two values representing CPE together and also it is quite closer to 1. Therefore, the R^2 value of P1w can be considered for defining the coefficient threshold for the calibration analysis.

Table 9. Resultant component values in different parameters

Component	Unit	R^2	X	Intercept	Lo D
R1	kΩ	0.16	$5.332 * 10^5$	$4.668 * 10^5$	1.32
R0	kΩ	0.201	2.086	5.45	1.26
P1n	T	0.341	-0.1	0.695	0.856
P1w	Φ	0.844	$5.627 * 10^{-7}$	$2.306 * 10^{-6}$	0.308

Based on the resultant values, the following calculations can be done to define a threshold level to differentiate between the absence and presence of microplastics in the solution for this particular test.

For the absence of microplastics,

$(0.56 * 10^{-6})$ Φ * (0) + $(2.306 * 10^{-6})$ Φ = $2.306 * 10^{-6}$ Φ =2.306 μΦ

For the presence of microplastics,

$(0.56 * 10^{-6})$ Φ * (1) + $(2.306 * 10^{-6})$ Φ = $2.866 * 10^{-6}$ Φ =2.866 μΦ

From the calculation, the coefficient threshold for calibration tests can be structured as follows:

P1w < 2.306 μΦ is aqueous solution with absence of microplastics

P1w > 2.306 μΦ is aqueous solution with possible presence of microplastics

P1w > 2.866 μΦ is aqueous solution with presence of microplastics

Similar calibration analysis on different concentrations of microplastics as shown in Section 4.4.1 was also carried out. The measurements carried out for this test were done in different test setups where the aqueous solution was taken differently, and the temperature of the aqueous solution might also have been different. Also, the surface area of the electrode that was submerged into the solution was also not the same as it was for the calibration test shown previously. Table 10 shows the resultant component values of different parameters in the calibration test for different microplastic concentrations. From the table, it is evident that the R^2 value of P1n in this case is the highest among the two values representing CPE together and also it is quite closer to 1. Therefore,

for this calibration test, P1n was taken as the defining coefficient threshold. Figure 4.23 shows the resultant plot for P1n values for different microplastic concentrations.

Table 10. Resultant component values of different parameters in calibration tests for several microplastics concentration level

Component	Unit	R^2	X	Intercept	Lo D
R1	kΩ	0.979	$2.314 * 10^4$	54.76	0.018
R0	kΩ	0.974	177	2.138	0.013
P1n	T	0.975	-4.879	0.798	$5.460 * 10^{-3}$
P1w	Φ	0.594	$-3.171 * 10^{-5}$	13.3	0.092

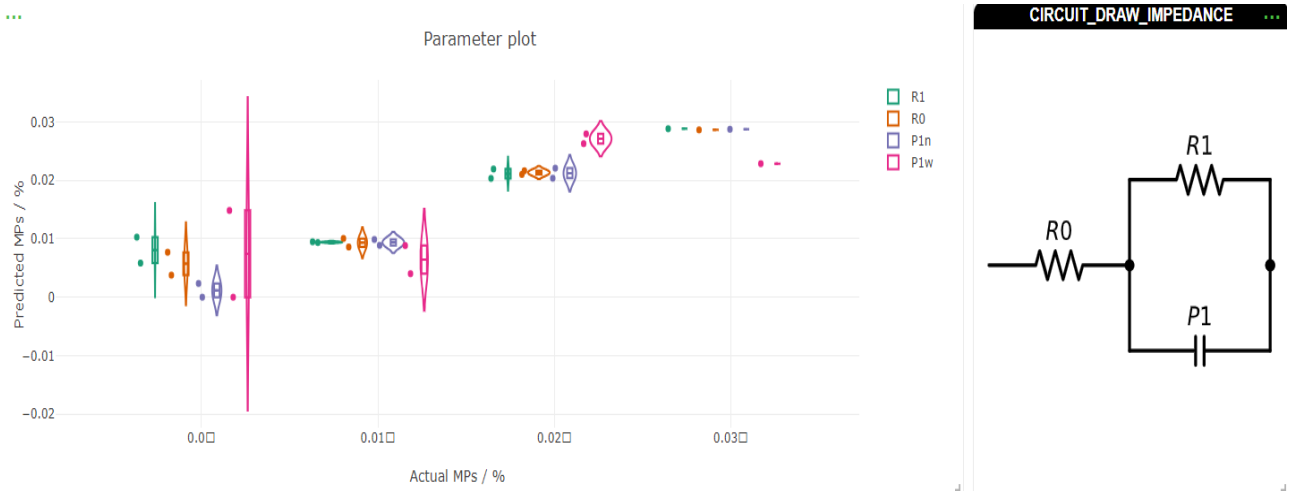

Figure 4.23 Parameter plot of P1n for different microplastics concentrations

Based on the resultant values, the following calculations can be done to define a threshold level to differentiate between different concentrations of microplastics in the solution for this particular test.

For absence of microplastics,

(-4.879) T * (0) + (0.798) T = 0.798 T

For 0.01% microplastics,

(-4.879) T * (0.01) + (0.798) T = 0.749 T

For 0.02% microplastics,

(-4.879) T * (0.02) + (0.798) T = 0.70 T

For 0.03% microplastics,

(-4.879) T * (0.03) + (0.798) T = 0.651 T

From the calculation, the coefficient threshold for calibration tests can be structured as following:

P1n ≥ 0.798 T is aqueous solution with absence of microplastics.

P1n ≈ 0.749 T is aqueous solution with presence of 0.01% microplastics concentration.

P1n ≈ 0.700 T is aqueous solution with presence of 0.02% microplastics concentration.

P1n ≈ 0.651 T is aqueous solution with presence of 0.03% microplastics concentration.

4.5 Signal Processing

Signal processing is considered to be the most crucial part of this project in order to make sense of the resultant signals obtained from different experiments and understand them properly. This section presents the pre-processing steps as well as the final stages of the signal-processing methods.

4.5.1 Microplastic Particles Count with Optical Microscope and Hemocytometer

For counting micro-particles visually, the hemocytometer is a quite helpful tool that can be used under an optical microscope. As per the methodology carried out for this step, the resultant images for a 1:10 dilution factor of microplastic particles are shown in Figure 4.24 by zooming in to one large square of the hemocytometer. Table 11 shows the estimated particles count for particular concentrations.

Here, each block consists of a certain number of microplastic particles. All 16 blocks together, would be considered as 1 large square block as shown in the figure. The resultant values are shown below:

Block 1 = 98, Block 2 = 93, Block 3 = 102, and Block 4 = 117 microparticles

Total = 410 microparticles

Total blocks in one large square = 16

Estimated total microplastics count in one large square = 410 * 4 = 1640 microparticles

Here,

Cell count Formula for Haemocytometer: Total number of particles/mL = average cell count per square (whole square containing 16 blocks) * dilution factor * 10^4

Therefore,

Total number of particles = 1640* 10 * 10^4 = 1.64*10^8/mL

= 1.64*10^5/µL

So, for 0.02%/mL microplastics concentration, Total number of particles = 20 * 1.64*10^5

$= 3.28*10^6$

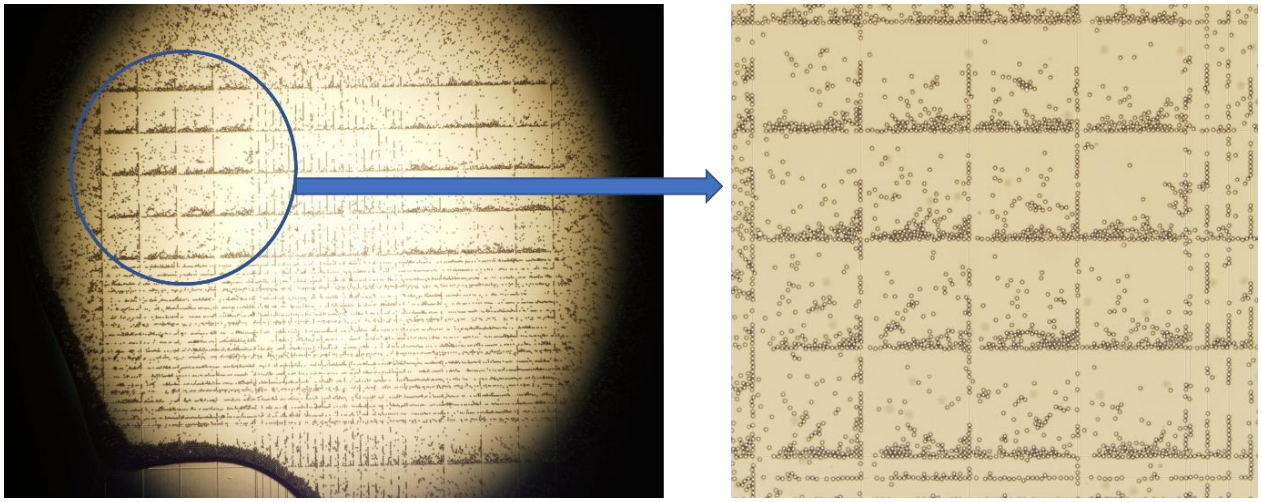

Figure 4.24 Microplastic particles on hemocytometer under the optical microscope, zoomed in to one large square

Table 11. Estimated microplastic particle count for particular concentration

Microplastics Concentration (solid% in v/v form)	Particles Count
0.01	$1.64*10^6$
0.02	$3.28*10^6$
0.03	$4.92*10^6$
0.04	$6.56*10^6$

4.5.2 Statistical Analysis of Spike Count

This section represents the statistical analysis of spike count that was carried out with Julia Programming Language.

4.5.2.1 Resultant Statistics on the Acquired Signals' Spikes

When a certain set of data consisting of different aqueous solutions (with or without microplastics, and deoxygenated solution) are compared through differentiation, their scans at each 0.05 ms time interval show the amplitude of the spike at that specific time. If a threshold is considered, a statistical representation can be attained to get the summary of how many spikes were attained above that certain threshold level. Figure 4.25 shows three differentiated signals of three

conditions overlaying on each other with a fixed threshold range. This analysis was done with Julia Programming language. Here, the X-axis displays the number of scannings required to attain a certain number of spikes, and the Y-axis displays the amplitude of the spikes. It is to be pointed out that the dataset represented in Figure 4.25 is to just visualize how the threshold range works and how the spikes above that threshold range are counted. These three signals were picked from a total dataset of 60 signals obtained from 60 measurements. Here, each condition had a contribution of 20 signals. In Figure 4.25, the threshold range was set to 7 duA/ds, which can be varied from 0 to 30 or any positive range, but only the number of spikes above the defined threshold range would be counted.

The total count of spikes for the whole dataset containing 60 signals above the defined threshold level, is represented in a statistical manner of violin plots and box plots in Figure 4.26. From this figure, it can be understood that the difference between the aqueous solution containing microplastics is hard to distinguish from the solution without microplastics by counting the spikes. The suspected reason was that the background oxygen in the aqueous media make it difficult to observe the change caused by microplastics alone. Even though the range of spike count for aqueous solution containing microplastics was slightly higher as shown in the box plot, it was still not entirely separated from the spike count range of the aqueous solution without any microplastics. However, the spike count went significantly high when the aqueous solution containing microplastics was deoxygenated. Both the box plot and the violin plot show a significant difference when the aqueous media was deoxygenated. This is because of the fact that all the background oxygen in the aqueous media was removed and only the oxygen remaining with the microplastics remain. Thus, the electrode only gets the oxygen released onto it from the microplastics when impacts occur and with no background oxygen, these spikes due to microplastics impacts cause a significant change in the resultant spike amplitude and are more distinguishable.

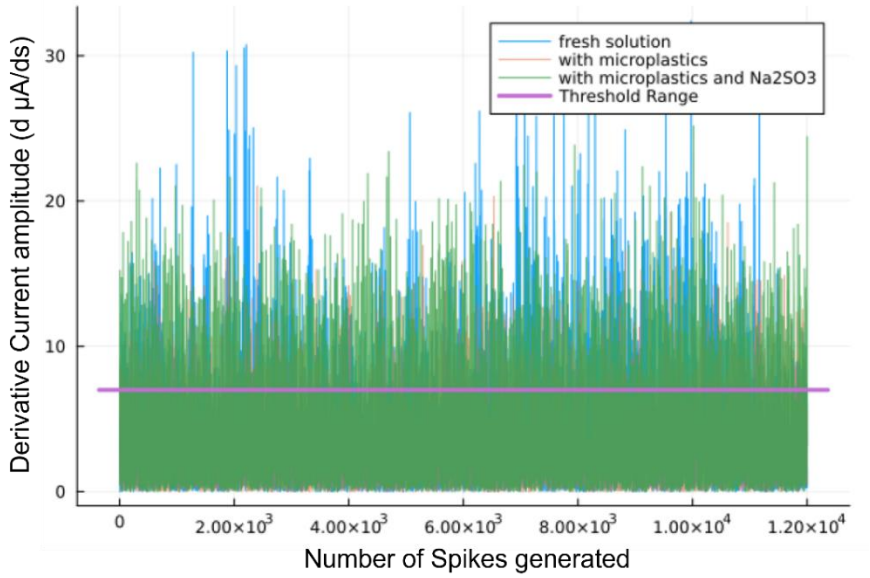

Figure 4.25 Representation of a defined threshold level 7 duA/ds in which the spikes above this threshold is counted.

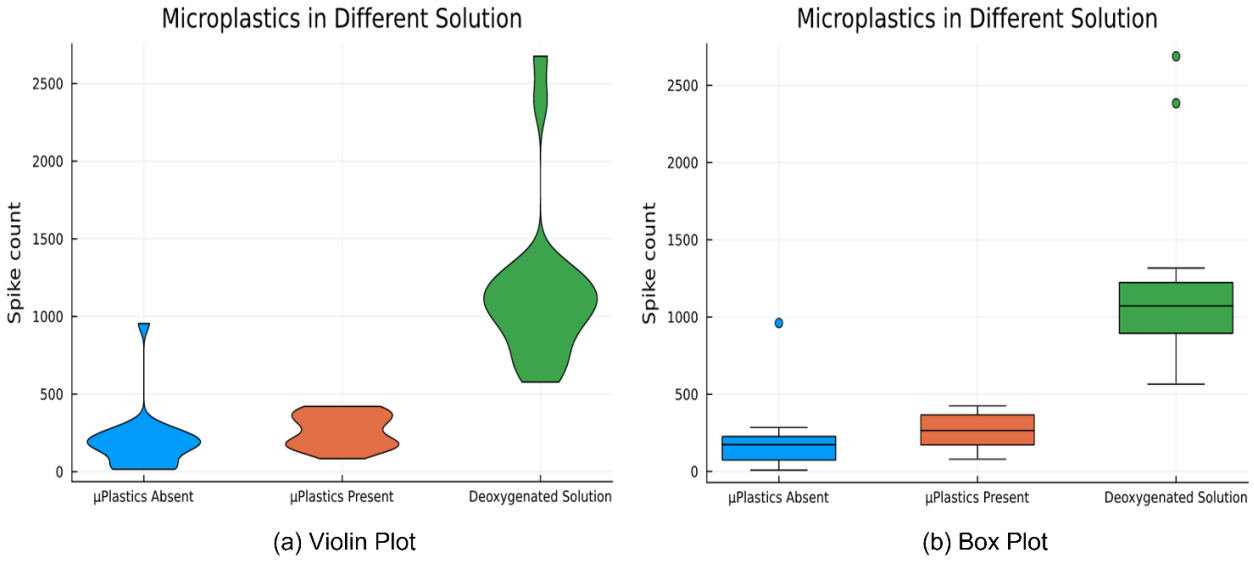

Figure 4.26 Statistical representation of Spike count above the threshold level 7 in oxygenated and deoxygenated solutions with and without microplastics.

4.5.2.2 Probable Impact Calculation

For the Type-4 electrode, it is quite difficult to count the exact number of impacts caused by the microplastics from the attained results. Also, the exact number of microplastic particles released into the aqueous solution is something that could not be pre-determined or counted with 100% accuracy. However, if some parameters were assumed with a realistic measurement so far, the probable number of microplastic particles making impacts with the electrode can be calculated.

We know,

Diameter of the Type-4 electrode = 0.04mm

The total volume of the aqueous solution = 10 mL

From the approximate count of microplastics with the optical microscope, there are $3.28 * 10^6$ particles per 0.02% concentration of microplastics and this amount was released into the 10mL aqueous solution.

Let's assume the following parameters for the sake of the calculation,

Height of the cylindrical-shaped electrode submerged into the aqueous solution = 0.5mm

Rotation speed of the solution with magnetic stirrer = 30 RPM

Now,

Radius, r = 0.04 mm / 2 = 0.02 mm.

We know, Volume of the wire = $\pi * (r)^2 *$ length

$= \pi * (0.02 \text{ mm})^2 * 0.5 \text{ mm}$

$\approx 0.0000628 \text{ mm}^3$

Number of particles hitting the wire per second = (Number of particles in the solution) * (Volume of the wire / Total volume of the solution) * (Stirring speed in revolutions per minute / 60 seconds)

$= (3.28 * 10^6 \text{ particles}) * (0.0000628 \text{ mm}^3 / 10000 \text{ mm}^3) * (30 \text{ RPM} / 60 \text{ seconds})$

$\approx (3.28 * 10^6) * (6.28 * 10^{-9}) * (0.5)$

≈ 10.3344 particles per second

Therefore, approximately 10.3344 microplastic particles would make impacts with the electrode every second.

From the calculation, it seems that there is a high possibility of microplastic particles hitting the electrode and producing such a high spike count without the interference of background oxygen.

4.5.3 Fast Fourier Transform (FFT) Analysis Results

With FFT analysis, the frequency spectrum of the recorded signal can be determined. For a specific concentration of microplastic particles released in the aqueous solution, there should be a certain frequency level associated with the impact events observed from the microplastics hitting the sensor. Figure 4.27 shows the difference between two aqueous solutions where one of them contains microplastics and the other one does not. Here, due to the presence of microplastics, there's a

significant rise in frequency between 5 Hz to 7 Hz, which is absent in the case of aqueous solution without any microplastics.

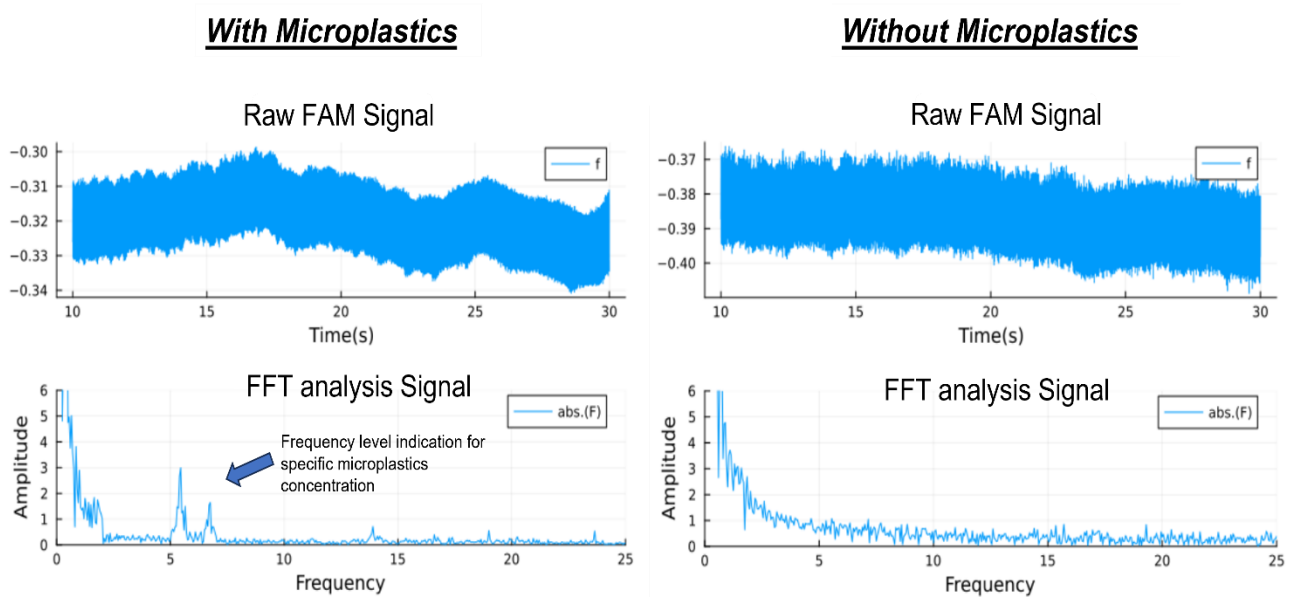

Figure 4.27 FFT analysis on raw signals obtained from FAM analysis for the aqueous solutions with microplastics and without microplastics

To verify whether this analysis was a reliable result or not, the same FAM measurement was carried out on the two solutions (with and without microplastics) multiple times to see whether the same pattern of the results repeat or not. Figure 4.28 shows the resultant plots from only FFT analysis on the obtained FAM signals. Here, it can be clearly understood that the aqueous solution with microplastics repeats the same result by showing a peak rise on the same frequency zone in almost every measurement as the concentration of microplastics remained unchanged in the solution. The frequency zone that had this peak rise was always in the 5 to 7 Hz zone with some random rise observed at other zones which were not repeated and can be neglected. On the other hand, there was no rise in any of the frequency zones for the aqueous solution without any microplastics. Multiple measurements were carried out in this solution as well to verify that these weren't random results and the final outcome proves that the results were indeed repeatable depending on the microplastic concentration of 0.005%.

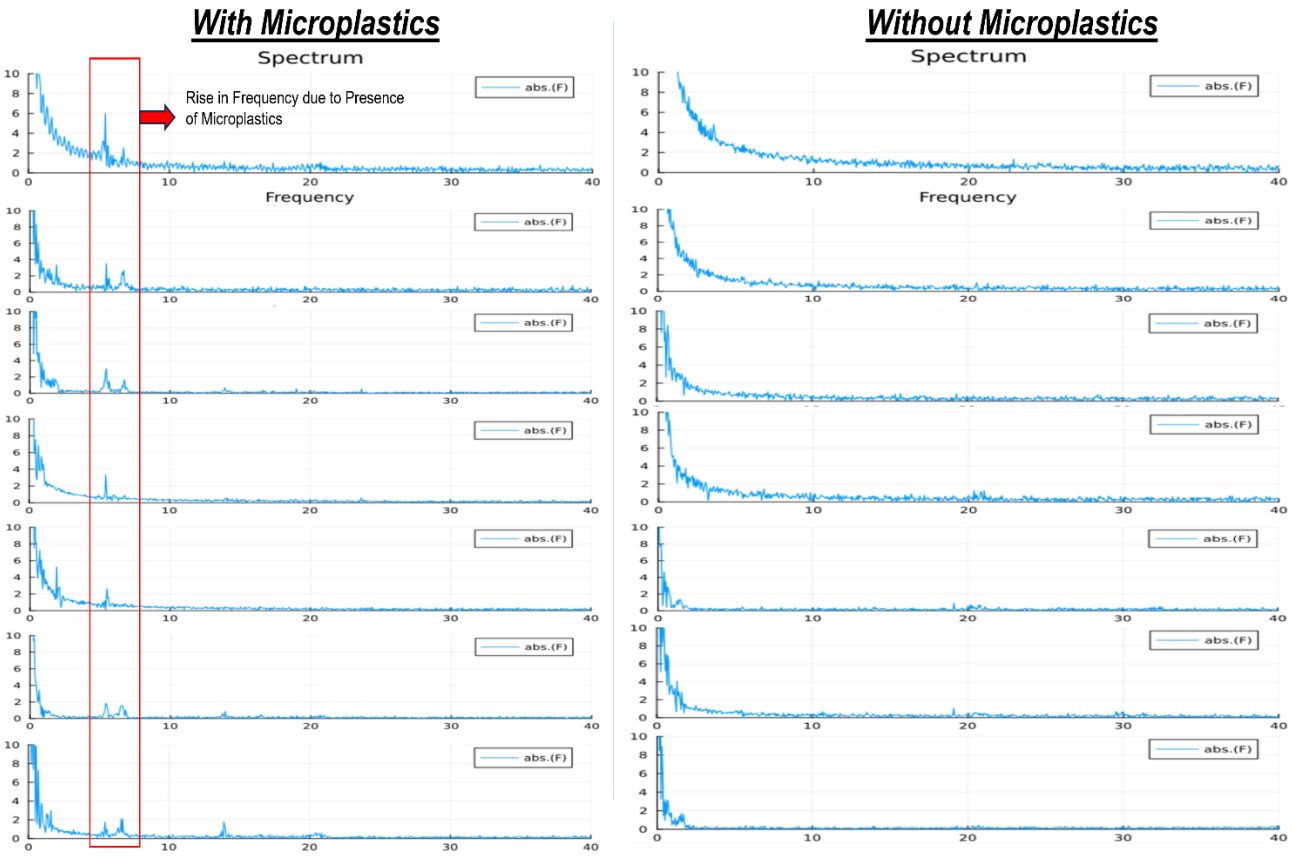

Figure 4.28 Multiple FFT Analysis results for the aqueous solutions with 0.005%/mL microplastics concentration and without any microplastics

However, the result presented above is not absolute, and there were also some exceptional results that break this pattern in some cases. Figure 4.29 shows some of these exceptions. On a statistical note, among the total number of measurements carried out for the same experiment setup, the rate of these results that break the pattern for the aqueous solution with microplastics was 26.31% and for the aqueous solution without microplastics was 26.66%. It should also be mentioned that if any of the measurements had any external disturbance in the experiment setup (e.g., external touch causing movement of the working electrode while running measurement), then the resultant signal would most likely show a disruption in the results. If Figure 4.29 was compared with the results shown in Figure 4.28, these exceptions and wrong patterns can be clearly observed as the results for the 'With Microplastics' condition didn't have the rise in frequency zone at 5 to 7 Hz whereas some random rise was observed for the 'Without Microplastics' condition.

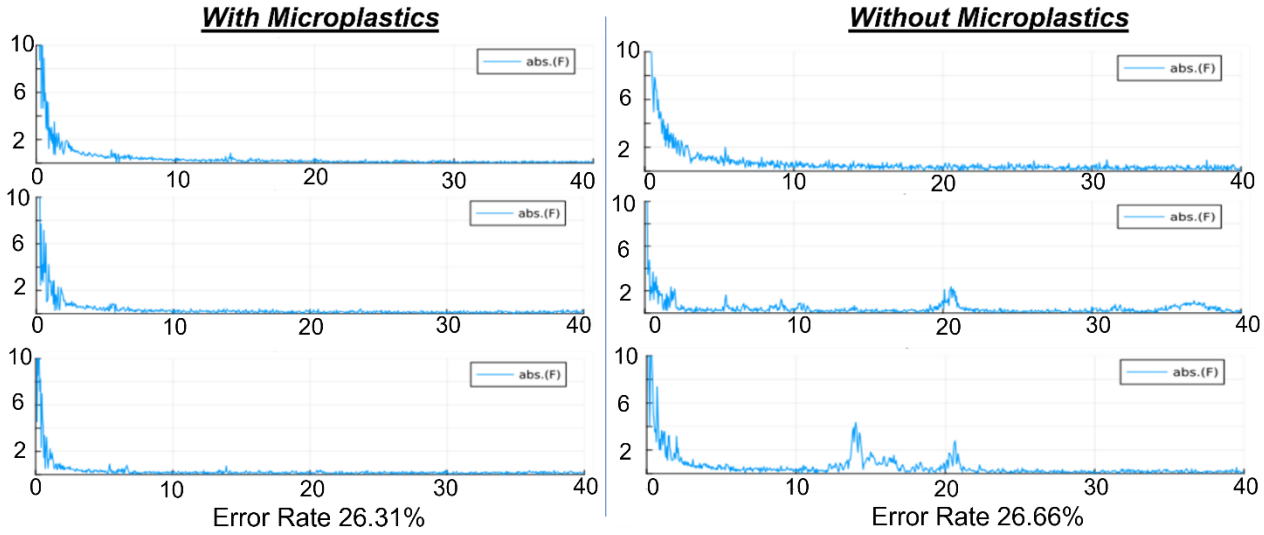

Figure 4.29 Exceptions and wrong results observed in some measurements most probably due to external interference

In order to verify whether this rise in the frequency shows any pattern of change for different microplastics concentrations, the experimental setup was modified where the concentration of microplastics was changed before running a set of measurements. Figure 4.30 shows the resultant raw FAM analysis signal along with its FFT analysis signal for the aqueous solution without any microplastics, with 20µL microplastics suspension for 0.02% microplastics concentration, 30µL microplastics suspension for 0.03% microplastics concentration, and 40µL microplastics suspension for 0.04% microplastics concentration. It is hard to find any significant pattern from the raw FAM signal. However, through FFT analysis, the resultant signal shows the difference in the frequency zone that had the rise in amplitude at a certain level. The signals obtained for aqueous solution without any microplastics, didn't have any rise in any of the frequency zone. However, for 20µL suspension, there is a significant rise observed at the 20 Hz with an amplitude of 5. In addition, for 30µL suspension, there is a significant rise observed at 21 Hz with an amplitude of 10. Lastly, for 30µL suspension, the rise was observed at 24 Hz with an amplitude of 9. Here, it should be noted that there are also rises observed at other frequency zones. But the amplitudes of the rise at these frequency zones are not the most dominant. Therefore, in the cases of multiple rises at different frequency zone, the highest amplitude rise is considered the dominant frequency zone, which is specific for certain concentration of microplastics.

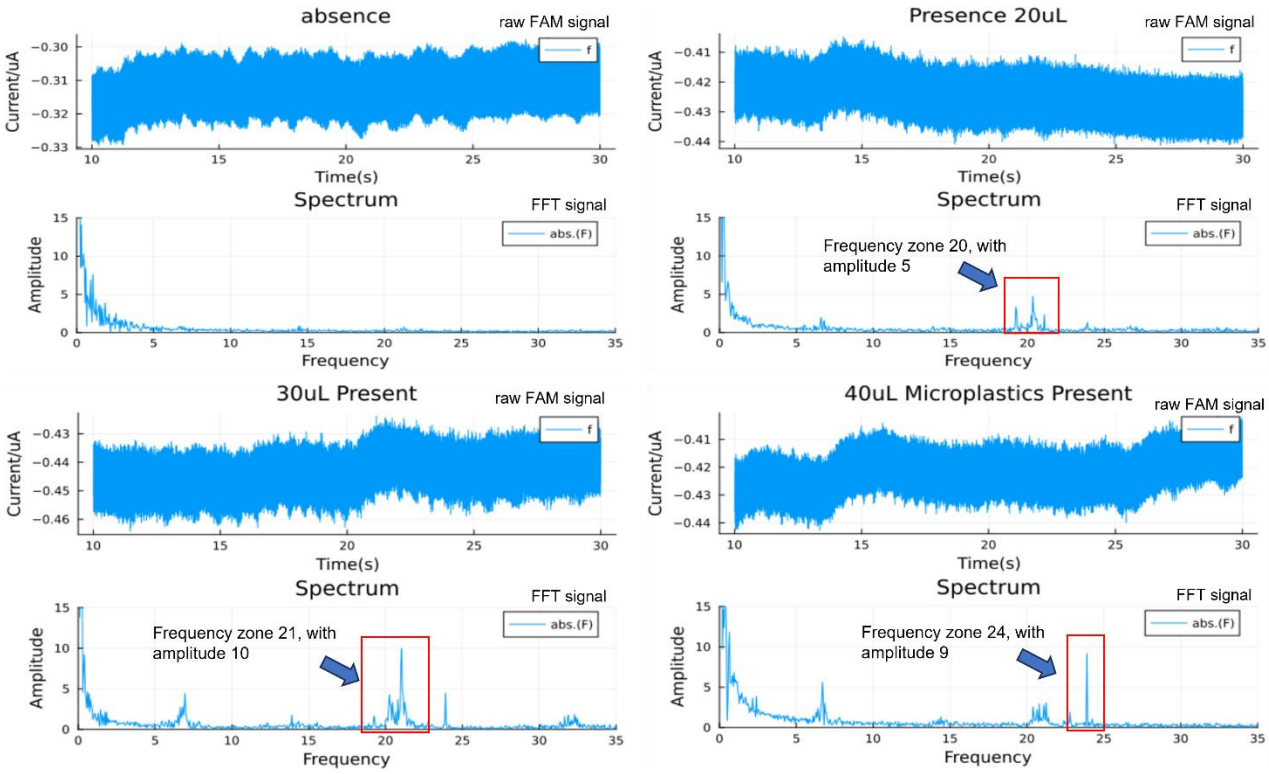

Figure 4.30 FFT analysis results on aqueous solutions at different microplastics concentration

Figure 4.31 shows multiple FFT analysis results obtained from multiple measurements carried out in the specified condition of the aqueous solution without any microplastics and with 20 µL suspension microplastics concentration. From the figure, it can be noticed that there is no significant rise at any of the frequency zone. However, the resultant FFT signals for 20 µL suspension had a significant rise at 20 Hz. Even though there are some rises at frequency zone 6.5, it is not the most dominant rise with the highest amplitude. Thus, for 20 µL suspension, the frequency zone of 20 Hz can be considered the dominant frequency zone. Furthermore, Figure 4.32 shows the resultant signals obtained from multiple FFT analyses on the obtained FAM signals from the aqueous solution with 30 µL microplastics suspension and 40 µL microplastics suspension. Here, one significant difference can be seen at 21 Hz and 24 Hz. The solution with a 30 µL microplastics concentration had peaks at both of these frequency zones, but only at 21 Hz, the results showed the highest amplitude in most of the cases. On the other hand, for 40µL suspension, the peak with the highest amplitude was at 24 Hz, even though it also had a rise at 21 Hz.

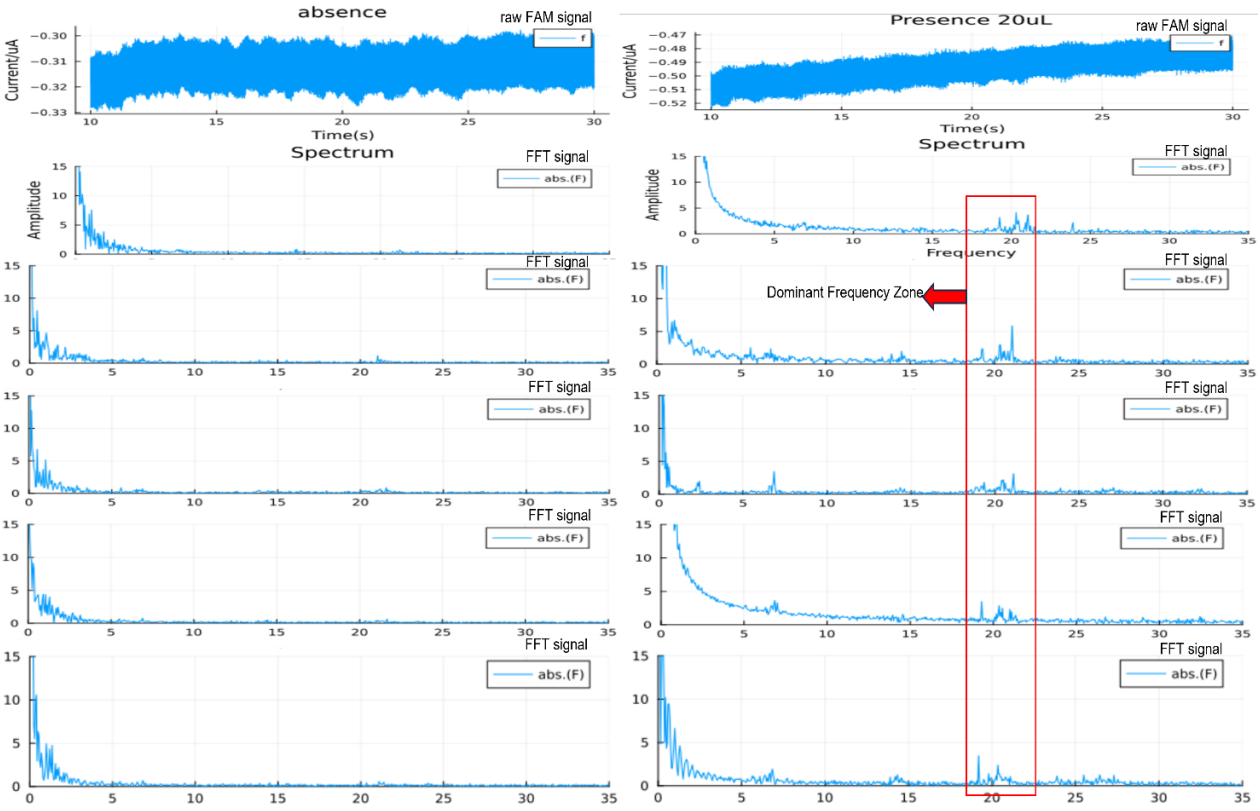

Figure 4.31 Resultant FFT signals obtained from multiple FAM signals for the aqueous solution without any microplastics and with 20µL microplastics suspension

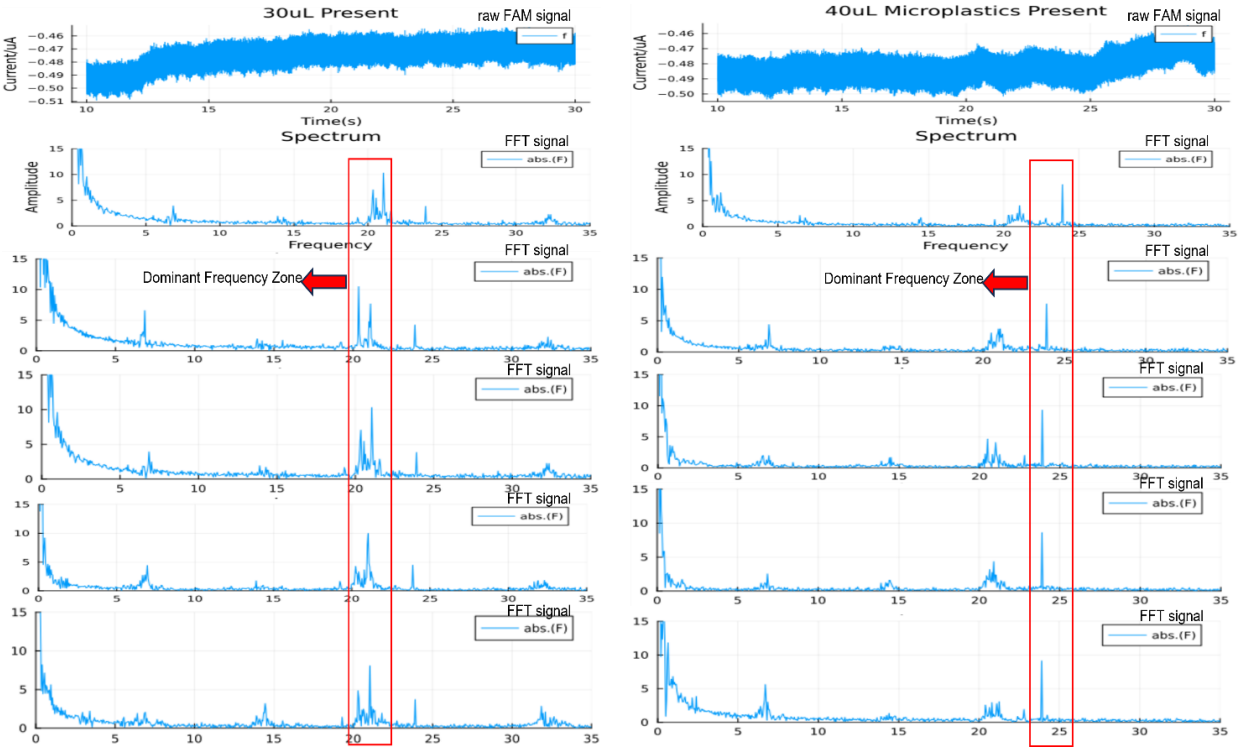

Figure 4.32 Resultant FFT signals obtained from multiple FAM signals for the aqueous solution with microplastics suspensions of 30µL and 40µL

A summarized representation is presented in Figure 4.33 showing the trendline for different frequency zone and amplitude variations that occurs when microplastic concentration is changed.

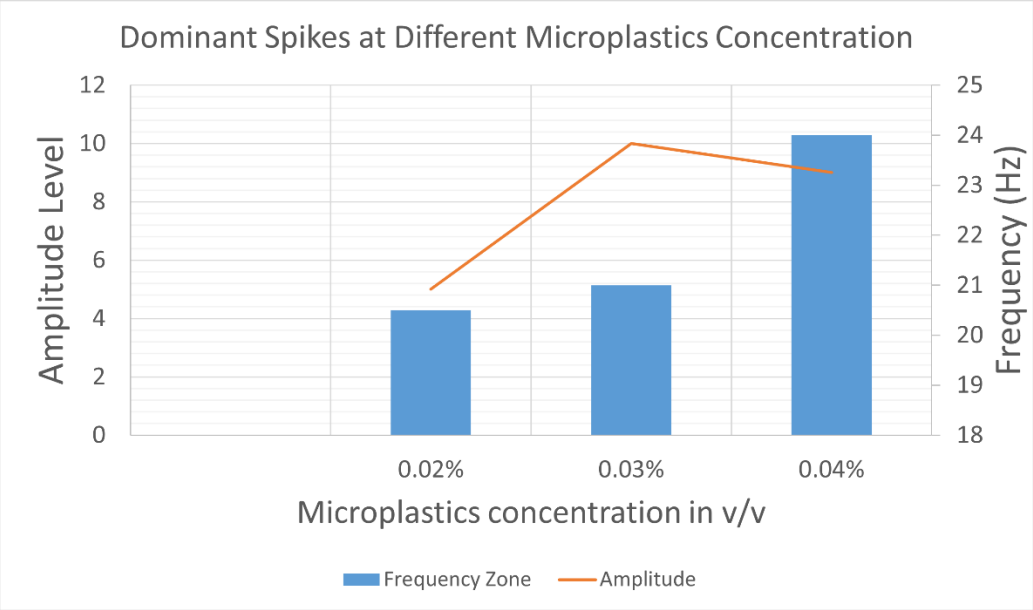

Figure 4.33 Summarized trendline representation on frequency zone and amplitude variations due to the change in microplastics concentration

In order to verify whether the microplastic particles work as oxygen carriers or not, the FFT analysis was also carried out for the deoxygenated solutions with and without microplastics. Although, previously the deoxygenation process was carried out with Na_2SO_3, this time it was carried out with $MgSO_4$. Figure 4.34 shows the resultant signals of two solutions prepared with deoxygenating agent $MgSO_4$, but only one of them contains microplastics. In the figure, it can be seen that the FFT signal for the aqueous solution containing microplastics has spikes with higher amplitudes of up to 6 in multiple frequency zone. However, such a rise of spikes was not observed in the aqueous solution without any microplastics. The $MgSO_4$ scavenges oxygen in the aqueous solution without being electrochemically active. This may have been a reason why it produces such a different result than Na_2SO_3, whereas Na_2SO_3 is electrochemically active in the aqueous solution. This also proves that the microplastics work as oxygen carriers and such behavior is more prominent when all the background oxygen in the aqueous media is removed.

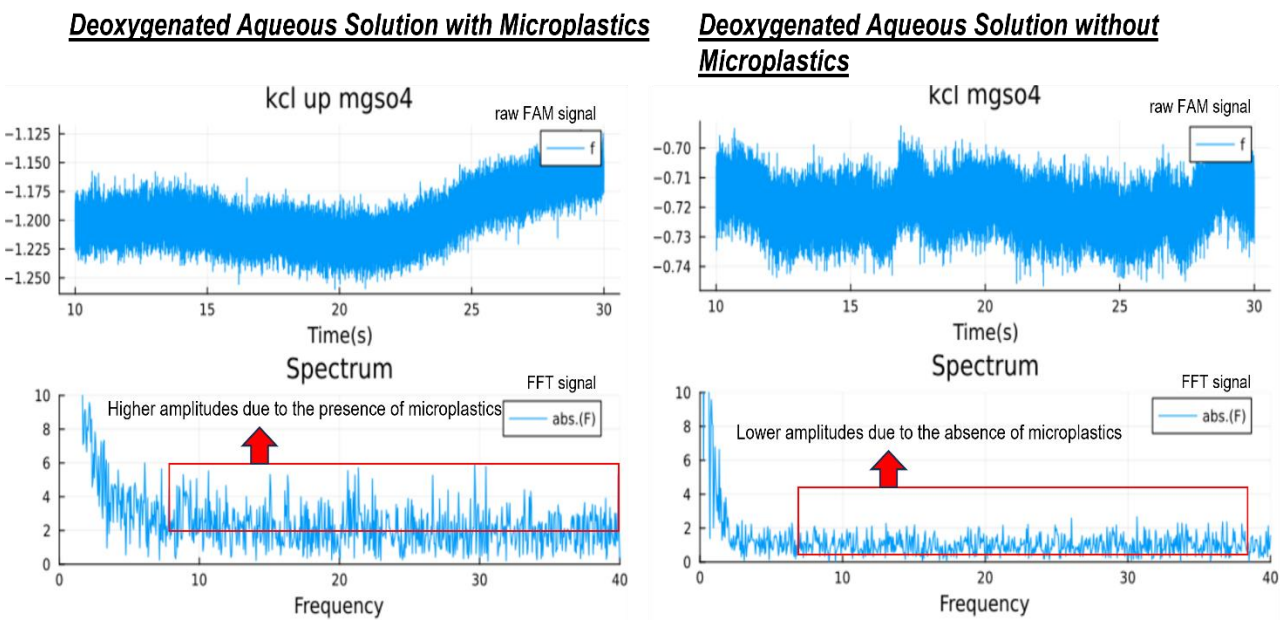

Figure 4.34 FFT analysis with deoxygenating agent $MgSO_4$ to observe the effect of microplastics without any background oxygen.

5 Discussion

This chapter discusses different aspects of the project including the challenges, limitations, advantages, and possible reasons for some of the outcomes of this project.

5.1 Comparison with other Microplastics Detection methods

There are several methods available for detecting microplastics, but almost all of them require high-tech laboratory technologies and trained personnel to operate. This project aimed to develop a simpler and cost-effective solution to detect microplastics. Figure 5.1 shows an overall comparison of the different techniques that are used for detecting microplastics in the aqueous media which were explained in Section 2.2. From the comparison, it can be clearly understood that the electrochemical sensor developed in this project does not require any high-tech laboratory facilities or any professional expertise. On the other hand, it paves the way for a detection technique that is efficient, easy to understand for general users, easier setup for analysis, low-cost, and has huge potential for large commercial usage. If the developed method is integrated fully into one system, it would become fairly easy to adopt as a microplastics concentration measuring method as it only requires the sensor to be in the aqueous concentration to run the measurement and then the analysis

would show a particular level depending on the concentration of microplastics present. For such a method, it would not require the users to have previous high-level expertise or knowledge of laboratory technologies. Instead, it would only require a simple training session for a user to use such an electrochemical sensor with the pre-defined tools and analysis method. From such a perspective, it can be envisioned as a rapid testing method to detect and determine microplastics concentrations in aqueous media. The fabrication of the sensor itself would be quite low-cost as it can be integrated into a screen printed electrode sensor. In this project, the screen printed CE and RE was used. If the WE had the structure of such a Type-4 electrode on a screen printed sensor with those Ag/AgCl CE and RE, then it would have been a functional sensor as well. For such a sensor, it would only need to be connected to a potentiostat for running the measurements. The collected data from the measurements could be easily used in a pre-defined system for spike count, FFT, and EIS analysis to determine the final results.

Detection Method	**High –Tech Lab Method**	**Requires Professional Expertise**	**Efficient and Reliable**	**Easy to understand and train on**	**Easier setup for analysis**	**Low-Cost**	**Potential large commercial use**	**Reference**
Microscopic Counting (Light microscopy, Stereomicroscope, Fluorescent microscopy, Hyperspectral imaging)	☑	☑	☑					[37]
Fourier Transform Infrared Spectroscopy (FTIR)	☑	☑	☑					[38]
Raman Spectroscopy	☑	☑	☑					[39]
Scanning Electron Microscopy (SEM)	☑	☑	☑					[40]
SEM coupled with EDS (energy dispersive x-ray spectroscopy)	☑	☑	☑					[40]
Pyrolysis GC/MS	☑	☑						[41]
Liquid Chromatography		☑						[40]
Optical Sensor				☑	☑			[43]
Thermal Analysis		☑						[45]
Surface plasmon resonance biosensor		☑	☑	☑				[46]
Electrochemical Sensor (This Work)			☑	☑	☑	☑	☑	

Figure 5.1 Comparison between different microplastic detection techniques and this work

5.2 Research outcomes

The electrochemical sensor was basically developed by taking inspiration from the work done by Shimizu et al. [6] and one of the main goals of this project was to prove the “impact concept” for detecting microplastics in the aqueous media. The reference research work utilized carbon microfiber as the WE in the aqueous media while limiting the exposure of the WE by inserting it through a pipette tip and sealing the remaining part. Inside the aqueous solution, the microplastics are suspended in a controlled test setup and each time a microplastic particle falls on the WE, it generates a spike in the acquiring chronoamperometry signal. Here, the small scale of the WE plays a crucial role to utilize low current ranging in the pA to nA level to recognize such a small particle’s impact signal. The resultant impact signal of one microplastic particle in the reference research work was 0.025 nA. Such a method can be used for counting the microplastics particles as well. Another hypothesis made by the researchers of the reference work was that the microplastics particles work as oxygen carriers and the oxygen is released onto the carbon WE upon impact.

The outcome of this project also utilized this “impact concept” with limited resources but was able to fulfill the main purpose of the project to detect changes in aqueous media caused by microplastics. Even with a large diameter compared to the reference work, the WE’s developed in this project (type 2-4) was able to utilize the “impact concept” to detect the spikes caused by microplastic particles impacting on the electrode in a manner of average scale. Here, the WE was not able to recognize each individual microplastic particle’s impact on a significant scale as the reference work by Shimizu et al., but it was able to detect the impacts over a longer period of time and the difference can be noticed when all the spikes above a certain threshold are counted and compared against the solution with no microplastics particles. Therefore, the developed method in this project might not be able to detect microplastic particles individually, but it can detect the overall concentration of the microplastics particles. Utilizing the FFT analysis, the results can be well defined to better represent this concentration level of the microplastics. For certain concentrations of microplastics, the FFT analysis would produce a specific frequency level that only represents the particular microplastics concentration. If the concentration is changed, this frequency level also changes accordingly to a lower level or higher level. In order to verify the hypothesis made in the reference work regarding microplastics acting as the oxygen carrier, the aqueous solution was deoxygenated in this project to remove all the background oxygen in the aqueous solution. In such a case, the amplitude of impact signals and spike count raised significantly. This could indicate the validity of the hypothesis as well, but the deoxygenation process used in this project might not be

the most accurate approach as the chemicals might cause some electrochemical effect that may deviate from the results.

For the CV analysis of the carbon electrode that produces the signature 'duck-shaped' plot, the anodic peak and cathodic peak occur due to the oxidative electrochemical reaction. Assuming the electrolyzing species are reversible, a lot of products are accumulated from the oxidation and then the initial state is achieved again through a reduction. The potential going negative of the reversal potential (midway between the two peaks) motivates the reaction to go in the opposite direction. When a conducting wire or fibre is not properly coated with carbon, disruption occurs in these oxidative electrochemical reactions, and the signature 'duck-shaped' plot is not attained. In this case, as the surface of the electrode does not have the same material in all surface areas, the same reaction can't take place in contrast to the materials of the electrode and the species present in the media.

At the 100 seconds of the multi-step amperometry analysis measurement presented in section 4.3.4, microplastics were added to the aqueous solution and the resultant signal was getting larger afterward. This could be because of a cumulative effect of the WE absorbing the oxygen from the microplastics, releasing afterward, and then absorbing more again at the next scan. Another possible reason could be some kind of element was being deposited or growing on the electrode electrochemically. However, these hypotheses were not investigated further in the project to confirm their validity entirely.

On the other hand, this project also utilized the EIS analysis to detect and quantify microplastics in the aqueous solution, which was not done by Shimizu et al. [6] in their work. A similar approach was made by Du et al. [65] to detect microplastics concentrations in aqueous media using graphene electrodes through EIS analysis. However, there are some inconsistencies in their work that can be noticed. One of them was that the applied electrode potential for their EIS analysis was not clear. One of their focuses was to prove that the EIS signal would change by varying the microplastics concentration for different sizes of the microplastics particles. Nonetheless, some of the resultant graphs did not have a consistent scale on the X and Y axis without any specific reason. This makes an uncertainty about the obtained results whether the variations in their obtained EIS signal were caused by the microplastics concentration change, or it might have been just because of the electrode itself. In this thesis project, the EIS analysis was carried out without changing or varying any of the parameters except for the microplastics concentration. The electrode settings were kept the same with the same submerged area in the aqueous solution. All the results were obtained without showing any inconsistencies in the scale of the X and Y axis. The results also indicate that the

impedance of the aqueous solution changes when the concentration of microplastics is varied. For calibration tests that were carried out, it was found that the calibration coefficient threshold has a significant dependency on the test setup as different test setups with variations in submerged electrode area, the temperature of the solution during a test, instrument-induced noise, and other variables cause the calibration coefficient to be different. For the calibration tests, the CPE elements that had the highest R^2 value were taken as the reference parameter. Such a selection procedure makes the calibration step easier and more effective. However, the calibration coefficient threshold for one particular test setup cannot be used for other tests. Therefore, it is a limitation of this method as well that a universal threshold level can't be defined with the utilized test setup.

5.3 Challenges, Limitations, and Possible Reasons

The project was basically developed from a concept to detect microplastics with an electrochemical sensor. Since there was not much work done on such a topic, it was a big challenge to understand different concepts and figure out the steps to develop such a sensor. When a problem arises, different options were considered to solve the problem and all of the options were practically tried out to finally figure out the most effective solution.

The reference work by Shimizu et al. utilized a carbon fibre electrode with a length of 1 mm and a diameter of 7 µm. This carbon fibre was manufactured by another company that has the technology to produce such carbon microfibers. However, for this project, carbon microfiber in such a low diameter was not available. Therefore, the wires or fibres at the smallest diameter were searched for in the in-house laboratory facilities and the smallest available wires or fibres were used for developing the working electrode. Thus, conductor string (Type-1, Type-2, Type-3) from electrical wire or fibre (Type-4) was coated with carbon paste to develop working electrodes. The lowest diameter possible to attain in such a case was 40 µm, which is quite large compared to the reference work. Therefore, it wasn't possible to attain the feature of individual microplastic particle counting using the developed WE, but it would have been possible to attain such a feature with a carbon microfiber in this project. Such a hypothesis was not fully proven in this project as the working electrode has too large a diameter to recognize particles of such small scales. However, the developed electrode proves to be able to detect microplastic concentration levels in the aqueous media collectively. So it proves to be an effective tool to detect microplastics.

Although the accuracy of the developed working electrode is not high enough, it could have been possible to obtain more accurate results if carbon nanofibers were available for use in this project. In

addition, the reference research paper hypothesized that such nanofibers can be used for detecting microplastic particles individually and counting them one by one through each impact caused by the particles individually. Such a hypothesis was not fully proven in this project as the working electrode has too large a diameter to recognize particles of such small scales. In addition, to mitigate the electrochemical issues with the deoxygenation process carried out in this project, the deoxygenation process could be carried out using argon gas. However, this approach was also not possible to carry out in this thesis work due to resource and time constraints.

Furthermore, due to the large diameter of the working electrode, the current range could not be brought down to a much lower level as such a large electrode is conducting current through it, it tends to conduct in a higher range. Thus, for this project, the minimum effective current range was attained at 100 nA for FAM analysis, and most of the measurements were carried out in this range. If carbon nanofiber was used as the working electrode, it might have been possible to bring the current range to an even lower level of pA range which is suspected to be the effective level for observing microplastics impact individually.

6 Conclusion and Future Works

Through this research work, an electrochemical sensor was developed to detect microplastics in aqueous media. The findings from this project supports that the “impact concept” can be considered as an effective method to detect microplastics in aqueous media. The findings also prove that the microplastic particles work as oxygen carriers and this characteristic may become more prominent when all the background oxygen in the aqueous media is absent. The working electrode absorbs the released oxygen from the microplastic particles and then releases it to produce hydrogen peroxide. This reaction generates the signal which is obtained as the “spike” in the FAM analysis. Combining FFT analysis and FAM analysis, the concentration of microplastics can be determined. The developed working electrode for this project proved to be a feasible part of the sensor’s mechanism. However, if the diameter of the WE were below or equal to 7 µm, one can assume that the accuracy of the system would have been better in detecting individual microplastic particles according to Shimizu et al. The research work also utilized impedance spectroscopy to prove that the developed sensor could detect the impedance of an aqueous solution containing microplastics and it can detect the change in concentration of microplastics.

The impact concept utilizing amperometry and FFT does not require very sophisticated electronics and it is quite a simple technique that could be used for detecting microplastics in

aqueous media. But it depends on a narrow current window to detect the impact and doesn't provide much mechanistic information as EIS. On the other hand, the EIS analysis also proved to be able to detect different microplastics concentrations and more information can be acquired by this method. However, it requires more sophisticated conditioning and readout circuitry and is highly dependent on the test setup as electrode submergence length, shielding, solution temperature, etc. affect the impedance, especially at high frequencies. Therefore, it can be concluded with the suggestion that both of these techniques (impact concept and EIS) should be improved and integrated together for an effective and highly efficient electrochemical microplastics detection method.

As for future work, the developed WE was used as a separate part of the sensor and it was not integrated with the RE and CE in the form of a screen-printed electrode. Therefore, much work can be done on this aspect of the project as well. Figure 6.1 shows an envisioned design that could be a possible model for a screen-printed sensor to detect microplastics in aqueous media. The working electrode of the envisioned sensor should be a free-standing electrode that should be exposed to the aqueous media from all angles. The reason behind such a concept is that the microplastic particles can flow and make impacts with the working electrode from any direction. If the exposed WE was printed on a flat surface, it would've constrained the ability of the WE to recognize half of the possible impacts as a flat surface only has the electrodes with only one side exposed.

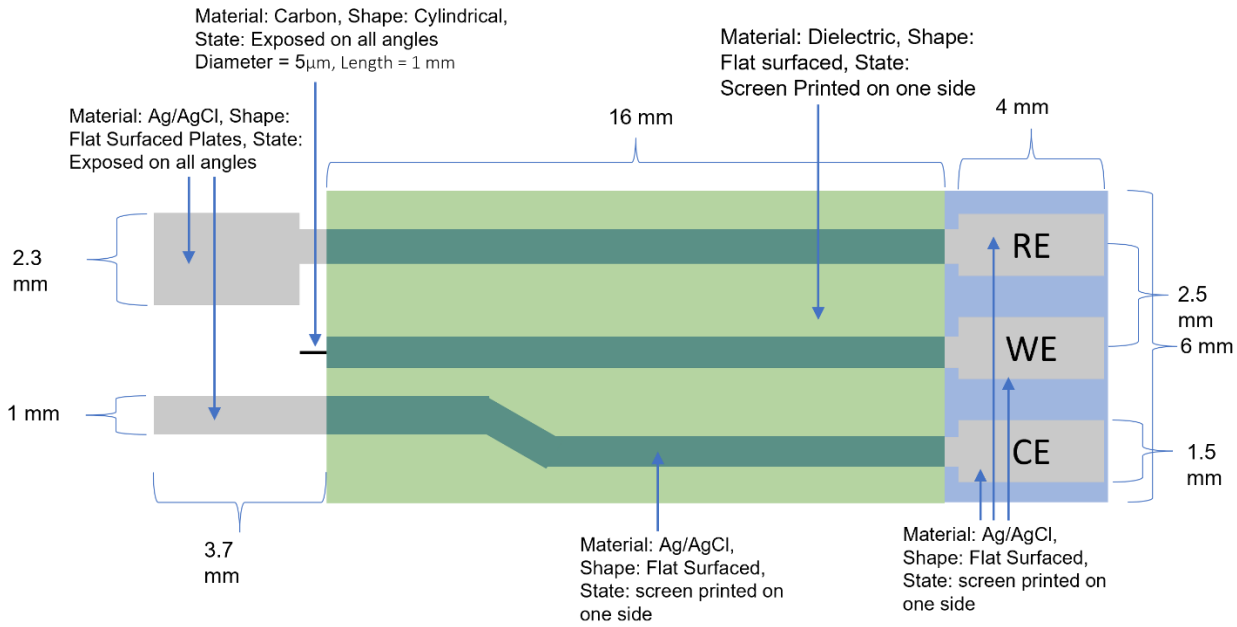

Figure 6.1 Envisioned design for screen printed sensor to detect microplastics in aqueous media

Another aspect of possible future work could be merging the developed electrochemical sensor with a microfluidic channel chamber where the microplastic particles would be guided toward the sensor by the acoustic actuator. Figure 6.2 shows a simulation of the envisioned microfluidic channel chamber. The sensor's WE would be placed in the microfluidic channel which would carry the microplastic particles. The microplastic particles would make an impact on the WE as they flow through the microfluidic channel.

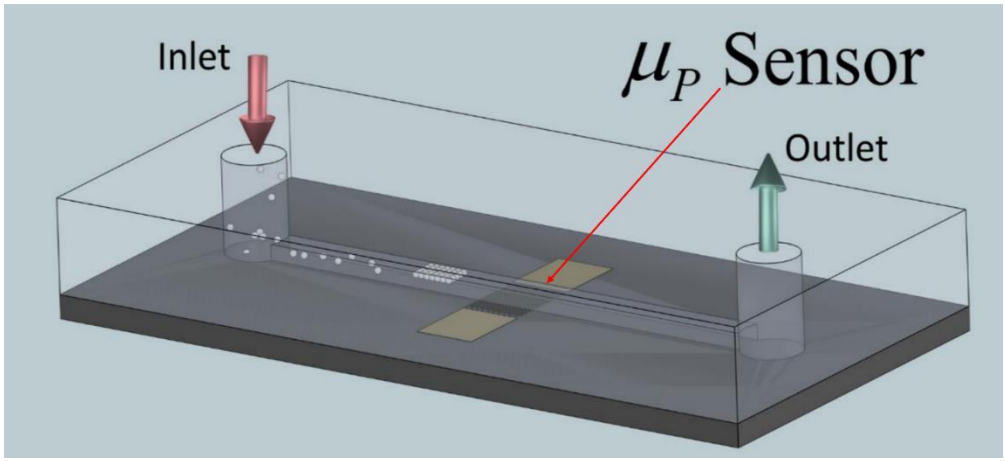

Figure 6.2 Envisioned microfluidic channel chamber that could be integrated with the electrochemical sensor to detect microplastics in aqueous media [66]

References

[1] C. M. Rochman *et al.*, 'Rethinking microplastics as a diverse contaminant suite', *Environ. Toxicol. Chem.*, vol. 38, no. 4, pp. 703–711, 2019, doi: 10.1002/etc.4371.

[2] A. A. Horton, A. Walton, D. J. Spurgeon, E. Lahive, and C. Svendsen, 'Microplastics in freshwater and terrestrial environments: Evaluating the current understanding to identify the knowledge gaps and future research priorities', *Sci. Total Environ.*, vol. 586, pp. 127–141, May 2017, doi: 10.1016/j.scitotenv.2017.01.190.

[3] J. R. Jambeck *et al.*, 'Plastic waste inputs from land into the ocean', *Science*, vol. 347, no. 6223, pp. 768–771, Feb. 2015, doi: 10.1126/science.1260352.

[4] D. Eerkes-Medrano, R. C. Thompson, and D. C. Aldridge, 'Microplastics in freshwater systems: A review of the emerging threats, identification of knowledge gaps and prioritisation of research needs', *Water Res.*, vol. 75, pp. 63–82, May 2015, doi: 10.1016/j.watres.2015.02.012.

[5] R. C. Thompson, C. J. Moore, F. S. vom Saal, and S. H. Swan, 'Plastics, the environment and human health: current consensus and future trends', *Philos. Trans. R. Soc. B Biol. Sci.*, vol. 364, no. 1526, pp. 2153–2166, Jul. 2009, doi: 10.1098/rstb.2009.0053.

[6] K. Shimizu, S. V. Sokolov, E. Kätelhön, J. Holter, N. P. Young, and R. G. Compton, 'In situ Detection of Microplastics: Single Microparticle-electrode Impacts', *Electroanalysis*, vol. 29, no. 10, pp. 2200–2207, 2017, doi: 10.1002/elan.201700213.

[7] J. G. B. Derraik, 'The pollution of the marine environment by plastic debris: a review', *Mar. Pollut. Bull.*, vol. 44, no. 9, pp. 842–852, Sep. 2002, doi: 10.1016/S0025-326X(02)00220-5.

[8] 'Plastics - the Facts 2022 • Plastics Europe', *Plastics Europe*. https://plasticseurope.org/knowledge-hub/plastics-the-facts-2022/ (accessed Jun. 21, 2023).

[9] D. K. A. Barnes, F. Galgani, R. C. Thompson, and M. Barlaz, 'Accumulation and fragmentation of plastic debris in global environments', *Philos. Trans. R. Soc. B Biol. Sci.*, vol. 364, no. 1526, pp. 1985–1998, Jul. 2009, doi: 10.1098/rstb.2008.0205.

[10] P. G. Ryan, C. J. Moore, J. A. van Franeker, and C. L. Moloney, 'Monitoring the abundance of plastic debris in the marine environment', *Philos. Trans. R. Soc. B Biol. Sci.*, vol. 364, no. 1526, pp. 1999–2012, Jul. 2009, doi: 10.1098/rstb.2008.0207.

[11] A. L. Andrady, 'Microplastics in the marine environment', *Mar. Pollut. Bull.*, vol. 62, no. 8, pp. 1596–1605, Aug. 2011, doi: 10.1016/j.marpolbul.2011.05.030.

[12] M. A. Browne, T. S. Galloway, and R. C. Thompson, 'Spatial Patterns of Plastic Debris along Estuarine Shorelines', *Environ. Sci. Technol.*, vol. 44, no. 9, pp. 3404–3409, May 2010, doi: 10.1021/es903784e.

[13] A. Bahraini, '7 Types of Plastic that You Need to Know', *Waste4Change*, Jul. 17, 2018. https://waste4change.com/blog/7-types-plastic-need-know/ (accessed Jun. 21, 2023).

[14] IFREMER *et al.*, *Marine strategy framework directive : task group 10 report (marine litter - april 2010)*. LU: Publications Office of the European Union, 2010. Accessed: Jun. 21, 2023. [Online]. Available: https://data.europa.eu/doi/10.2788/86941

[15] A. A. Koelmans, N. H. Mohamed Nor, E. Hermsen, M. Kooi, S. M. Mintenig, and J. De France, 'Microplastics in freshwaters and drinking water: Critical review and assessment of data quality', *Water Res.*, vol. 155, pp. 410–422, May 2019, doi: 10.1016/j.watres.2019.02.054.

[16] J. Li, H. Liu, and J. Paul Chen, 'Microplastics in freshwater systems: A review on occurrence, environmental effects, and methods for microplastics detection', *Water Res.*, vol. 137, pp. 362–374, Jun. 2018, doi: 10.1016/j.watres.2017.12.056.

[17] G. Liebezeit and E. Liebezeit, 'Non-pollen particulates in honey and sugar', *Food Addit. Contam. Part A*, vol. 30, no. 12, pp. 2136–2140, Dec. 2013, doi: 10.1080/19440049.2013.843025.

[18] G. Liebezeit and E. Liebezeit, 'Synthetic particles as contaminants in German beers', *Food Addit. Contam. Part A*, vol. 31, no. 9, pp. 1574–1578, Sep. 2014, doi: 10.1080/19440049.2014.945099.
[19] A. Karami, A. Golieskardi, C. Keong Choo, V. Larat, T. S. Galloway, and B. Salamatinia, 'The presence of microplastics in commercial salts from different countries', *Sci. Rep.*, vol. 7, no. 1, Art. no. 1, Apr. 2017, doi: 10.1038/srep46173.
[20] E. Besseling *et al.*, 'Microplastic in a macro filter feeder: Humpback whale Megaptera novaeangliae', *Mar. Pollut. Bull.*, vol. 95, no. 1, pp. 248–252, Jun. 2015, doi: 10.1016/j.marpolbul.2015.04.007.
[21] C. J. Foley, Z. S. Feiner, T. D. Malinich, and T. O. Höök, 'A meta-analysis of the effects of exposure to microplastics on fish and aquatic invertebrates', *Sci. Total Environ.*, vol. 631–632, pp. 550–559, Aug. 2018, doi: 10.1016/j.scitotenv.2018.03.046.
[22] C. G. Alimba and C. Faggio, 'Microplastics in the marine environment: Current trends in environmental pollution and mechanisms of toxicological profile', *Environ. Toxicol. Pharmacol.*, vol. 68, pp. 61–74, May 2019, doi: 10.1016/j.etap.2019.03.001.
[23] D. Lithner, Å. Larsson, and G. Dave, 'Environmental and health hazard ranking and assessment of plastic polymers based on chemical composition', *Sci. Total Environ.*, vol. 409, no. 18, pp. 3309–3324, Aug. 2011, doi: 10.1016/j.scitotenv.2011.04.038.
[24] C. M. Rochman, 'The Complex Mixture, Fate and Toxicity of Chemicals Associated with Plastic Debris in the Marine Environment', in *Marine Anthropogenic Litter*, M. Bergmann, L. Gutow, and M. Klages, Eds., Cham: Springer International Publishing, 2015, pp. 117–140. doi: 10.1007/978-3-319-16510-3_5.
[25] A. Lusher, P. C. H. Hollman, and J. Mendoza-Hill, *Microplastics in fisheries and aquaculture: status of knowledge on their occurrence and implications for aquatic organisms and food safety*. in FAO fisheries and aquaculture technical paper, no. 615. Rome: Food and Agriculture Organization of the United Nations, 2017.
[26] J.-P. W. Desforges, M. Galbraith, and P. S. Ross, 'Ingestion of Microplastics by Zooplankton in the Northeast Pacific Ocean', *Arch. Environ. Contam. Toxicol.*, vol. 69, no. 3, pp. 320–330, Oct. 2015, doi: 10.1007/s00244-015-0172-5.
[27] A. L. Lusher, M. McHugh, and R. C. Thompson, 'Occurrence of microplastics in the gastrointestinal tract of pelagic and demersal fish from the English Channel', *Mar. Pollut. Bull.*, vol. 67, no. 1, pp. 94–99, Feb. 2013, doi: 10.1016/j.marpolbul.2012.11.028.
[28] A. Ragusa *et al.*, 'Plasticenta: First evidence of microplastics in human placenta', *Environ. Int.*, vol. 146, p. 106274, Jan. 2021, doi: 10.1016/j.envint.2020.106274.
[29] F. J. Kelly and J. C. Fussell, 'Toxicity of airborne particles—established evidence, knowledge gaps and emerging areas of importance', *Philos. Trans. R. Soc. Math. Phys. Eng. Sci.*, vol. 378, no. 2183, p. 20190322, Sep. 2020, doi: 10.1098/rsta.2019.0322.
[30] '4.4: Studying Cells - Cell Size', *Biology LibreTexts*, Jul. 05, 2018. https://bio.libretexts.org/Bookshelves/Introductory_and_General_Biology/Book%3A_General_Biology_(Boundless)/04%3A_Cell_Structure/4.04%3A_Studying_Cells_-_Cell_Size (accessed Jun. 24, 2023).
[31] C. Q. Y. Yong, S. Valiyaveettil, and B. L. Tang, 'Toxicity of Microplastics and Nanoplastics in Mammalian Systems', *Int. J. Environ. Res. Public. Health*, vol. 17, no. 5, Art. no. 5, Jan. 2020, doi: 10.3390/ijerph17051509.
[32] S. L. Wright and F. J. Kelly, 'Plastic and Human Health: A Micro Issue?', *Environ. Sci. Technol.*, vol. 51, no. 12, pp. 6634–6647, Jun. 2017, doi: 10.1021/acs.est.7b00423.
[33] 'Fourier Transform Infrared Spectroscopic Analysis of Protein Secondary Structures', *Acta Biochim. Biophys. Sin.*, pp. 549–559, Aug. 2007, doi: 10.1111/j.1745-7270.2007.00320.x.

[34] ‘What is FTIR Spectroscopy?’ https://www.sigmaaldrich.com/NO/en/technical-documents/technical-article/analytical-chemistry/photometry-and-reflectometry/ftir-spectroscopy (accessed Jun. 24, 2023).
[35] Granite, ‘What is Raman Spectroscopy? | Raman Spectroscopy Principle’, *Edinburgh Instruments*. https://www.edinst.com/blog/what-is-raman-spectroscopy/ (accessed Jun. 24, 2023).
[36] S. Nie and S. R. Emory, ‘Probing Single Molecules and Single Nanoparticles by Surface-Enhanced Raman Scattering’, *Science*, vol. 275, no. 5303, pp. 1102–1106, Feb. 1997, doi: 10.1126/science.275.5303.1102.
[37] C. M. Free, O. P. Jensen, S. A. Mason, M. Eriksen, N. J. Williamson, and B. Boldgiv, ‘High-levels of microplastic pollution in a large, remote, mountain lake’, *Mar. Pollut. Bull.*, vol. 85, no. 1, pp. 156–163, Aug. 2014, doi: 10.1016/j.marpolbul.2014.06.001.
[38] A. Turner and L. Holmes, ‘Occurrence, distribution and characteristics of beached plastic production pellets on the island of Malta (central Mediterranean)’, *Mar. Pollut. Bull.*, vol. 62, no. 2, pp. 377–381, Feb. 2011, doi: 10.1016/j.marpolbul.2010.09.027.
[39] F. Collard, B. Gilbert, G. Eppe, E. Parmentier, and K. Das, ‘Detection of Anthropogenic Particles in Fish Stomachs: An Isolation Method Adapted to Identification by Raman Spectroscopy’, *Arch. Environ. Contam. Toxicol.*, vol. 69, no. 3, pp. 331–339, Oct. 2015, doi: 10.1007/s00244-015-0221-0.
[40] Z.-M. Wang, J. Wagner, S. Ghosal, G. Bedi, and S. Wall, ‘SEM/EDS and optical microscopy analyses of microplastics in ocean trawl and fish guts’, *Sci. Total Environ.*, vol. 603–604, pp. 616–626, Dec. 2017, doi: 10.1016/j.scitotenv.2017.06.047.
[41] M. Funck, A. Yildirim, C. Nickel, J. Schram, T. C. Schmidt, and J. Tuerk, ‘Identification of microplastics in wastewater after cascade filtration using Pyrolysis-GC–MS’, *MethodsX*, vol. 7, p. 100778, Jan. 2020, doi: 10.1016/j.mex.2019.100778.
[42] E. Hengstmann and E. K. Fischer, ‘Nile red staining in microplastic analysis—proposal for a reliable and fast identification approach for large microplastics’, *Environ. Monit. Assess.*, vol. 191, no. 10, p. 612, Sep. 2019, doi: 10.1007/s10661-019-7786-4.
[43] B. O. Asamoah, B. Kanyathare, M. Roussey, and K.-E. Peiponen, ‘A prototype of a portable optical sensor for the detection of transparent and translucent microplastics in freshwater’, *Chemosphere*, vol. 231, pp. 161–167, Sep. 2019, doi: 10.1016/j.chemosphere.2019.05.114.
[44] A. H. Iri *et al.*, ‘Optical detection of microplastics in water’, *Environ. Sci. Pollut. Res.*, vol. 28, no. 45, pp. 63860–63866, Dec. 2021, doi: 10.1007/s11356-021-12358-2.
[45] B. J. Holland and J. N. Hay, ‘The thermal degradation of PET and analogous polyesters measured by thermal analysis–Fourier transform infrared spectroscopy’, *Polymer*, vol. 43, no. 6, pp. 1835–1847, Mar. 2002, doi: 10.1016/S0032-3861(01)00775-3.
[46] C.-J. Huang, G. V. Narasimha, Y.-C. Chen, J.-K. Chen, and G.-C. Dong, ‘Measurement of Low Concentration of Micro-Plastics by Detection of Bioaffinity-Induced Particle Retention Using Surface Plasmon Resonance Biosensors’, *Biosensors*, vol. 11, no. 7, Art. no. 7, Jul. 2021, doi: 10.3390/bios11070219.
[47] J. G. Webster, ‘The Measurement, Instrumentation and Sensors Handbook’, 1999.
[48] X. Zhang, H. Ju, and J. Wang, *Electrochemical Sensors, Biosensors and their Biomedical Applications*. Academic Press, 2011.
[49] A. J. Bard and L. R. Faulkner, *Electrochemical methods: fundamentals and applications*, 2nd ed. New York: Wiley, 2001.
[50] ‘Hyper Value Screen Printed Electrodes’, *zimmerandpeacock*. http://www.zimmerpeacocktech.com/products/electrochemical-sensors/hyper-value-screen-printed-electrodes/ (accessed May 30, 2023).

[51] ‘Fast Amperometry (FAM)’, *PalmSens*. https://www.palmsens.com/knowledgebase-article/fast-amperometry-fam/ (accessed May 30, 2023).
[52] ‘Cyclic Voltammetry 2/4- What is a Cyclic Voltammogram?’, *PalmSens*. https://www.palmsens.com/knowledgebase-article/cyclic-voltammetry/ (accessed May 30, 2023).
[53] Instituto Nacional de Metrologia, Qualidade e Tecnologia, Avenida Nossa Senhora das Graças, 50, 25250-020, Duque de Caxias, RJ, Brasil. and K. L. S. Castro, ‘Electrochemical Response of Glassy Carbon Electrodes Modified using Graphene Sheets of Different Sizes’, *Int. J. Electrochem. Sci.*, pp. 71–87, Jan. 2018, doi: 10.20964/2018.01.02.
[54] ‘Cyclic voltammetry’, *zimmerandpeacock*. http://www.zimmerpeacocktech.com/knowledge-base/faq/cyclic-voltammetry/ (accessed Jul. 01, 2023).
[55] ‘Electrochemical Impedance Spectroscopy (EIS)’, *PalmSens*. https://www.palmsens.com/knowledgebase-article/electrochemical-impedance-spectroscopy-eis/ (accessed Nov. 07, 2022).
[56] C. Tian *et al.*, ‘Oxygen management in carbon electrode for high-performance printable perovskite solar cells’, *Nano Energy*, vol. 53, pp. 160–167, Nov. 2018, doi: 10.1016/j.nanoen.2018.08.050.
[57] D. Qu, ‘Investigation of oxygen reduction on activated carbon electrodes in alkaline solution’, *Carbon*, vol. 45, no. 6, pp. 1296–1301, May 2007, doi: 10.1016/j.carbon.2007.01.013.
[58] A. I. Belova, D. G. Kwabi, L. V. Yashina, Y. Shao-Horn, and D. M. Itkis, ‘Mechanism of Oxygen Reduction in Aprotic Li–Air Batteries: The Role of Carbon Electrode Surface Structure’, *J. Phys. Chem. C*, vol. 121, no. 3, pp. 1569–1577, Jan. 2017, doi: 10.1021/acs.jpcc.6b12221.
[59] P. Ashdhir, J. Arya, C. E. Rani, and Anshika, ‘Exploring the fundamentals of fast Fourier transform technique and its elementary applications in physics’, *Eur. J. Phys.*, vol. 42, no. 6, p. 065805, Sep. 2021, doi: 10.1088/1361-6404/ac20ad.
[60] M. Cerna and A. F. Harvey, ‘The Fundamentals of FFT-Based Signal Analysis and Measurement’.
[61] ‘Micro particles based on polystyrene size: 10 µm | Sigma-Aldrich’. http://www.sigmaaldrich.com/ (accessed Jun. 01, 2023).
[62] Labconco, ‘What’s the difference between RO and DI water purification? Reverse osmosis vs. deionized water’, *Labconco*. https://www.labconco.com/articles/whats-the-difference-between-ro-and-di-water-pur (accessed May 31, 2023).
[63] A. E. F. Oliveira and A. C. Pereira, ‘Development of a Simple and Cheap Conductive Graphite Ink’, *J. Electrochem. Soc.*, vol. 168, no. 8, p. 087508, Aug. 2021, doi: 10.1149/1945-7111/ac1b02.
[64] M. B. Rooney, D. C. Coomber, and A. M. Bond, ‘Achievement of Near-Reversible Behavior for the [Fe(CN)6]3-/4- Redox Couple Using Cyclic Voltammetry at Glassy Carbon, Gold, and Platinum Macrodisk Electrodes in the Absence of Added Supporting Electrolyte’, *Anal. Chem.*, vol. 72, no. 15, pp. 3486–3491, Aug. 2000, doi: 10.1021/ac991464m.
[65] H. Du, G. Chen, and J. Wang, ‘Highly selective electrochemical impedance spectroscopy-based graphene electrode for rapid detection of microplastics’, *Sci. Total Environ.*, vol. 862, p. 160873, Mar. 2023, doi: 10.1016/j.scitotenv.2022.160873.
[66] F. F. Bolamiri and H. Salmani, *Master’s Thesis work of Farshad Bolamiri on Microfluidic Channel*.

List of Tables

List of Figures